

MODELING WATER TABLE RESPONSE TO SUBIRRIGATION WITH A BURIED
MICROIRRIGATION LINE SOURCE FOR POTATO PRODUCTION

By

JADIR APARECIDO ROSA

A DISSERTATION PRESENTED TO THE GRADUATE SCHOOL
OF THE UNIVERSITY OF FLORIDA IN PARTIAL FULFILLMENT
OF THE REQUIREMENTS FOR THE DEGREE OF
DOCTOR OF PHILOSOPHY

UNIVERSITY OF FLORIDA

2000

to
Bruna and Lucas

100

ACKNOWLEDGMENTS

The author wishes to express his sincere appreciation to Dr. Kenneth L. Campbell for his guidance, assistance and encouragement during the last part of my course of study. Special gratitude is due to the late Prof. Allen G. Smajstrla who was much more than an adviser to me. He was a brilliant scientist and an esteemed friend. I would like to express my deep admiration and respect for him in every possible way. He welcomed and helped me in adjusting to living in a different country. Without his excellent advice, guidance, patience and time, my work would not have been possible. It was a great pleasure and precious experience working with him.

Special thanks are also due to the other members of my committee, Dr. D. Z. Haman, Dr. F. S. Zazueta, Dr. S. J. Locascio, and Dr. L. H. Motz for their support.

The author is indebted to the Agricultural and Biological Engineering Department for the use of its facilities. Appreciation is also expressed to other graduate students, and faculty and staff members for their assistance, especially to Mr. Danny Burch for his technical assistance.

Special gratitude goes to the taxpayers of Brazil, few of whom will ever read this dissertation, but all of whom have contributed to it. Thanks to CAPES, my scholarship's sponsor, and to IAPAR, my employer.

Finally, behind the scenes were my loving kids, Bruna and Lucas, who rejoiced with me in good times and cheered me up in the bad.

TABLE OF CONTENTS

	<u>page</u>
ACKNOWLEDGMENTS.....	iii
LIST OF TABLES.....	vii
LIST OF FIGURES.....	viii
ABSTRACT.....	x
 CHAPTERS	
1 INTRODUCTION.....	1
2 REVIEW OF LITERATURE.....	5
Variably Saturated Water Flow	5
Flux Density Equation: Darcy's Law	5
Conservation of Mass: Continuity Equation	6
General Unsaturated Flow Equation: Richards Equation	7
Solutions of the Water Flow Equation	9
Soil Hydraulic Properties	12
Soil Water Characteristic Curve.....	13
Unsaturated Hydraulic Conductivity Curve	16
Soil Water Capacity	17
Hysteresis in Soil Hydraulic Properties	18
Root Water Uptake.....	20
Water Table Management	22
Subsurface Drip Irrigation.....	27
3 MODEL DEVELOPMENT.....	30
Two-Dimensional Model Development.....	30
Initial Conditions.....	34
Boundary Conditions.....	34
Top Surface Boundary.....	34
Bottom Surface Boundary.....	35
Left Surface Boundary	36
Right Surface Boundary Condition	36
Seepage Surface Boundary.....	37
Surface Runoff	38

Irrigation.....	40
Corner Nodes.....	41
Time Step Update.....	41
Grid Size.....	42
Estimation of Internode Hydraulic Conductivity	43
Evaluation of the Soil Hydraulic Properties.....	44
Water Uptake by Plant Roots.....	45
Solution of the Two-Dimensional Model.....	46
Mass Balance Computation.....	47
4 MODEL TESTING.....	49
Infiltration in a Large Caisson.....	49
Water Movement in a Cropped Soil Profile.....	50
Transient, Two-Dimensional, Variably Saturated Water Table Recharge.....	54
Transient, Two-Dimensional, Unconfined Drainage	55
5 EXPERIMENTAL PROCEDURE.....	58
Subirrigation System.....	58
Runoff Measurement.....	61
Soil Hydraulic Characteristics.....	62
Soil Water Retention Curve	62
Saturated Hydraulic Conductivity	64
Climate Data.....	66
6 NUMERICAL SOLUTION: CALIBRATION.....	68
Soil Hydraulic Properties	68
Estimated Daily ET	71
Deep Percolation	75
Water Table Levels	77
Runoff.....	79
Irrigation.....	82
Water Balance	87
7 MODEL VERIFICATION AND SENSITIVITY ANALYSIS.....	89
Model Verification	89
Estimated Daily ET	89
Water Table Levels	91
Irrigation.....	91
Runoff.....	96
Deep Percolation	100
Water Balance	101
Sensitivity Analysis.....	102

8	SUMMARY, CONCLUSIONS AND RECOMMENDATIONS.....	106
	Summary	106
	Conclusions	107
	Recommendations for Future Research	108
APPENDICES		
A	MODEL ORGANIZATION.....	109
B	NUMERICAL MODEL PROGRAM LISTING.....	115
LIST OF REFERENCES.....		153
BIOGRAPHICAL SKETCH.....		162

LIST OF TABLES

<u>Table</u>		<u>page</u>
4-1. Soil hydraulic parameters of crushed Bandelier Tuff used in the caisson flow example.....		49
4-2. Soil hydraulic parameters for the second example		51
4-3. Soil hydraulic parameters used in the third example.....		54
5-1. Parameters used in van Genuchten's equation to describe the soil hydraulic properties of Placid Fine Sand.....		62
6-1. Parameters in van Genuchten's equation determined using original and calibrated soil water retention curves for Placid Fine Sand.....		69
6-2. Lengths of the stages and crop coefficients for potato used in this work.....		74
6-3. Measured and simulated runoff volumes for three storm events in 1996.....		82
6-4. Water Balance for the 1996-simulation period.....		87
7-1. Water Balance for the 1997-simulation period.....		102
7-2. Sensitivity analysis of selected parameters for the 1997 simulation period.....		105
A-1. Input files and type of information read.....		110
A-2. Output files and type of data printed.....		112
A-3. List of significant variables of the two-dimensional model		113

LIST OF FIGURES

<u>Figure</u>		<u>page</u>
2-1. Schematic of the plant water stress response, $a(h)$, as used by Feddes et al. (1978).....		21
3-1. Grid system for finite difference two-dimensional model after discretizing equation (2.9). Nodes are located at the centroid of the cells.....		31
3-2 Finite difference grid for the field problem.....		39
4-1 Predicted water pressure head during transient infiltration in Bandelier Tuff.....		50
4-2. Simulated pressure heads at the surface for the second example, as simulated with HYDRUS and this work.....		52
4-3. Simulated water content at selected times (days) with HYDRUS (symbols) and this work (lines) for the second example.....		52
4-4. Precipitation and location of the water table level for the second example, as simulated with the HYDRUS and this work computer program.....		53
4-5. Simulation of transient water table mounding, comparing results from this work and experimental data collected by Vauclin et al. (1979).....		55
4-6. Simulation of transient drainage, comparing results from this work and experimental data collected by Vauclin et al. (1975).....		57
5-1. Layout of the field research experiment.....		59
5-2. Soil moisture curve for Placid Fine Sand		63
5-3. Fitted and observed soil moisture retention curves for one equivalent layer of Placid Fine Sand.....		63
6-1. Fitted soil moisture retention curves with original and calibrated parameters.....		70
6-2. Predicted hydraulic conductivity with original and calibrated parameters.....		71

6-3.	Simulated distribution of the daily ET over a 24-hr cycle.....	73
6-4.	Crop coefficient curve for potato used in this study.....	74
6-5.	Daily values of potential evapotranspiration (Penman) and crop ET for the 1996 simulated period.....	76
6-6.	Relationship between flux and hydraulic head at the bottom of the soil profile.....	78
6-7.	Observed and simulated water table in the 1996 growing season.....	80
6-8.	Cumulative observed and simulated irrigation in the 1996 growing season.....	86
6-9.	Simulated and observed water tables during a period of irrigation late in the 1996 growing season.....	88
7-1.	Daily values of potential evapotranspiration (Penman) and crop ET for the 1997 simulated period.....	90
7-2.	Observed and simulated water table in the 1997 growing season.....	92
7-3.	Scattergram of observed and simulated water table depth (taken positive downward) in the 1997 simulation.....	93
7-4.	Cumulative observed and simulated irrigation in the 1997 growing season.....	94
7-5.	Water table profile during irrigation in the early and mid seasons.....	97
7-6.	Water table profile during irrigation in the early and mid hours of the day.....	97
7-7.	Cumulative observed and simulated runoff in the 1997 growing season.....	98
7-8.	Measured rainfall versus simulated and observed runoff during the 1997 simulation period.....	101

Abstract of Dissertation Presented to the Graduate School
of the University of Florida in Partial Fulfillment of the
Requirements for the Degree of Doctor of Philosophy

MODELING WATER TABLE RESPONSE TO SUBIRRIGATION WITH A BURIED
MICROIRRIGATION LINE SOURCE FOR POTATO PRODUCTION

By

Jadir Aparecido Rosa

May 2000

Chairman: Kenneth L. Campbell

Major Department: Agricultural and Biological Engineering

In northeast Florida, the greatest use of fresh water resources is for supplemental irrigation of agricultural crops, including potato, one of the major crops in this area. Potatoes are grown on beds in soils that require irrigation even though if they are subject to naturally occurring high water tables. Most potato fields are irrigated using conventional semi-closed seepage systems that are not as efficient as most other irrigation methods. Research has shown the technical feasibility of subirrigation with a buried microirrigation system for vegetable crops in Florida, with a reduction in runoff rates and irrigation requirements as compared to the conventional semi-closed seepage irrigation system.

The contribution of high water tables to soil water extracted by agricultural crops in combination with subsurface drip irrigation had not been studied accurately. Field plots were installed at the University of Florida Hastings Agricultural Research Center Yelvington Farm, and potatoes were produced during three spring growing seasons to

compare buried microirrigation and conventional seepage irrigation systems. Water table levels, precipitation, irrigation and runoff volumes were continuously monitored.

A two-dimensional finite difference model was developed to simulate water movement from a buried microirrigation line source with an automated controller for the water table level and the response of the water table to precipitation, evapotranspiration, and deep percolation. The water uptake by plant roots was simulated by an extraction function with a root distribution term. Deep percolation was modeled with a water table-drainage flux relationship. Runoff was simulated at the surface and at the face of the water furrow located at the right boundary.

The model was calibrated and verified by comparing simulated results with experimental field observations. The model performed very well in simulating seasonal runoff, irrigation volumes, and water table levels during crop growth. A sensitivity analysis, to observe the influence of some parameters on model response, identified the high sensitivity of the model to the parameter n used in the model to describe the soil hydraulic functions.

The two-dimensional model can be used to investigate different irrigation strategies involving water table management control. Applications of the model include using it to optimize the depth of water table for each growth stage, and to optimize the duration, frequency, and rate of irrigation.

CHAPTER 1

INTRODUCTION

Irrigation of agricultural crops is one of the primary uses of water. Supplemental water is provided to crops during periods of low rainfall to maintain optimal crop performance. An effective method of application is required to minimize water losses. Wind, evaporation, surface runoff, and deep percolation can cause these losses.

The design of efficient agricultural water management systems is becoming more and more critical as competitive uses for water resources increase, and as installation and operational costs climb. In humid regions, artificial drainage is necessary to permit farming of some of the most productive soils. Drainage is needed to provide trafficable conditions for seedbed preparation and planting, and to insure a suitable environment for plant growth. At the same time, excessive drainage is undesirable as it reduces soil water available to growing plants and leaches fertilizer nutrients, carrying them to receiving streams where they act as pollutants. In some cases, water table control or subirrigation can be used to maintain a relatively high water table during the growing season, thereby supplying irrigation water for crop growth, as well as preventing excessive drainage.

Water table management can play an important role in stabilizing crop production by reducing moisture stress in the root environment. In addition, an automatic-controlled irrigation system promotes more efficient use of natural resources and may decrease the amount of pumped irrigation water. Water table management can be efficient using subirrigation combined with drainage systems.

Tools to quantify the effects of different water table management systems allow irrigation and drainage designers to make correct decisions in the system design and management. In such cases, computer simulation provides a logical base for informed management decisions.

In the last thirty years, computer models have been developed to simulate the day-by-day performance of drainage and water table control systems (Skaggs, 1992). Different approaches have been used in the models, ranging from very complex numerical solutions of differential equations to approximate methods for conducting a water balance in the soil profile.

However, all models have their limitations. Extensive amounts of data are often required, some of which will not be readily available. In some cases, more is known about the governing processes than can be implemented in a model due to computational and data limitations. Understanding of the details of the governing processes in the natural system also is limited. There is a tremendous amount of variability in the response of any natural system, and while current physically-based models may be able to predict mean responses with some certainty, much of the variability is not addressed as the causal processes are not completely understood.

In northeast Florida, potatoes are grown on beds in soils that require irrigation even if they are subject to naturally occurring high water tables. Most potato fields are irrigated using conventional semi-closed seepage systems that are not as efficient as most other irrigation methods (Smajstrla et al., 1991). The technical feasibility of subirrigation with buried microirrigation for vegetables crops in Florida has been shown, with reduction of runoff rates and irrigation requirements as compared to conventional semi-

closed seepage irrigation (Stanley and Clark, 1991; Smajstrla et al., 1995; Smajstrla et al., 2000).

Because no studies were found on the dynamic soil-plant-water-climate relationships that occur when agricultural crops are grown on sandy soils, irrigated by buried microirrigation line sources, and subject to naturally occurring high water tables, the objectives of this research were:

1. To conduct field studies on potatoes grown on sandy soils and irrigated by buried microirrigation line sources.
2. To record the dynamics of water table depth under subirrigation with buried microirrigation line sources and drainage.
3. To develop a mathematical model that describes the transient movement of the water table during drainage, subirrigation, rainfall, and root extraction.
4. To verify the computer simulation by comparing model results with field observations on water table management research plots and with other published studies.

The dissertation is organized in the following manner: Chapter 2 contains the Literature Review, where literature used to develop the model is discussed. The development and components of the model are described in Chapter 3. Comparisons of simulation results of the model and published numerical solutions are presented in Chapter 4. The experimental procedure of the field research used to calibrate and verify the model is presented in Chapter 5. The model calibration and the model verification using data from the field research plots are presented in Chapters 6 and 7, respectively.

Finally, Chapter 8 contains a summary, conclusions and recommendations for future research.

CHAPTER 2 REVIEW OF LITERATURE

Variably Saturated Water Flow

Prediction of fluid movement in unsaturated soils is an important role in many branches of science and engineering, including soil science, agricultural engineering, environmental engineering, and groundwater hydrology (Celia et al., 1990). The general equations governing soil water flow are Darcy's law and the continuity of flow equation, which combined, yield the general flow equation for unsaturated flow (Richards equation).

Flux Density Equation: Darcy's Law

Darcy's law¹ postulates that the flow of a viscous liquid (namely water) through a porous medium is in the direction of, and at a rate proportional to, the *driving force* (i.e., the *hydraulic gradient*) and also proportional to the ability of the conducting medium to transmit the liquid (namely the *hydraulic conductivity*).

For the two-dimensional flow of water in both saturated and unsaturated soil, Darcy's law can be written as:

$$q = -K(h)\nabla H \quad (2.1)$$

where

q = discharge per unit area or flux density (LT^{-1}),

¹ After Henry Darcy, the French engineer who discovered it in the course of his classic investigation of seepage rates through sand filters in the city of Dijon.

h = soil moisture pressure head (L),

K = hydraulic conductivity (LT^{-1}),

∇ = differential operator, and

H = hydraulic potential (L).

Defining hydraulic potential (H) as

$$H = h - z \quad (2.2)$$

where z is elevation head or gravitational head (L) taken as positive in the downward direction, Darcy's law for unsaturated soils can be expressed as

$$q_x = -K_x(h) \frac{\partial h}{\partial x} \quad (2.3a)$$

$$q_z = -K_z(h) \left(\frac{\partial h}{\partial z} - 1 \right) \quad (2.3b)$$

where q_x and q_z are the components of soil water flux in two dimensions.

Conservation of Mass: Continuity Equation

The mass conservation law, expressed in the equation of continuity, states that if the rate of inflow into a volume element is greater than the rate of outflow, the volume element must be storing the excess and increasing its water content (and, conversely, if outflow exceeds inflow, water content must decrease in time).

The equation of continuity in multidimensional systems according to Hillel (1998) can be written as

$$\frac{\partial \theta}{\partial t} = -\nabla \cdot q \quad (2.4)$$

where

θ = soil water content (L^3L^{-3}), and

T = time (T).

In some situations, positive and negative accumulations of a component are due not only to changes in the direction of transport, but also to local addition to or extraction from outside the system. For the flow of water in soils the proper continuity equation (Koorevaar et al., 1983) is then

$$\frac{\partial \theta}{\partial t} = -\nabla q - S \quad (2.5)$$

where S is an extraction term.

General Unsaturated Flow Equation: Richards Equation

The flux density equation and the continuity equation must both be satisfied in solving a particular water flow problem. Substitution of equation (2.1) into the continuity equation (2.5) yields the combined flow equation that can be written as

$$\frac{\partial \theta}{\partial t} = -\nabla[K(h)\nabla H] - S(h) \quad (2.6)$$

This equation, along with various alternative formulations, is known as the *Richards equation*. Note that the extraction term is also considered a term dependent on the actual soil water pressure.

Full expansion of Richards equation in two dimensions yields the pressure head form of the flow equation

$$\frac{\partial \theta}{\partial t} = \frac{\partial}{\partial x} \left[K_x(h) \frac{\partial h}{\partial x} \right] + \frac{\partial}{\partial z} \left[K_z(h) \left(\frac{\partial h}{\partial z} - 1 \right) \right] - S(h) \quad (2.7)$$

In equation (2.7) time and space dimensions are independent variables, whereas soil water pressure and volume water content are the dependent variables. The equation can be simplified introducing a soil differential capacity defined as

$$C = \frac{d\theta}{dh} \quad (2.8)$$

C (L^{-1}) is called *soil water capacity* and its use provides the option of expressing the Richards equation in either an h -based form, a θ -based form, or a mixed-form.

Applying equation (2.8) into equation (2.7) the general flow equation in two-dimensional form and h -based can be expressed as

$$C(h) \frac{\partial h}{\partial t} = \frac{\partial}{\partial x} \left[K_x(h) \frac{\partial h}{\partial x} \right] + \frac{\partial}{\partial z} \left[K_z(h) \left(\frac{\partial h}{\partial z} - 1 \right) \right] - S(h) \quad (2.9)$$

The θ -based equation can be written as

$$\frac{\partial \theta}{\partial t} = \frac{\partial}{\partial x} \left[D_x(\theta) \frac{\partial \theta}{\partial x} \right] + \frac{\partial}{\partial z} \left[D_z(\theta) \left(\frac{\partial \theta}{\partial z} - 1 \right) \right] - S(\theta) \quad (2.10)$$

where $D(\theta) \equiv K(\theta)/C(\theta)$ is the unsaturated diffusivity ($L^2 T^{-1}$).

The most commonly used form of the Richards equation is the h -based form. Its advantages are that it can be applied to both saturated and unsaturated conditions, as well as to layered soils, where h is generally continuous but θ may not be (Hanks and Ashcroft, 1980). However, these models suffer from poor mass balance for unsaturated soils, and from unacceptable time step limitations or poor CPU efficiency especially for very dry initial conditions (Pan and Wierenga, 1995). On the other hand, numerical models of the θ -based form (eq. 2.10) have demonstrated significantly improved performance when modeling infiltration into very dry soil and heterogeneous soils, but

cannot be used for simulating water flow in soils with saturated regions. (Hills et al., 1989). These models also require special treatment for material discontinuities.

Equations (2.9) and (2.10) assume that:

1. The porous medium is homogeneous (if isotropic, $K_x = K_z = K$).
2. There is no air resistance to the flow, i.e., the porous medium contains only water and empty voids.
3. The hydraulic conductivity is a single valued function of soil water pressure (or water content).
4. Darcy's law is applicable.
5. The flow is isothermal.
6. There is no swelling or shrinking of the soil mass and the liquid is incompressible.
7. Vegetative, bacterial, and chemical effects are neglected.

Solutions of the Water Flow Equation

Richards equation is highly nonlinear due to the functional nature of soil properties to pressure head, and cannot be solved analytically, except in special cases (Hillel, 1998).

Analytical methods to solve the nonlinear water flow equation search for the exact solution in terms of analytical functions. Such an exact solution, if it exists, requires transformation, separation of variables, and usually a series of error functions. Boltzman transformation is commonly used to reduce the partial differential equations to ordinary differential equations. The Laplace transformation results in removing the time variable. The solution of an equation modified this way yields a dependent variable as a function

of the space variables. The nonlinear mass conservation can be analytically solved only using various types of relaxation techniques such as linearization, quasilinearization and transformation to steady state (Feddes et al., 1988).

Numerical methods are used to represent a continuous differential equation as an approximate algebraic equation (or set of such equations) in which the domain of interest is cut into discrete intervals and derivatives are replaced by differences that can be solved with the aid of a computer for successive times.

A number of numerical methods have been introduced in recent decades. The methods that are most appropriate to the problem of soil water dynamics are finite difference and finite element methods.

The finite difference method, either explicit or implicit, is the numerical technique most frequently used in modeling unsaturated flow conditions (Remson et al., 1971). Different forms of finite difference have been formulated to face the difficulties encountered when solving the governing equation, and various features have been introduced in order to reduce computer time, stability problems, and convergence problems (Jensen, 1983).

The advantage of the finite difference method is its simplicity and efficiency in treating the time derivatives, but the method is rather limited in dealing with complex geometries of flow regions. A slow convergence, a restriction to bilinear grids and difficulties in treating moving boundary conditions are other serious drawbacks of the method.

Several researchers have presented finite difference algorithms for modeling transient water flow in unsaturated soils. Examples of finite difference models include

those presented by Brandt et al. (1971), Dane and Mathis (1981), Haverkamp and Vauclin (1981), Haverkamp et al. (1977), and Vauclin et al. (1979).

With finite element methods the domain is divided into a number of rigid elements. In modeling soil water flow problems, triangular elements can be efficiently used to represent difficult geometries and to concentrate coordinate functions in regions where changes are anticipated – such as near the soil surface or wetting fronts. The corners of such triangular elements are designated as nodal points. These nodes serve the purpose of locating state variables, e.g. water pressure heads. Each element is characterized by local coordinate functions. This permits the application of variational or weighted residual principles, with Galerkin's method being the most widely used (Feddes et al., 1988). Examples of finite element based unsaturated flow algorithms include those of Lappala et al. (1993), Šimunek et al. (1994), and Vogel et al. (1996).

Until recently most numerical studies have used either the h - or θ -based form of the Richards equation. The objectives of these studies include obtaining more stable numerical algorithms, speeding up the calculations, minimizing mass balance errors, and achieving more accurate solutions for different soil types or initial and boundary conditions (Huang et al., 1996). For example, Milly (1985) presented a mass-conservative solution procedure in which an effective element soil water capacity term was used. By introducing a source term, Hills et al. (1989) successfully solved the problem involving one-dimensional water flow into layered soils with the θ -based formulation. Rathfelder and Abriola (1994) proposed a mass-conservative solution for the h -based equation by expanding and discretizing the soil water capacity term. Kirkland et

al. (1992) developed a θ -based form algorithm involving a transformation of variable to model variably saturated soils in two dimensions.

Because of the existing problems with the h - and θ -based forms of the Richards equation, many researchers have tried to combine the advantages of the two methods. The mixed form (eq. 2.7) of the governing equation was thought to maintain the mass conservative property inherent in the θ -based form, while providing solutions in terms of the pressure head. Brutsaert (1971) was one of the first researchers to present a finite difference algorithm that combined the mixed-form of Richards equation with a Newton iteration scheme to effectively deal with steep wetting fronts. Celia et al. (1990) proposed a mass-conservative numerical scheme to solve the mixed-form of Richards equation using modified Picard iteration, resulting in perfect mass balance. This approach showed much promise in modeling unsaturated flow with steep wetting fronts. Huang et al. (1996) proposed a new nonlinear convergence criterion in the mixed-form algorithm of Celia et al. (1990) to improve further the computational efficiency as compared with standard convergence criteria used in most numerical studies.

Soil Hydraulic Properties

The prime goal for model simulations of transient, unsaturated water flow in soil profiles is to accurately predict temporal and spatial distributions of water content, pressure head, and flux. Such simulations involve the use of numerical methods to solve Richards equation for water flow under specified initial and boundary conditions. Hydraulic property submodels are needed to provide mathematical relationship of suction head to water content ($\theta(h)$) and to hydraulic conductivity, $K(h)$. These functions provide

continuous representations of $\theta(h)$ and $K(h)$ as input information for the water flow model.

While a large number of laboratory and field methods have been developed over the years to measure the soil hydraulic functions (Klute and Dirksen, 1986) most methods are relatively costly and difficult to implement. Accurate in situ measurement of the unsaturated hydraulic conductivity has remained especially cumbersome and time-consuming (Stephens, 1995). Thus, cheaper and more expedient methods for estimating the hydraulic properties are needed if we are to implement improved practices for managing water in the unsaturated zone.

Soil Water Characteristic Curve

The soil water characteristic curve (SWCC) defines the degree of saturation (or water content) for a particular suction (negative water pressure) in the soil (Hillel, 1998). The SWCC is primarily determined by the textural and structural composition of the soil. A characteristic feature of many SWCC is that moisture content decreases fairly rapidly with suction, except for a transition range, which introduces an S-shape in the curves.

The relationship between the soil moisture content and water pressure is not always included as a part of hydrological measuring programs, and to supplement this deficit several investigators have proposed empirical equations to predict the relationship. In general, it must be concluded that the parameters involved in these equations are of minor physical relevance. However, to solve the general flow equation numerically or analytically, the SWCC has to be supplied in a mathematically tractable form, and hence

the various empirical equations can be used for this purpose simply by fitting the equations to the available data on soil moisture retention (Jensen, 1983).

One of the most popular functions used to describe the SWCC is the equation of Brooks and Corey (1964):

$$\theta = \begin{cases} \theta_r + (\theta_s - \theta_r)(\alpha h)^{-\lambda} & (\alpha h > 1) \\ \theta_s & (\alpha h \leq 1) \end{cases} \quad (2.11)$$

where

θ = water content ($L^3 L^{-3}$),

θ_r = residual water content ($L^3 L^{-3}$),

θ_s = saturated water content ($L^3 L^{-3}$),

α = empirical parameter whose inverse is often referred to as the air entry value or bubbling pressure and taken positive for unsaturated soils (L^{-1}),

h = water pressure taken positive for unsaturated soils (L), and

λ = pore-size distribution parameter affecting the slope of the retention function.

Because of its simple form, equation (2.11) has been shown to produce relatively accurate results for many coarse-textured soils characterized by relatively narrow pore- or particle-size distribution (large λ -values). Results have generally been less accurate for many fine-textured and undisturbed field soils because of the absence of a well-defined air-entry value for these soils (van Genuchten et al., 1991).

Several continuously differentiable (smooth) equations have been proposed to improve the description of soil water retention near saturation. While these functions were able to reproduce observed soil water retention data more accurately, most are too complicated mathematically to be easily incorporated into predictive pore-size

distribution models for hydraulic conductivity (to be discussed later), or possess other features (notably the lack of a simple inverse relationship), which make them less attractive in soil water studies. A related smooth function with attractive properties is the equation of van Genuchten (1980):

$$\theta = \theta_r + \frac{(\theta_s - \theta_r)}{\left[1 + (\alpha|h|)^n\right]^m} \quad (2.12)$$

where α , n and m are empirical constants affecting the shape of the retention curve.

The residual water content (θ_r) specifies the maximum amount of water in a soil that will not contribute to liquid flow because of a blockage from the flow paths or strong adsorption onto the solid phase. Formally, θ_r may be defined as the water content at which $d\theta/dh$ goes to zero when h becomes very large. The saturated water content (θ_s) denotes the maximum volumetric water content of a soil, and should not be equated to the porosity of soils; θ_s of field soils is generally 5 to 10% smaller than the porosity because of entrapped or dissolved air. In the equation (2.12) θ_r and θ_s are viewed as being essentially empirical constants in soil water retention functions and without much physical meaning (van Genuchten et al., 1991).

Recently, Fredlund et al. (1997) presented a method to estimate the SWCC from the grain-size distribution curve and volume-mass properties of the soil. The prediction of SWCC was found to be particularly accurate for sands, and reasonable for silts. Clays, tills and loams were more difficult to predict although the accuracy of the algorithm appeared to be reasonable. Results of this research tended to be sensitive to the packing porosity and they suggested that more research is required in this regard.

Unsaturated Hydraulic Conductivity Curve

According to Darcy's equation (eq. 2.1), hydraulic conductivity is the ratio of the flux to the potential gradient, or the slope of the flux versus gradient curve (Hillel, 1998). For saturated flux, the total soil pore space is available for water flow. However, for unsaturated flow, part of the pores is filled with air and the unsaturated hydraulic conductivity (K) is smaller than the saturated hydraulic conductivity. So, K is dependent upon the soil water content θ or the water pressure h (Kutilek and Nielsen, 1994).

Reliable estimates of the K are especially difficult to obtain, partly because of its extensive variability in the field, and partly because measuring this parameter is time-consuming and expensive (van Genuchten, 1980). Several investigators have, for these reasons, used models for predicting the K from the more easily measured soil water characteristic curve.

Because of their simplicity and ease of use, predictive models for the K have become very popular in numerical studies of unsaturated flow. Results thus far suggest that predictive models work reasonably well for many coarse-textured soils and other porous media having relatively narrow pore-size distributions, but that predictions for many fine-textured and structured field soils remain inaccurate. Because of the time-consuming nature of direct field measurement of the hydraulic conductivity, and in view of the field-scale spatial variability problem, it nevertheless seems likely that predictive models (including those that predict the hydraulic properties from soil texture and related data) provide the only viable means of characterizing the hydraulic properties of large areas of land, whereas direct measurement may prove to be cost-effective only for site-specific problems (Wösten and van Genuchten, 1988).

The theory of hydraulic conductivity prediction has been expanded and generalized by Mualem (1976) and by van Genuchten (1980). Consideration of additional factors such as tortuosity and hysteresis are presented by Mualem (1986) in an extensive review and analysis of alternative models.

van Genuchten et al. (1991) presented a code for quantifying the unsaturated hydraulic conductivity using different pore-size distribution models. The code has the possibility of evaluating the model parameters from observed conductivity data, from measured retention data or from both simultaneously. Based on Mualem's (1976) model, the relative hydraulic conductivity (K_r), defined as the ratio of unsaturated to saturated hydraulic conductivity (K_s), was expressed in terms of pressure head by

$$K_r(h) = \frac{\{1 - (\alpha|h|)^{n-1} [1 + (\alpha|h|)^n]^{-m}\}^2}{[1 + (\alpha|h|)^n]^{0.5}} \quad (2.13)$$

where all variables are as defined for equation (2.12). The actual value of $K(h)$ (LT^{-1}) is given by

$$K(h) = K_s K_r \quad (2.14)$$

Soil Water Capacity

The soil water capacity (C) is defined by equation (2.8) as the slope of the soil water characteristic curve at a given pressure. In the Richards equation of unsaturated flow (equation 2.9) C represents the volume of water released from or taken into storage, per unit bulk volume of soil, per unit change in pressure head (Stephens, 1995). This definition is essentially identical to that for specific storage coefficient in aquifers, and

both terms have units of inverse length (L^{-1}). C can be obtained by differentiating equation (2.12) to give

$$C = \frac{-\alpha m(\theta_s - \theta_r)}{1-m} \left[\frac{1}{1 + (\alpha|h|)^n} \right] \left\{ 1 - \left[\frac{1}{1 + (\alpha|h|)^n} \right] \right\}^m \quad (2.15)$$

where all variables were previously defined.

Hysteresis in Soil Hydraulic Properties

The relation between water pressure and water content can be obtained in two ways: (1) in desorption, by starting with a saturated sample and applying increasing suction to gradually dry the soil while taking successive measurements of wetness versus suction; (2) in sorption, by gradually wetting an initially dry soil sample while reducing the suction incrementally (Hillel, 1998). The equilibrium soil wetness at a given suction is greater in desorption (drying) than in sorption (wetting). This dependence of the equilibrium content and state of water upon the direction of the process leading up to it is called *hysteresis*.

Hysteresis is attributed to the action of several factors – the enclosed air in “blind pores”, the ink bottle effect of the rosary shaped pores where the radius of the meniscus depends upon the direction of reaching a given level and, moreover, the difference in wetting angle occurring for an advancing versus receding liquid front over the solid surface (Kutilek and Nielsen, 1994).

Problems in which hysteresis may be important to consider involve periods of both wetting and drying, such as can occur during infiltration and subsequent redistribution of a pulse of infiltrated water that is drawn both downward by gravity and

capillarity and also upward due to evapotranspiration (Stephens, 1995). Earlier numerical simulation work by Rubin (1967) showed the importance of hysteresis in the soil hydraulic properties to accurately predict redistribution. In general, the effect of hysteresis is to retard redistribution, so that water is retained at the top layers of the profile.

One major factor that complicates the accurate measurement of the unsaturated soil hydraulic properties is their hysteretic nature when two immiscible fluids like air and water, or water and hydrocarbons, simultaneously occupy the pore space. Luckner et al. (1989) developed a set of parametric models for the unsaturated fluid phase content and hydraulic conductivity functions of typical immiscible two-phase systems. The fluid saturation (soil water retention) curves were described with modifications of the high-order continuous S-shaped retention function of van Genuchten (1980). The functions were modified to allow inclusion of both wetting and nonwetting residual fluid saturations. To avoid theoretical and experimental complications, the researchers emphasized the need to match the predicted and experimental hydraulic conductivity at fluid phase contents less than full saturation.

Simulating unsaturated flow using hysteretic soil-hydraulic properties is numerically always a relatively complicated task (Vogel et al., 1996). Including hysteresis in numerical models may increase the chances of producing unstable or even non-convergent results, especially when long-term transient simulations are being carried out.

Root Water Uptake

The sink term, S , in equation (2.9) can define the volume of water removed per unit time from a unit volume of soil due to plant root uptake. The rate at which water is extracted from a cropped soil profile is limited by the amount of available energy as given by the potential evapotranspiration rate (ET). The actual rate of extraction is also affected by the rate at which the soil can transmit water to the roots (or indirectly by the soil water pressure head, h) and hence may be less than the ET . A large number of models have been proposed in the soil physics and plant physiology literature to quantitatively describe root water uptake as a function of h and/or θ . Molz (1981) presented an interesting review of models of water transport in the soil-plant system.

Feddes et al. (1978) defined S as

$$S(h) = a(h)S_p \quad (2.16)$$

where the water stress response function $a(h)$ is a prescribed dimensionless function of the soil water pressure head ($0 \leq a \leq 1$), and S_p is the potential water uptake rate (T^{-1}). Figure 2-1 gives a schematic plot of the stress response function as used by Feddes et al. (1978). Notice that water uptake is assumed to be zero close to saturation (i.e. wetter than some arbitrary anaerobiosis point, h_1). For $h < h_4$ (the wilting point pressure head), water uptake is also assumed to be zero. Water uptake is considered optimal between pressure heads h_2 and h_3 , whereas for pressure head between h_3 and h_4 (or h_1 and h_2), water uptake decreases (or increases) linearly with h . S_p is equal to the water uptake rate during periods of no stress when $a(h) = 1$.

When the potential water uptake rate is equally distributed over a two-dimensional rectangular root domain, S_p becomes

$$S_p = \frac{1}{L_x L_z} L_t T_p \quad (2.17)$$

where T_p is the potential transpiration rate (LT^{-1}), L_z is the depth (L) of the root zone, L_x is the width (l) of the root zone, and L_t is the width (L) of the soil surface associated with the transpiration process. Notice that S_p reduces to T_p/L_z when $L_t = L_x$.

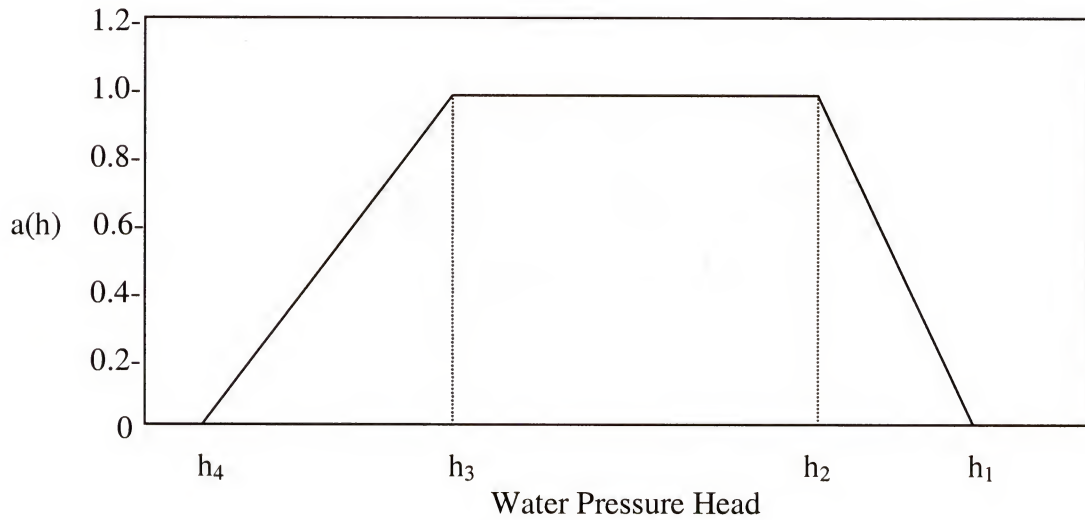


Figure 2-1. Schematic of the plant water stress response function, $a(h)$, as used by Feddes et al. (1978).

Smajstrla (1982) presented an extraction function, S (LT^{-1}), based on potential extraction rate and soil water status, defined as

$$S = T_p R^{(T_p / CR)} \quad (2.18)$$

where

T_p = potential transpiration rate (LT^{-1}), and

C = calibration constant.

R was defined as the relative available soil water content, given by

$$R = \frac{\theta - \theta_{wp}}{\theta_{fc} - \theta_{wp}} \quad (2.19)$$

where

θ = actual soil water content,

θ_{wp} = soil water content at the wilting point, and

θ_{fc} = soil water content at field capacity.

The model was calibrated using the rate of soil water content change observed during lysimeter field experiments with soybeans. The function allows a rapid rate of soil water extraction when soil water is readily available. As the water is depleted, the extraction rate declines logarithmically. Extraction is limited during periods of high potential evapotranspiration and is allowed to recover to near potential rates during periods of low potential evapotranspiration. The function limits extraction to very low rates as the permanent wilting point is approached. Stone (1987) modified the extraction term to include a root distribution function and substituted potential transpiration (T_p) with actual evapotranspiration. The extraction term was used with success in two-dimensional models simulating extraction patterns under field and lysimeter conditions (Stone, 1987; Vellidis, 1989).

Water Table Management

Using water table management practices to help maintain agricultural productivity and profitability, without causing any degradation of water quality, is important in most areas in the United States. It has been practiced for many years in scattered locations, such as Florida in both the sandy flatwoods soils (Campbell et al., 1974; Pitts et al., 1993) and the organic soils near the Everglades (Snyder et al., 1978), in the Lower Mississippi

Valley (Bengtson et al., 1993), in the Georgia Flatwoods (Shirmohammadi et al., 1991; Johnson et al., 1993), in the Coastal Plain Soils of Virginia and North Carolina (Evans and Skaggs, 1989), in the organic soils of the Great Lake States of Michigan, Indiana, Ohio, and Minnesota, and in the Sacramento-San Joaquin Delta in Central California (Fouss et al., 1990). Some of these applications date back to the 1920's. Water table control is also practiced in other countries: Brazil (Rosa, 1993), Egypt (Kandil and Willardson, 1992; Ragab and Amer, 1986), Canada (Madramootoo et al., 1993; Prasher et al., 1994), and Nigeria (Nwadukwe et al., 1989).

There are two limiting depths of water tables to be considered when designing a water table management system. The upper limit is determined by the soil characteristics and the root requirement for aeration. The lower limit is the lowest elevation that will provide water for plant growth. Williamson and Kriz (1970) identified four representative water table (WT) conditions: (1) when the WT is maintained constant; (2) when the WT is maintained fluctuating; (3) when the WT is far below the root zone so water logging will not occur unless the soil surface is flooded; and (4) when the WT is at or above the soil surface. The authors found that, with a 15-cm water table depth, maximum crop yield was produced only with certain crops under certain conditions, i.e., relatively low temperatures. Other crops performed best with a 150-cm deep water table.

Sieben (see Bower, 1974) studied the effect of a fluctuating water table by analyzing the hydrograph of the water table and by considering the top 30 cm of the soil profile as the critical depth. Sieben introduced the SEW_{30} factor, expressed as

$$SEW_{30} = \int_0^T (30 - x_i) dt \quad \text{for } x_i \leq 30 \quad (2.16)$$

where x_i = the daily water table depth below the soil surface (cm) and T = the length of the growing period (days). For example, a value of $SEW_{30} = 25$ could mean one day with a water table 5 cm below the soil surface or five days with a water table 25 cm below the soil surface. Generally, high SEW_{30} would indicate poor drainage or a long period with a shallow water table.

The depth of the water table has an effect not only on the quantity of water used but also on the determination of effective rainfall. Effective rainfall is defined as a rainfall that is temporarily stored in the soil without causing runoff and seepage to the groundwater. Effective rainfall is an important element used to estimate the needs for supplemental irrigation and drainage, and is primarily influenced by the rainfall amounts and temporal distributions, potential evapotranspiration rates, and soil hydraulic characteristics. The antecedent soil moisture also strongly affects the effective rainfall (Jones et al., 1984).

Most water table management systems are currently designed to hold the water level at a constant level from the soil surface with only minor changes in its position occurring due to diurnal variations in evapotranspiration. It is known that controlling the system such that the water table is allowed to fluctuate within prescribed limits could minimize runoff and excess drainage. In such a system, the water table would be allowed to fall due to evapotranspiration until it reaches a depth that could no longer supply adequate water to the root zone. At this point, the pump would be started and the water table raised to some maximum height that would not interfere with plant growth. Then, the pump would be turned off and the cycle repeated.

In recent years computer models have been developed to simulate the day-by-day performance of drainage and water table control systems. They range from very complex numerical solutions of differential equations to approximate methods for conducting a water balance in the soil profile. Many of these models have been field tested and provide means of describing the hydrology of shallow water table soils, including effects of drainage and related water management practices on yields.

The first computer simulation models were based on a water balance in the soil profile. An example is DRAINMOD which used functional algorithms to approximate the components of shallow water table soils (Skaggs, 1978). Approximate methods are used to simulate infiltration, drainage, surface runoff, evapotranspiration, and seepage processes on an hour-by-hour, day-by-day basis. An important feature of the model is the ability to provide information on the influence of excess and deficit water stresses on relative crop yields.

The water balance approach has also been used to develop other models. The ADAPT (Agricultural Drainage and Pesticide Transport) model (Chung et al., 1992) was developed by modifying the Groundwater Loading Effects of Agricultural Management Systems (GLEAMS) model (Leonard et al., 1987) and extending its use by adding drainage and subirrigation algorithms from DRAINMOD. The hydrology component of the ADAPT model includes snowmelt, surface runoff, macropore flow, evapotranspiration, infiltration, subsurface drainage, subirrigation and deep seepage.

Another approach used in water table management models is based on numerical solutions to the one-dimensional Richards equation for vertical flow. Lateral water movement due to drainage is evaluated using approximate equations that are imposed as

boundary conditions on the solutions to the Richards equation. The SWATRE model (Feddes et al., 1978; Belmans et al., 1983) is an example of this approach. SWATRE is a detailed root-water unsaturated flow model that does not need modifications to deal with water tables rising to the surface, but is limited in its capability to describe saturated flow for water table management systems, due to the use of approximate methods which cannot account for field heterogeneity (Havard, 1993).

The PREFLO model (Workman and Skaggs, 1990) also uses a finite difference solution to the one-dimensional Richards equation. The model simulates soil evaporation, plant transpiration, subsurface drainage, subirrigation, infiltration, and surface runoff. The PREFLO model uses the same input data and parameters as DRAINMOD, and the main difference between the two models is the computation of the soil water movement; PREFLO considers preferential flow through large cylindrical pores and subsequent infiltration from the large pores into the mass. Workman and Skaggs (1991) reported excellent agreement between water table simulated with PREFLO and DRAINMOD, and good agreement between PREFLO and field data in a five-year period of data record.

Direct comparison of ADAPT with the three models, DRAINMOD, SWATRE, and PREFLO showed that all models were capable of predicting water table depths with similar accuracy (Desmond et al., 1996). SWATRE and DRAINMOD are the most widely used water table management models in Europe and the United States, respectively. Several other models are listed in the literature, but generally are modifications or improvements of the models listed above.

Subsurface Drip Irrigation

Subsurface drip irrigation (SDI) is defined as “application of water below the soil surface through emitters, with discharge rates generally in the same range as surface drip irrigation” (ASAE, 1996). This method of water application should not be confused with subirrigation, which is defined by ASAE as “application of irrigation water below the ground surface by raising the water table to within or near the root zone”. However, the nomenclature in the literature is inconsistent yet, and commonly “subirrigation” is used to refer to both subsurface drip irrigation and subirrigation (water table management).

A major difference between surface and subsurface drip irrigation is that in the first case the emitter will always discharge water at atmospheric pressure. However, in the SDI case a positive pressure can be developed in the vicinity of the emitter. Extensive studies have been done to describe flow from surface drip irrigation, including analytical and quasi-analytical solutions (e.g., Philip, 1971; Zazueta et al., 1994), and numerical solutions (e.g., Zazueta et al., 1985; Lafolie et al., 1989). Few studies have been conducted to investigate flow from SDI. Philip (1968) developed a quasi-analytical solution for flow from a buried point source, but his solution was limited to steady state cases. Warrick (1974) developed a quasi-analytical solution for flow from a buried point source, considering transient flow. However, in his solution, he assumed the value of the hydraulic conductivity with respect to soil moisture to be constant, limiting the solution to cases where the value of soil moisture varies over a small range only. Examples of numerical models developed to describe flow from a SDI system are based on the steady-state form of the Richards equation in two dimensions (Gilley and Allred, 1974; Oron, 1981) or transient in three dimensions (Jnad et al., 1998).

The design of a SDI system requires the proper placement of the lateral line in the soil profile, i.e., adequate depth below the soil surface and spacing between the laterals. This placement depends upon the nature of the soil water movement and the soil water content extraction pattern of the irrigated crop. Specific guidelines for design, installation, and management for SDI systems are generally available from state extension offices, other government agencies, dealers, consultants, and manufacturers, and are often specific to the geographic or climatic region. Much information is currently available on web sites related to irrigation, or the interested person can post specific questions regarding the system in on-line groups of discussion.

SDI has been used in a large variety of crops, including cotton, corn, sugarcane, peanut, turfgrass, wheat, grain sorghum, alfalfa, tomato, vine crops, potato, etc. Camp (1998) presented an excellent summary of information reported for SDI systems on agronomic and horticultural crops, including comparison with other irrigation systems.

The primary objective of SDI systems is to apply water directly in or a little below the root zone to meet evapotranspiration requirements and minimize losses by deep percolation. However, in some conditions the system can be used as a source of water for water table management.

Clark et al. (1990) introduced the concept of a fully enclosed subirrigation (FES) system as a water application method for subirrigation purposes on Florida flatwoods soils. The FES system used drip irrigation tubing buried at 10 cm deep as water conveyance. They reported reduced runoff rates and reduced irrigation requirements with FES as compared to conventional semi-closed seepage irrigation systems for vegetable crops in south Florida.

Stanley and Clark (1991) and Clark and Stanley (1992) studied the feasibility of using FES (substituting for open lateral ditches) as a means of water conveyance for subirrigation. They reported that the application rates with FES represent a 30 - 40% water savings when compared to rates commonly used for ditch-conveyed seepage irrigation.

A feasibility study of FES was conducted by Smajstrla et al. (1998) in potatoes, in northeast Florida. The FES system was improved by automatically controlling the irrigation according to the depth of the water table to be maintained. They found a reduction of 36% in water applied with FES compared to ditch-conveyed seepage irrigation, in a three-year experiment without any change in crop yield.

CHAPTER 3 MODEL DEVELOPMENT

The development of the computer model used in this dissertation is described in this chapter. Each component of the model, its representation, the methods of solution and the structure of computer program, are described.

Two-Dimensional Model Development

The water pressure –based form of the Richards equation (2.9) was used in this study because it is more useful for problems involving flow in layered or spatially heterogeneous soils, as well as for variably saturated flow problems. The assumptions employed in the development of the numerical model also were listed in Chapter 2.

A totally implicit scheme was chosen to solve the independent variable h , and linearization (estimation of $C(h)$ and $K(h)$ in time) was obtained by considering C and K constant during Δt and equal to their values calculated at the preceding time step. Any weighting method (arithmetic, geometric, harmonic, etc.) can be used to estimate $K(h)$ over space. The linearized equation was solved by a Gaussian elimination method.

The two-dimensional flow domain was divided utilizing a block centered finite difference grid. The pressure head was evaluated at nodes located at the center of each block. The spatial increments in the x (horizontal) and in the z (vertical) directions were indicated by Δx and Δz . The index j ($j = 1, 2, \dots, J$) was used to number the nodes in the vertical direction, and the index i ($i = 1, 2, \dots, I$) was used to number the nodes in the horizontal direction (Fig. 3-1).

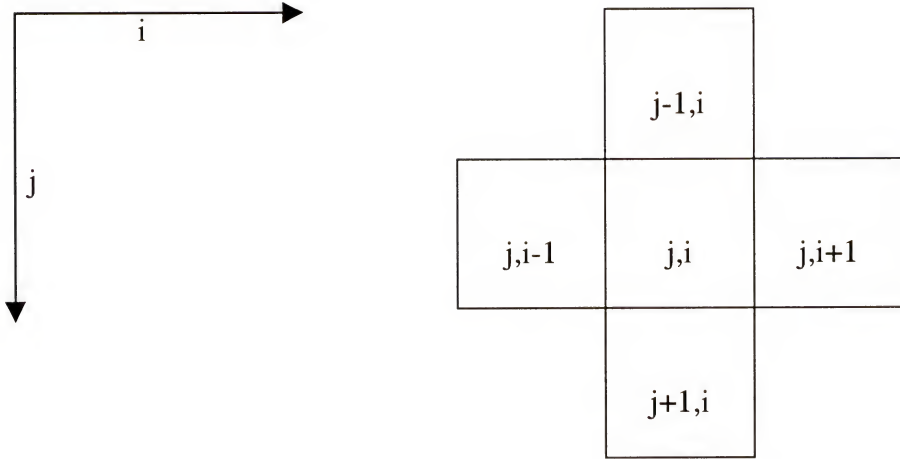


Figure 3-1: Grid system for finite difference two-dimensional model after discretizing equation (2.9). Nodes are located at the centroid of the cells.

The finite difference approximation of equation (2.9) was obtained by discretizing the right hand side of (2.9) as

$$\frac{\partial}{\partial x} \left[K_x(h) \left(\frac{\partial h}{\partial x} \right) \right] = \frac{1}{\Delta x} \left\{ \left[K_{j,i+\frac{1}{2}} \left(\frac{\partial h}{\partial x} \right)_{j,i+\frac{1}{2}} \right] - \left[K_{j,i-\frac{1}{2}} \left(\frac{\partial h}{\partial x} \right)_{j,i-\frac{1}{2}} \right] \right\} \quad (3.1)$$

and

$$\frac{\partial}{\partial z} \left[K_z(h) \left(\frac{\partial h}{\partial z} - 1 \right) \right] = \frac{1}{\Delta z} \left\{ \left[K_{j+\frac{1}{2},i} \left(\frac{\partial h}{\partial z} - 1 \right)_{j+\frac{1}{2},i} \right] - \left[K_{j-\frac{1}{2},i} \left(\frac{\partial h}{\partial z} - 1 \right)_{j-\frac{1}{2},i} \right] \right\} \quad (3.2)$$

For simplicity, the parameters $K(h)$ were represented by K . The derivatives of h with respect to x and z were approximated by

$$\left(\frac{\partial h}{\partial x} \right)_{j,i+\frac{1}{2}} = \frac{h_{j,i+1} - h_{j,i}}{\Delta x} \quad (3.3)$$

$$\left(\frac{\partial h}{\partial z} \right)_{j,i-\frac{1}{2}} = \frac{h_{j,i} - h_{j,i-1}}{\Delta z} \quad (3.4)$$

$$\left(\frac{\partial h}{\partial z} - 1 \right)_{j+\frac{1}{2},i} = \frac{h_{j+1,i} - h_{j,i}}{\Delta z} - 1 \quad (3.5)$$

$$\left(\frac{\partial h}{\partial z} - 1 \right)_{j-\frac{1}{2},i} = \frac{h_{j,i} - h_{j-1,i}}{\Delta z} - 1 \quad (3.6)$$

which when substituted back into equations (3.1) and (3.2) gave

$$\frac{\partial}{\partial x} \left[K_x \left(\frac{\partial h}{\partial x} \right) \right] = \frac{1}{\Delta x} \left\{ \left[K_{j,i+\frac{1}{2}} \left(\frac{h_{j,i+1} - h_{j,i}}{\Delta x} \right) \right] - \left[K_{j,i-\frac{1}{2}} \left(\frac{h_{j,i} - h_{j,i-1}}{\Delta x} \right) \right] \right\} \quad (3.7)$$

and

$$\frac{\partial}{\partial z} \left[K_z \left(\frac{\partial h}{\partial z} - 1 \right) \right] = \frac{1}{\Delta z} \left\{ \left[K_{j+\frac{1}{2},i} \left(\frac{h_{j+1,i} - h_{j,i}}{\Delta z} - 1 \right) \right] - \left[K_{j-\frac{1}{2},i} \left(\frac{h_{j,i} - h_{j-1,i}}{\Delta z} - 1 \right) \right] \right\} \quad (3.8)$$

Equations (3.7) and (3.8) represent the horizontal and vertical flows, respectively.

The implicit formulation of (2.9) was obtained by substituting back equations (3.7) and (3.8) into (2.9) and evaluating water pressure at the $n+1$ time level. The time derivative in equation (2.9) was then replaced by a backward-difference approximation relative to the $n+1$ time level. For simplicity, parameters $C(h)$ and $S(h)$ were expressed as C and S . The result is a two-dimensional finite difference equation for flow through a porous medium expressed as

$$\begin{aligned} C_{j,i}^n \frac{h_{j,i}^{n+1} - h_{j,i}^n}{\Delta t} &= \frac{1}{\Delta x} \left\{ \left[K_{j,i+\frac{1}{2}}^n \left(\frac{h_{j,i+1}^{n+1} - h_{j,i}^{n+1}}{\Delta x} \right) \right] - \left[K_{j,i-\frac{1}{2}}^n \left(\frac{h_{j,i}^{n+1} - h_{j,i-1}^{n+1}}{\Delta x} \right) \right] \right\} \\ &+ \frac{1}{\Delta z} \left\{ \left[K_{j+\frac{1}{2},i}^n \left(\frac{h_{j+1,i}^{n+1} - h_{j,i}^{n+1}}{\Delta z} - 1 \right) \right] - \left[K_{j-\frac{1}{2},i}^n \left(\frac{h_{j,i}^{n+1} - h_{j-1,i}^{n+1}}{\Delta z} - 1 \right) \right] \right\} - S_{j,i}^n \end{aligned} \quad (3.9)$$

Equation (3.9) was then rearranged so that the unknown parameters were on the left hand side and the known parameters were on the right hand side. In a more useful form the equation can be expressed as

$$A_{j,i}h_{j-1,i}^{n+1} + B_{j,i}h_{j,i-1}^{n+1} + D_{j,i}h_{j,i}^{n+1} + E_{j,i}h_{j,i+1}^{n+1} + F_{j,i}h_{j+1,i}^{n+1} = R_{j,i} \quad (3.10)$$

where

$$A_{j,i} = -\frac{K_{j-\frac{1}{2},i}^n}{\Delta z^2} \quad (3.11)$$

$$B_{j,i} = -\frac{K_{j,i-\frac{1}{2}}^n}{\Delta x^2} \quad (3.12)$$

$$D_{j,i} = \frac{C_{j,i}^n}{\Delta t} - A_{j,i} - B_{j,i} - E_{j,i} - F_{j,i} \quad (3.13)$$

$$E_{j,i} = -\frac{K_{j,i+\frac{1}{2}}^n}{\Delta x^2} \quad (3.14)$$

$$F_{j,i} = -\frac{K_{j+\frac{1}{2},i}^n}{\Delta z^2} \quad (3.15)$$

$$R_{j,i} = \frac{C_{j,i}^n}{\Delta t} h_{j,i}^n + \frac{K_{j-\frac{1}{2},i}^n - K_{j+\frac{1}{2},i}^n}{\Delta z} - S_{j,i}^n \quad (3.16)$$

Equation (3.10) was written for each of the interior nodes in the soil profile. The grids bordering the boundaries required equation (3.10) to be modified so that the equation would describe the boundary conditions.

Initial Conditions

The solution to equation (3.10) requires that initial values of h be specified everywhere in the solution domain:

$$h(x, z, t) = h_0(x, z) \quad \text{for } t=t_0 \quad (3.17)$$

where h_0 is a prescribed function of (x, z) and t_0 is the time when the simulation begins. Although $h_0(x, z)$ can be any arbitrary function, the initial conditions usually represent some type of steady state or equilibrium. If initial conditions are used that do not represent steady state, any simulation results will include transient effects from the difference between the specified initial conditions and equilibrium conditions.

Boundary Conditions

Solutions to equation (3.10) require boundary conditions that specify either the flux of liquid across the boundary, the water pressure along the boundary, or some combination of specified head and specified flux.

Top Surface Boundary

A flux boundary condition was employed for the surface grids to represent infiltration by precipitation. To describe the top surface boundary for the nodes $2 \leq i \leq I-1$ at $j = 1$, equation (3.10) was modified to

$$B_{j,i}h_{j,i-1}^{n+1} + D_{j,i}h_{j,i}^{n+1} + E_{j,i}h_{j,i+1}^{n+1} + F_{j,i}h_{j+1,i}^{n+1} = R_{j,i} \quad (3.18)$$

where

$$D_{j,i} = \frac{C_{j,i}^n}{\Delta t} - B_{j,i} - E_{j,i} - F_{j,i} \quad (3.19)$$

$$R_{j,i} = \frac{C_{j,i}^n}{\Delta t} h_{j,i}^n + \frac{QS_i - K_{j+\frac{1}{2},i}^n}{\Delta z} - S_{j,i}^n \quad (3.20)$$

$QS(i)$ is the surface flux (LT^{-1}) and $B_{j,i}$, $E_{j,i}$ and $F_{j,i}$ are as previously defined.

Bottom Surface Boundary

Vertical drainage across the lower boundary of the soil profile was approximated by a flux that depended on the position of the water table level. The bottom boundary condition consisted of a prescribed drainage flux-water table relationship, $QB(h)$, as given by Hopmans and Stricker (1989):

$$QB(h) = ae^{b|h|} \quad (3.21)$$

where a and b are parameters determined from calibration of QB and h . This type of boundary condition suggests that there is at all times some downward flux leaving the soil water system at the bottom, although its magnitude can be very small as compared to the upward flux.

The modification of equation (3.10) to describe the lower boundary for the nodes $2 \leq i \leq I-1$ at $j = J$ was

$$A_{j,i} h_{j-1,i}^{n+1} + B_{j,i} h_{j,i-1}^{n+1} + D_{j,i} h_{j,i}^{n+1} + E_{j,i} h_{j,i+1}^{n+1} = R_{j,i} \quad (3.22)$$

where

$$D_{j,i} = \frac{C_{j,i}^n}{\Delta t} - A_{j,i} - B_{j,i} - E_{j,i} \quad (3.23)$$

$$R_{j,i} = \frac{C_{j,i}^n}{\Delta t} h_{j,i}^n + \frac{K_{j-\frac{1}{2},i}^n - QB(i)}{\Delta z} - S_{j,i}^n \quad (3.24)$$

$QB(i)$ is the bottom flux (LT^{-1}) for each node that fell on the lower boundary, and $A_{j,i}$, $B_{j,I}$, and $E_{j,i}$ are as previously defined.

Left Surface Boundary

The left boundary of the grid was defined as a plane of symmetry that passed through the center of the field. Usually, in this situation there is no flux across a plane of symmetry, so this boundary was simulated with a no-flux boundary condition. To describe the left surface boundary for the nodes $2 \leq j \leq J-1$ at $i = 1$, equation (3.10) was modified to

$$A_{j,i}h_{j-1,i}^{n+1} + D_{j,i}h_{j,i}^{n+1} + E_{j,i}h_{j,i+1}^{n+1} + F_{j,i}h_{j+1,i}^{n+1} = R_{j,i} \quad (3.25)$$

where

$$D_{j,i} = \frac{C_{j,i}^n}{\Delta t} - A_{j,i} - E_{j,i} - F_{j,i} \quad (3.26)$$

and $A_{j,i}$, $E_{j,i}$, $F_{j,i}$, and $R_{j,i}$ are as previously defined.

Right Surface Boundary Condition

The last column of cells at the right boundary of the grid ($I = IX$) represented the center of the water furrow and was simulated as a pressure head boundary condition. There are two cases to consider:

1. Cells that make part of the water furrow: these cells were treated as constant pressure head cells to represent the open furrow (atmospheric cells, $h=-1000$ cm). A very simple equation was used to represent these cells:

$$D_{j,i}h_{j,i}^{n+1} = R_{j,i} \quad (3.27)$$

where

$$D_{j,i} = \frac{C_{j,i}^n}{\Delta t} \quad (3.28)$$

$$R_{j,i} = \frac{C_{j,i}^n}{\Delta t} h_{j,i}^n \quad (3.29)$$

2. Cells below water furrow: these cells were treated differently depending if the condition for runoff had been reached. When the water level at the water furrow reached the maximum allowed, runoff would begin and the water pressure at these cells was maintained constant in equilibrium with the water level. In this case, a lateral flux between adjacent cells ($I = IX-1$ and $I = IX$) occurred because the water table level inside the soil profile continued to rise and there was a water pressure gradient toward the water furrow. If the condition for runoff was not reached, the cells were assigned to the same water pressure value as the adjacent grid ($I = IX-1$) and there was no lateral flux between the adjacent cells. At the right side of the last column of cells ($I = IX$) there was no flux because of another plane of symmetry that passed by at the center of the water furrow.

In both cases above, equation (3.27) was applied. This boundary was very demanding to develop because of its peculiarities. It was tested against literature data for this kind of boundary (see examples in the Chapter 4) and was shown very successful.

Seepage Surface Boundary

Seepage occurred at the face of the water furrow ($I = IX-1$). When the level of water at the furrow was not enough to cause runoff, there was no seepage because the

cells at the last two columns of the grid were in equilibrium (anterior condition). When runoff occurred, the flux at the cells below the bottom of the water furrow was calculated by Darcy's equation, and the seepage at the cells above the bottom of the water furrow was set to the value of the incoming flux from the soil profile (flux at left side of I = IX - 1). In both cases, the equation used to represent this boundary was

$$A_{j,i}h_{j-1,i}^{n+1} + B_{j,i}h_{j,i-1}^{n+1} + D_{j,i}h_{j,i}^{n+1} + F_{j,i}h_{j+1,i}^{n+1} = R_{j,i} \quad (3.30)$$

where

$$D_{j,i} = \frac{C_{j,i}^n}{\Delta t} - A_{j,i} - B_{j,i} - F_{j,i} \quad (3.31)$$

$$R_{j,i} = \frac{C_{j,i}^n}{\Delta t} h_{j,i}^n + \frac{K_{j-\frac{1}{2},i}^n - K_{j+\frac{1}{2},i}^n}{\Delta z} - \frac{QR(j)}{\Delta x} - S_{j,i}^n \quad (3.32)$$

and $QR(j)$ was the flux out of the system (seepage).

Surface Runoff

Surface runoff occurred when the water table level reached some distance below the surface of the grid. This was done because the grid used in the model was different from the geometry of the field. The model used a flat top surface that corresponded to the middle section of the beds in the field (Figure 3-2). Then, the surface runoff was calculated when $h_{j,i} > 0$ at the position that corresponded to the bottom of the beds in the field. The "surface runoff" was then calculated by a very simple statement: if the condition established for surface runoff was satisfied at the determined column of cells, the surface infiltration at that grid (precipitation) was considered as runoff and $QS(i) = 0$ at the current time step. For the next time step, infiltration could occur again and then

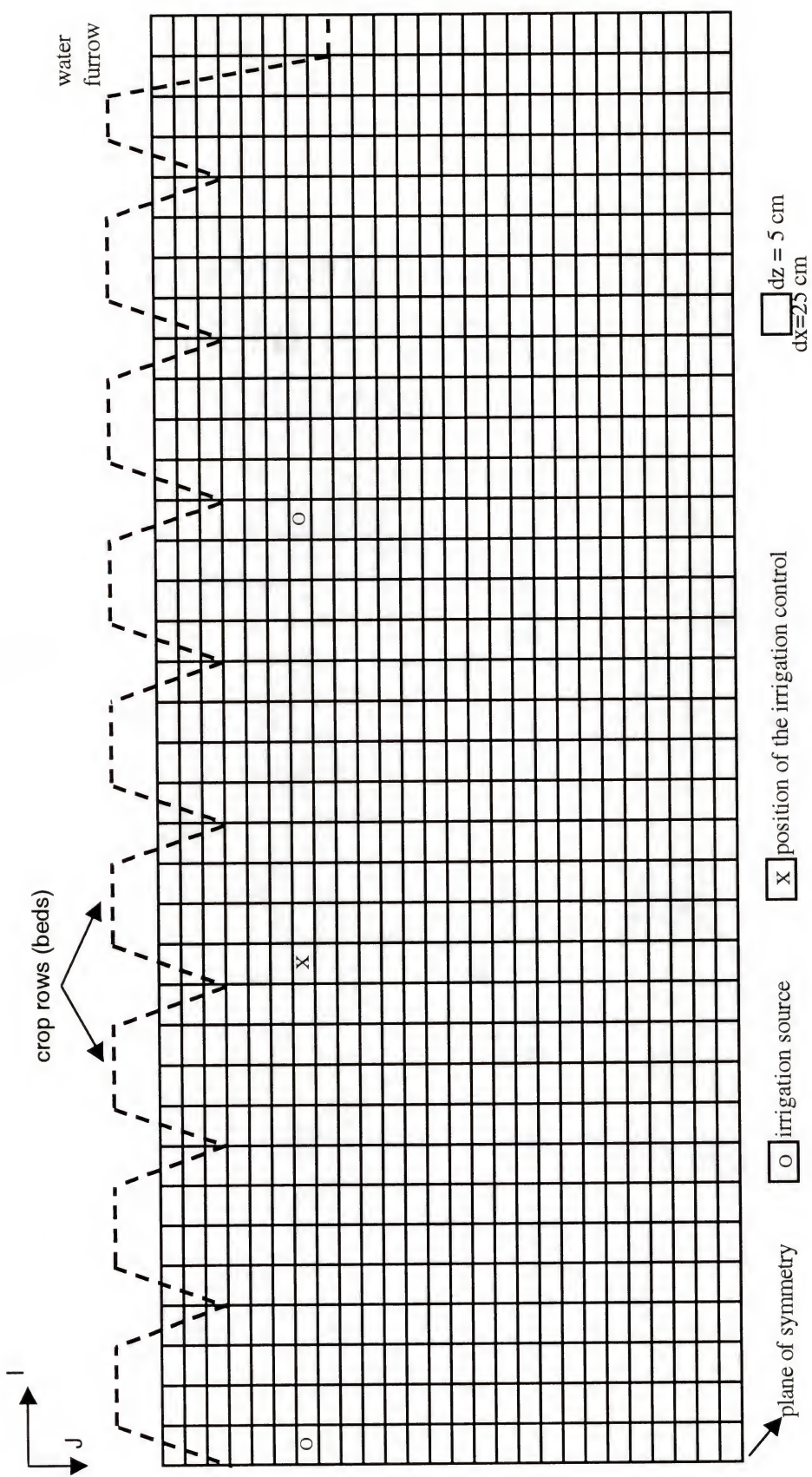


Figure 3-2. Finite difference grid for the field problem.

successively for later time steps. There was very little variation (positive and negative) around $h_{j,i} = 0$ when this procedure was adopted, maybe reflecting what occurs in the field where infiltration and runoff are not steady state processes. It was not necessary to modify the equation and runoff are not steady state processes. It was not necessary to modify the equation used for the nodes at the row where surface runoff occurred and the same equation for interior nodes (eq. 3.10) was used. In reality, the only modification necessary was to set $QS(i) = 0$ at the top surface boundary (eq. 3.20).

Irrigation

The subirrigation with buried microirrigation line sources was simulated by placing two irrigation lines at the depth corresponding to the depth in the field (Figure 3-2). One of the irrigation lines was placed at the line of symmetry ($I=1$), so that only half of the flux from the line was considered to enter in the simulated soil profile. The irrigation flux was included as source at the nodes where the lines were placed, as suggested by Jnad et al. (1998). The equations used to solve h for these irrigating nodes were equation (3.10) for the interior node with the modification

$$R_{j,i} = \frac{C_{j,i}^n}{\Delta t} h_{j,i}^n + \frac{K_{j-\frac{1}{2},i}^n - K_{j+\frac{1}{2},i}^n}{\Delta z} - S_{j,i}^n + \frac{QIRR}{\Delta Z} \quad (3.33)$$

and equation (3.25) for the node at the line of symmetry with the modification

$$R_{j,i} = \frac{C_{j,i}^n}{\Delta t} h_{j,i}^n + \frac{K_{j-\frac{1}{2},i}^n - K_{j+\frac{1}{2},i}^n}{\Delta z} - S_{j,i}^n + \frac{1}{2} \frac{QIRR}{\Delta Z} \quad (3.34)$$

where QIRR was the irrigation flux (LT^{-1}).

In the experimental field, controllers installed at the mid-point between irrigation lines turned the irrigation system on or off in order to maintain the water table at an

established depth. In the model, an irrigation control was simulated by assigning a node-control, where the water table was allowed to fluctuate in depth; if the position of the water level was above the range of fluctuation the irrigation was turned off, and if the water level was below that range the irrigation was turned on. Because of the rainfall events, when the system in the field was turned off manually and the water table was allowed to drop below the depth-control after the rain, it was also necessary to establish periods when the irrigation system was turned off during the simulations, even though the water level was below the range of control. More details about irrigation management are presented in Chapter 5.

Corner Nodes

Because the four cells found in each of the corners of the two-dimensional grid were influenced by two boundaries, special equations had to be written for them. They were derived by evaluating equation (3.10) at the appropriate nodes (1,1), (J,1), (1,I), and (J,I).

Time Step Update

Although the time step $\Delta t = t_{n+1} - t_n$ could be assigned arbitrarily, its value in this model was determined according to a self-adjusting algorithm. The time step was taken as variable and was explicitly estimated as proposed by Belmans et al. (1983):

$$\Delta t^{n+1} = \frac{\Delta \theta_{\max}}{\left(\Delta \theta / \Delta t\right)_{\max}^n} \quad (3.35)$$

where a specific value for $\Delta \theta_{\max}$ was assigned.

The empirically obtained range of this value was based on a number of computed flow cases, which were rather different in type of soil and magnitude of fluxes. Belmans et al. (1983) recommended that $0.002 \leq \Delta\theta_{max} \leq 0.03$. Values below this range result in increasing computing times with only a slight improvement of the water balance. Values above the range result in poor water balances.

The denominator of equation (3.35) was obtained from the equation

$$\left(\frac{\Delta\theta}{\Delta t}\right)_{max}^n = \text{Max} \left[S(j,i) + SINK(j,i) + \left| \frac{\Delta q_z(j,i)}{\Delta z} + \frac{\Delta q_x(j,i)}{\Delta x} \right| \right] \quad (3.36)$$

where $S(i,j)$ is the extraction term, $SINK(j,i)$ is a sink term (if existing), and $q_x(j,i)$ and $q_z(j,i)$ are the fluxes through the boundaries of the node.

The time step Δt^{n+1} as calculated from equations (3.35) and (3.36) was restricted by three additional conditions: (1) a maximum was prescribed; (2) a minimum was prescribed; and (3) $\Delta t^{n+1} \leq 1.2 \Delta t^n$.

Grid Size

Proper spatial discretization of the flow domain is crucial for achieving maximum accuracy and numerical stability in numerical solutions, either by finite difference or finite element. The number and location of nodal points in the flow domain is usually a compromise between criteria of accuracy, stability, and computational efficiency (Vogel et al. 1996). For example, a very fine spatial grid (i.e., having a large number of very small elements) could dramatically increase the CPU time, but may not always improve the numerical results.

The influence of finite difference grid size on soil water flow model accuracy has been studied. Amerman and Monke (1977) presented a review of works on the subject,

and also studied the effect of the grid size in different conditions of simulations. They concluded that there is no computational advantage gained by modeling a large cross section with a geometrically similar smaller one because, when using a finite difference technique, both required about the same number of nodes. Also, the authors concluded that: 1) Spatial grid spacing was a function of curvature of equipotential lines and of the spatial rate of change of hydraulic gradient in the direction of flow, and 2) Computational savings could be realized with very little loss of accuracy by designing an irregular mesh where the smallest grid sizes were used in regions of the expected sharpest curvature of equipotentials or greatest rate of change of gradient; larger grid sizes might be used elsewhere.

In this work, a uniform size in each direction was used (Figure 3-2).

Estimation of Internode Hydraulic Conductivity

When node-centered finite difference discretization schemes are used, as in this model, it is necessary to average the conductivity terms for adjacent nodes to develop internodal conductivities. Various methods of estimation have been proposed and compared in the finite difference framework (Haverkamp and Vauclin, 1979; Schnabel and Richie, 1984; Warrick, 1991).

Haverkamp and Vauclin (1979) used nine different methods of weighting internodal hydraulic conductivity values in studying two test problems using different types of soil and boundary conditions. Some of their weighting schemes were:

1. *Arithmetic mean*

$$K_{i\pm\frac{1}{2}} = 0.5(K_i + K_{i\pm1}) \quad (3.37)$$

2. *Harmonic mean*

$$K_{i\pm\frac{1}{2}} = \frac{2K_i K_{i\pm 1}}{K_i + K_{i\pm 1}} \quad (3.38)$$

3. *Geometric mean*

$$K_{i\pm\frac{1}{2}} = (K_i K_{i\pm 1})^{\frac{1}{2}} \quad (3.39)$$

4. *Upstream mobility* concept, where the conductivity of the grid cell from which the fluid originates is used. In cases where the flow is originating from upstream grids

$$K_{i+\frac{1}{2}} = K_i \quad \text{and} \quad K_{i-\frac{1}{2}} = K_{i-1} \quad (3.40)$$

Haverkamp and Vauclin (1979) found that the geometric mean was the only method that generated little weighting error. The accuracy of their model using this method was affected negligibly by the changing of space increments. This was confirmed not only for an exact analytical case, but also under experimental conditions. As a consequence, the model using the geometric mean as a weighting relation was found preferable in terms of flexibility, precision, and feasibility for simulating transient water flow in partially saturated soil. Because of this, in the model used in this work, geometric mean was chosen to represent the internodal hydraulic conductivity. However, an option for using the arithmetic method has been included in the model in such a way that either one can be specified at every nodepoint.

Evaluation of the Soil Hydraulic Properties

The soil hydraulic properties water content, $\theta(h)$, unsaturated hydraulic conductivity, $K(h)$, and soil water capacity, $C(h)$ were evaluated at the end of each time

step from equations (2.12), (2.14), and (2.15). An option to read the parameter values from tables generated prior to simulation is not presented in this model, but it can be implemented easily by adding one subroutine to the computer code.

Water Uptake by Plant Roots

This model considers a root distribution term to determine the fraction of the total water use extracted from each node in the finite difference grid.

A macroscopic extraction function developed by Smajstrla (1982) (equation 2.18), and modified by Stone (1987), was used. The extraction function was

$$S_{j,i} = ET_r * A_t * RDT_{j,i} * R_{j,i}^{(ET_r/C/R_{j,i})} \quad (3.41)$$

where

$S_{j,i}$ = soil water extraction rate ($L^3 T^{-1}$),

ET_r = evapotranspiration rate (LT^{-1}),

$RDT_{j,i}$ = root distribution term or the percentage of water extraction for the soil cell,

A_t = total surface area of the grid (L^2),

$R_{j,i}$ = relative available soil water content, given by equation (2.19), and

C = calibration constant.

The evapotranspiration rate, ET_r , in equation (3.41) was calculated by distributing the daily crop evapotranspiration over a 24-hr period. A sinusoidal type distribution, as used with success by Vellidis (1989), was selected and given by

$$ET_r = \frac{ET}{T_{cycle}} \left[1 + \sin \left(\frac{2\pi T_{day}}{T_{cycle}} - \frac{\pi}{2} \right) \right] \quad (3.42)$$

where

- ET_r = predicted evapotranspiration rate (LT^{-1}),
- ET = daily crop evapotranspiration (LT^{-1}),
- T_{cycle} = the period of the cycle (hr), in this case 24 hr, and
- T_{day} = the current time on the 24-hr clock minus the beginning time of the cycle (hr).

Equation (3.41) was used to calculate the water extraction rate from each cell at every time step. To make sure that the total water extraction calculated matched the actual ET_r , a comparison between the two values was done, and if necessary, the calculated water extraction for each cell was adjusted by

$$S_{j,i} = S_{j,i} \frac{ET_r * A_t}{\sum S_{j,i}} \quad (3.43)$$

Finally, to be consistent with the units in equation (3.10) $S_{j,i}$ was converted in units of T^{-1} , by

$$S_{j,i} = \frac{S_{j,i}}{dz * dx * dy} \quad (3.44)$$

where dz , dx , and dy are the dimensions of the node (L), with $dy = 1$ unit of length.

Solution of the Two-Dimensional Model

The system of equations for the two-dimensional model produced a banded matrix equation with 5 nonzero diagonals. An example of the matrix equation for a 3x3 mesh is given by

$$\begin{array}{cccccc|c|c}
 D_{1,1} & E_{1,1} & 0 & F_{1,1} & & & h(1,1) & R(1,1) \\
 B_{1,2} & D_{1,2} & E_{1,2} & 0 & F_{1,2} & & h(1,2) & R(1,2) \\
 0 & B_{1,3} & D_{1,3} & 0 & 0 & F_{1,3} & h(1,3) & R(1,3) \\
 A_{2,1} & 0 & 0 & D_{2,1} & E_{2,1} & 0 & F_{2,1} & h(2,1) & R(2,1) \\
 A_{2,2} & 0 & B_{2,2} & D_{2,2} & E_{2,2} & 0 & F_{2,2} & h(2,2) & R(2,2) \\
 & A_{2,3} & 0 & B_{2,3} & D_{2,3} & 0 & 0 & F_{2,3} & h(2,3) & R(2,3) \\
 & A_{3,1} & 0 & 0 & D_{3,1} & E_{3,1} & 0 & h(3,1) & R(3,1) \\
 & A_{3,2} & 0 & B_{3,2} & D_{3,2} & E_{3,2} & 0 & h(3,2) & R(3,2) \\
 & A_{3,3} & 0 & B_{3,3} & D_{3,3} & 0 & 0 & h(3,3) & R(3,3)
 \end{array} = \begin{array}{c}
 h(1,1) \\
 h(1,2) \\
 h(1,3) \\
 h(2,1) \\
 h(2,2) \\
 h(2,3) \\
 h(3,1) \\
 h(3,2) \\
 h(3,3)
 \end{array} \quad (3.45)$$

An algorithm was used to solve a large, sparse matrix with a narrow band centered on the main diagonal. The algorithm operates only on the banded part of the matrix and does not require computer storage for the elements above or below the band; it has been used to solve two-dimensional water flow models with success (Stone, 1987; Vellidis, 1989).

A computer program was written in ANSI FORTRAN 90 to execute the mathematical model presented here and designed to run on personal computers. The program organization, description of program units, and list of significant variables are presented in Appendix A and the program code is presented in Appendix B.

Mass Balance Computation

The model code calculates a water balance at the end of each time step for the entire flow domain. The accuracy of the mass balance in the numerical solution is determined by means of the relative error, as follows

$$\varepsilon_r = 100 \frac{\varepsilon_a}{V} \quad [\%] \quad (3.46)$$

where ε_a is the absolute error in the water balance as given by

$$\varepsilon_a = V_0 + \sum_0^t I - \sum_0^t O - V_t \quad (3.47)$$

in which V_0 and V_t are the volumes of mobile water in the flow domain at the initial and current times, respectively. The second term on the right-hand side represents the cumulative inflow to the flow domain (precipitation and irrigation), while the third term gives the cumulative outflow from the flow domain (root extraction, runoff, seepage, and deep percolation). All the terms are in units of volume. The term V in the denominator of (3.46) represents the total volume of water in the flow domain given by

$$V = V_0 + \sum_0^t I \quad (3.48)$$

The mass balance was printed at prescribed times defined by the user.

CHAPTER 4 MODEL TESTING

The accuracy of the model in simulating infiltration and redistribution of soil water was determined by comparison with other computer simulations from the literature. The comparisons were selected to test the applicability and accuracy of the model with soils that had widely varying hydraulic properties.

Infiltration in a Large Caisson

The first example was taken from the one-dimensional HYDRUS code (Vogel et al. 1996). The example considers transient infiltration of water in a large caisson. The soil was assumed to be at a uniform initial water content of 10% volume. Hydraulic parameters of the soil are listed in Table 4-1. In the simulation, the caisson was wetted by applying water by ponding. The bottom boundary consisted of free drainage with a unit hydraulic gradient. For the flow simulation, the 6 m deep caisson was discretized into 120 cells of uniform size, leading to a cell size of 5 cm. As shown in Figure 4-1, results for the two simulations agreed very well.

Table 4-1: Soil hydraulic parameters of crushed Bandelier Tuff used in the caisson flow example.

Hydraulic Parameter	Unit	Value
θ_s	$(\text{cm}^3 \text{cm}^{-3})$	0.3308
θ_r	$(\text{cm}^3 \text{cm}^{-3})$	0.0000
α	cm^{-1}	0.01433
n	-	1.506
K_s	cm hr^{-1}	25.0

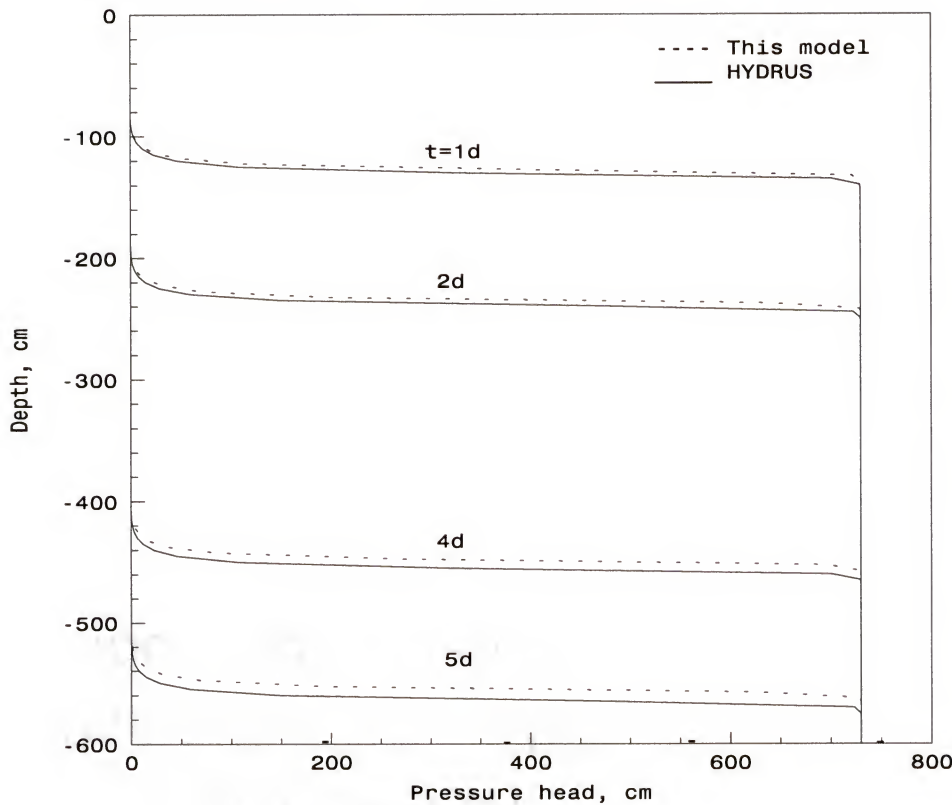


Figure 4-1: Predicted water pressure head during transient infiltration in Bandelier Tuff.

Water Movement in a Cropped Soil Profile

The second example considers water movement in a cropped field profile in the Hupselse Beek watershed of the Netherlands. Atmospheric data and observed ground water levels provided the required boundary conditions for the numerical model. Calculations were performed for the period of April 1 to September 30 of the relatively dry year 1982. Parts of this problem were previously simulated using the SWATRE (Feddes et al., 1978; Belmans et al., 1983), SWMS_2D (Šimunek et al., 1994) and HYDRUS (Vogel et al. 1996) computer programs.

The soil profile consisted of two layers: a 40-cm thick A-horizon, and a B/C-horizon that extended to a depth of about 300 cm. The depth of the root zone was 30 cm. The mean scaled hydraulic parameters of the two soil layers are listed in Table 4-2.

Table 4-2: Soil hydraulic parameters for the second example.

Parameter	1 st layer	2 nd layer
θ_s (cm ³ cm ⁻³)	0.399	0.339
θ_r (cm ³ cm ⁻³)	0.0001	0.0001
α (cm ⁻¹)	0.0174	0.0139
n (-)	1.3757	1.6024
K_s (cm hr ⁻¹)	1.242	1.892

The soil surface boundary conditions involved actual precipitation and potential transpiration rates for a grass cover. The surface fluxes were incorporated by using average daily rates distributed uniformly over each day. The bottom boundary consisted of a prescribed drainage flux-groundwater level relationship as used in this work. In this example, the relationship was given by

$$q(h) = -0.1687 \exp(-0.02674|h - 230|) \quad (4.1)$$

where q is the drainage flux (cm/day) and h is the pressure at the bottom boundary (cm).

The groundwater level was initially set at 55 cm below the soil surface. The initial moisture profile was taken to be in equilibrium with the initial ground water level. Figure 4-2 presents the pressure head at the soil surface as simulated with HYDRUS and this work. Simulated water content at selected times is presented in Figure 4-3. Finally, Figure 4-4 shows variations in the calculated groundwater level with time. In all cases, simulations with the two computer models agreed very well.

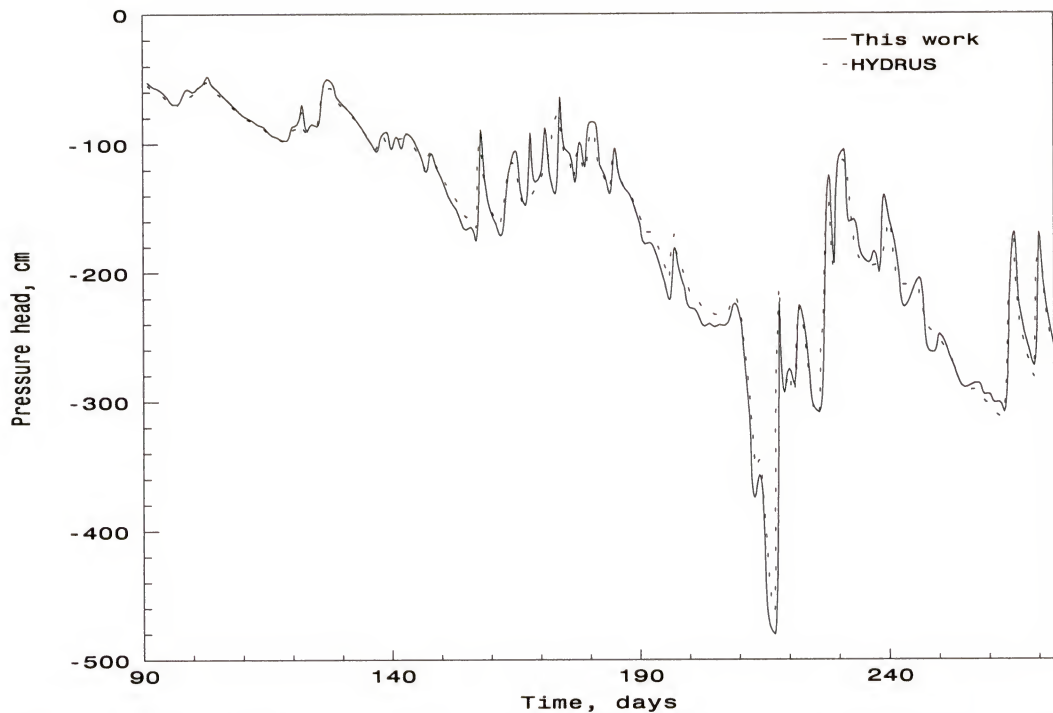


Figure 4-2: Simulated pressure heads at the surface for the second example, as simulated with HYDRUS and this work.

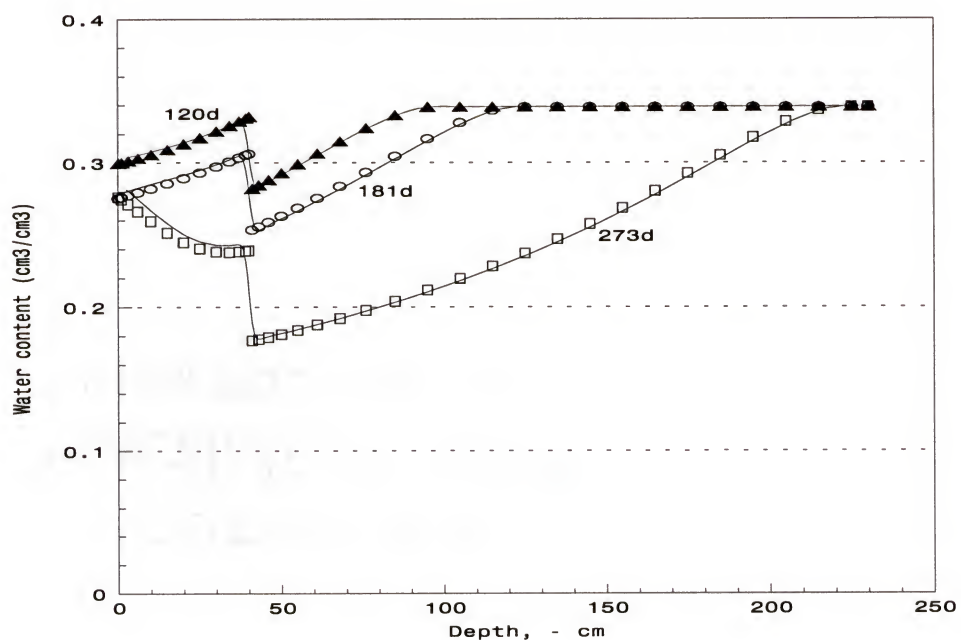


Figure 4-3: Simulated water content at selected times (days) with HYDRUS (symbols) and this work (lines) for the second example.

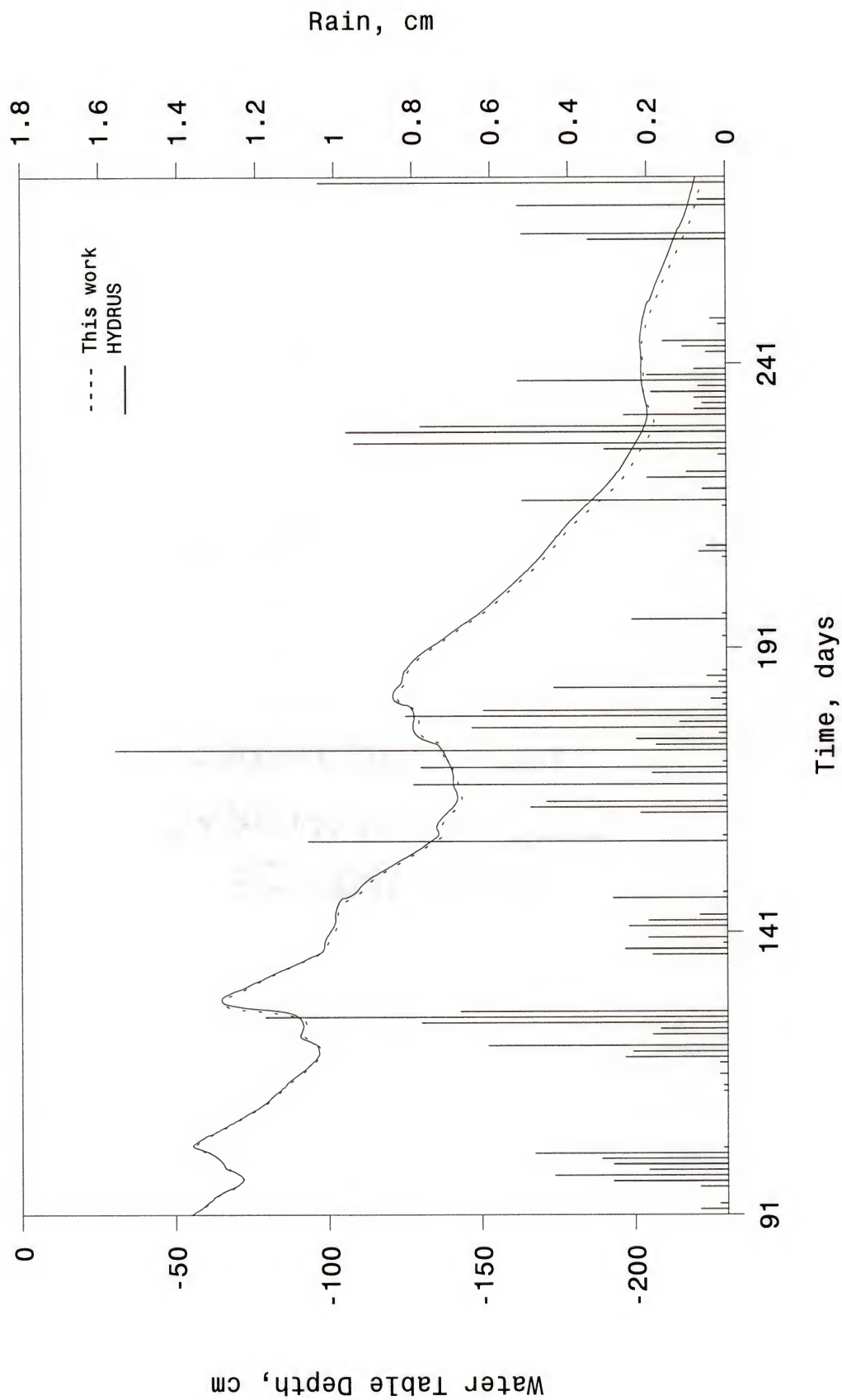


Figure 4-4: Precipitation and location of the water table level for the second example, as simulated with the HYDRUS and this work computer programs.

Transient, Two-Dimensional, Variably Saturated Water Table Recharge

This example was selected to verify the performance of the numerical model for a two-dimensional, transient, variably saturated flow condition. The experiment has been presented in detail by Vauclin et al.(1979). The same example was used by Clement et al. (1994) to verify their two-dimensional variably saturated model and by Dogan (1999) to verify his three-dimensional variably saturated model.

The flow domain consisted of a rectangular slab of soil, 300 cm long x 200 cm deep. The vertical right-hand side of the slab was connected to a constant head reservoir to maintain the water level constant at a depth of 135 cm at this side. At the soil surface a constant flux of 14.8 cm/hr was applied over the left 50 cm of the top of the modeled domain. The remaining soil surface at the top, the left-hand side and the bottom of the slab were no-flow boundaries. A water table was imposed at the depth of 135 cm and the experiment began when hydrostatic equilibrium was obtained throughout the flow domain.

The van Genuchten (1980) model was fitted to the soil hydraulic parameters given by Vauclin et al. (1979) (Table 4-3). The nodal spacings in the x and z directions were 10 cm and 5 cm, respectively.

Table 4-3: Soil hydraulic parameters used in the third example.

Hydraulic parameter	Unit	Value
θ_s	$\text{cm}^3 \text{cm}^{-3}$	0.30
θ_r	$\text{cm}^3 \text{cm}^{-3}$	0.01
α	cm^{-1}	0.033
n	-	4.10
K_s	cm hr^{-1}	35.0

Transient positions of the water table predicted by this numerical model are compared with the experimental results presented by Vauclin et al. (1979) in Figure 4-5, which illustrates that there is a very good agreement between the two sets of data.

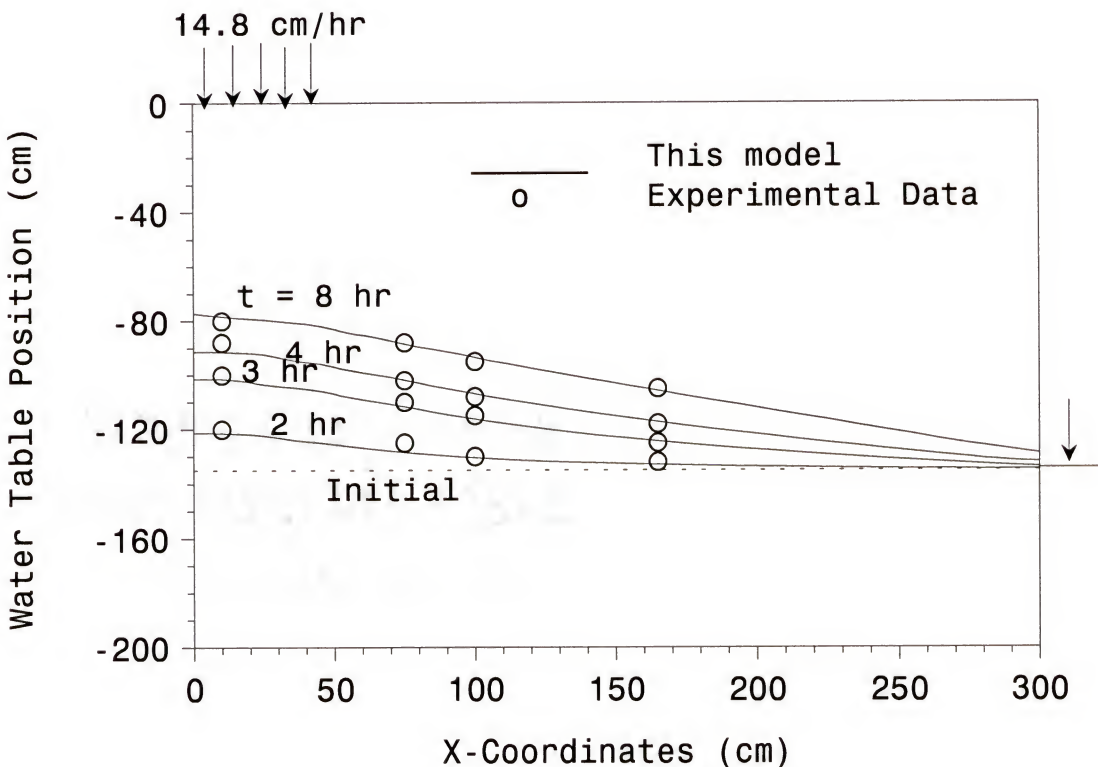


Figure 4-5: Simulation of transient water table mounding, comparing results from this work and experimental data collected by Vauclin et al. (1979).

Transient, Two-Dimensional, Unconfined Drainage

This example was chosen to verify the performance of the numerical model in modeling transient, unconfined drainage problems with seepage-face boundaries. The experimental data were taken from Vauclin et al. (1975). A saturated slab of soil, similar to that used in the previous example, was allowed to drain after a sudden drop in the external water table. Before drainage, the water table was maintained at the depth of 55

cm. At the time $t=0$, the external water table was dropped instantaneously to the depth of 125 cm at the right-hand side, and was maintained there subsequently. No-flow boundaries were imposed at the left-hand side, on the bottom, and on the top of the flow domain. Hence, on the right side, the seepage face boundary was transiently determined between the depth of 125 and 55 cm. Below the external water table level of 125 cm, a constant head boundary was applied.

Vauclin et al. (1975) fitted an analytical expression for the water content versus pressure head (h) to experimental data:

$$\theta = \theta_s \frac{A}{A + |h|^B} \quad (4.2)$$

with

$$A = 4.00 \times 10^5, B = 2.9, \theta_s = 0.30 \text{ cm}^3 \text{ cm}^{-3}, \theta \text{ in } \text{cm}^3 \text{ cm}^{-3}, h \text{ in cm of water.}$$

Their analytical expression for the unsaturated hydraulic conductivity was given by

$$K = K_s \frac{C}{C + |h|^D} \quad (4.3)$$

where

$$C = 3.6 \times 10^5, D = 4.5, K_s = 40 \text{ cm day}^{-1}, K \text{ in } \text{cm day}^{-1}, h \text{ in cm of water.}$$

The nodal spacings are the same as the previous example. The transient simulation was continued until steady state was approached. Numerically simulated water table positions were compared with experimental results (Vauclin et al. 1975) in Figure 4-6, in which the numerical model was able to reproduce closely the experimental results.

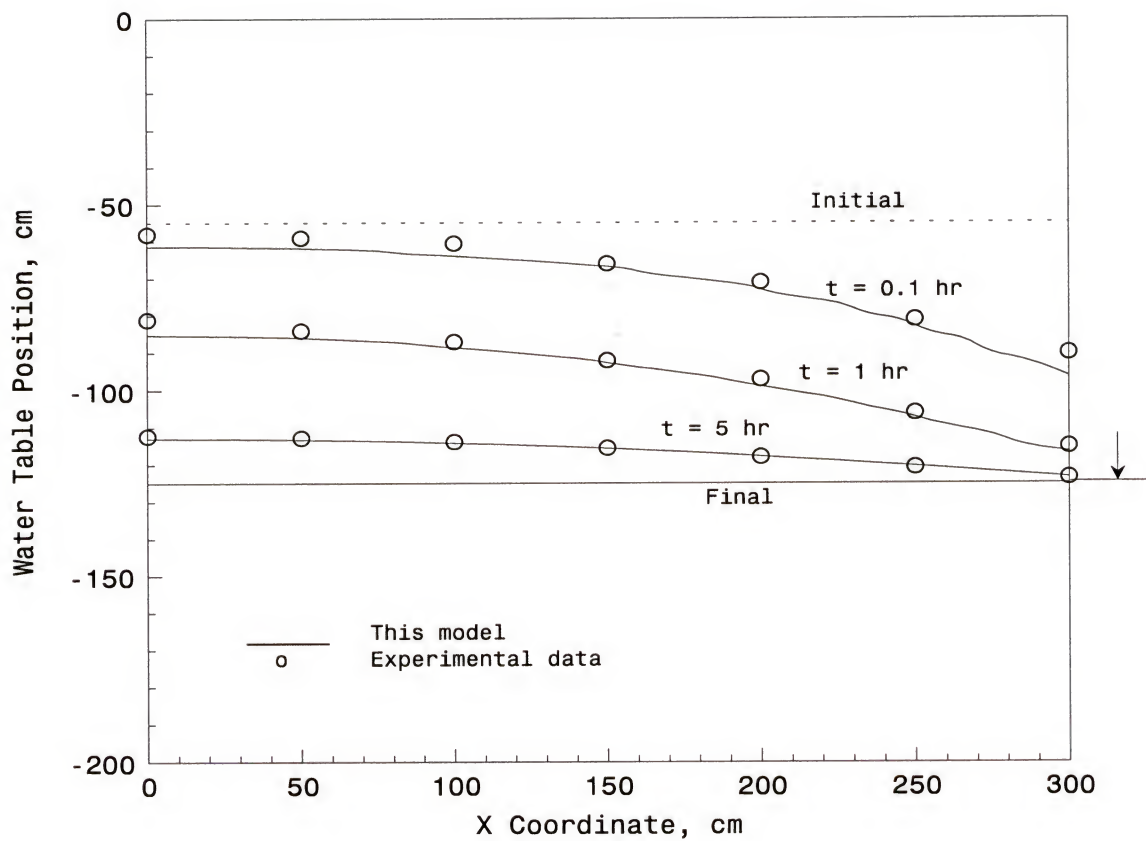


Figure 4-6: Simulation of transient drainage, comparing results from this work and experimental data collected by Vauclin et al. (1975).

CHAPTER 5 EXPERIMENTAL PROCEDURE

Field data from a research project were used to calibrate and verify the mathematical model. The main objective of the research project was to conduct a field-scale study of the use of automatically-controlled subirrigation with buried microirrigation line sources to control field water tables as compared to conventional seepage (Smajstrla et al., 1996). Field research plots installed at the University of Florida Hastings Agricultural Research Center Yelvington Farm were used in this research.

Potatoes were produced during the 1995, 1996, and 1997 spring growing seasons. Field scale research plots 18.3 m wide and 183 m long were used (Fig. 5-1). The soil type was Placid Fine Sand (Typic Humaquepts), a typical high water table soil of the area.

Field operations for potato production followed typical grower practices in the area. A cover crop of sorghum sudan was grown during the summer and early fall months each year to increase the soil organic matter. Details on potato production practices were presented by Smajstrla et al. (1996).

Subirrigation System

The subirrigation system consisted of Netafim microirrigation tubing with 3.8-l per hour Triton emitters spaced at 1.2-m intervals. Laterals (shown as dashed lines in Fig. 5-1) were spaced 6 m apart and extended the 183-m length of the beds. Laterals were buried by chiseling them to a depth of about 0.5 m. Each group of three laterals per bed was connected with a polyethylene manifold pipeline at each end of the field.

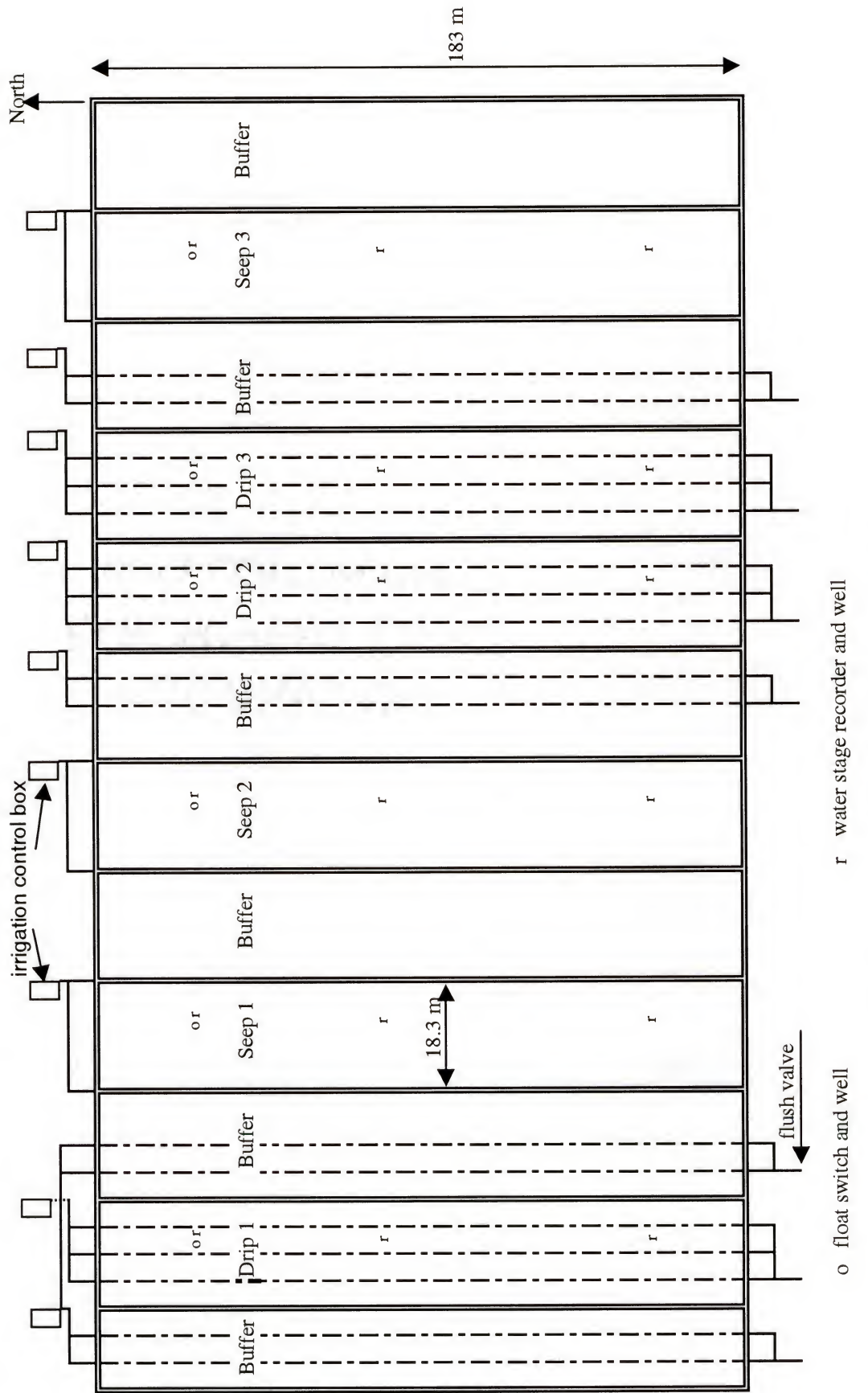


Figure 5-1. Layout of the field research experiment.

At the inlet end water was supplied to the manifold through an automatic solenoid valve, pressure regulator, flow meter, and vacuum breaker. At the downstream end, a ball valve, filter, flow meter, and automatic flush valve were installed to permit automatic flushing of the pipelines and monitoring of the volume of flush water. The filters were required to prevent sand in the laterals from plugging the flow meters.

Automatic flush valves were installed on the microirrigation laterals. These valves operate for approximately 1 minute each time the irrigation system is turned on, thus flushing accumulated materials from pipelines to help prevent emitter plugging. This type of valve was a necessary component of the microirrigation system because fine sand particles were found regularly in the laterals. These apparently moved backwards through the emitters and into the pipelines. If they were not flushed, they would accumulate and possibly form larger aggregates with other materials in the pipelines, causing plugging problems (Smajstrla et. al., 1996).

Irrigation of each of the plots was independently controlled with a float-actuated mercury tilt switch located in a shallow well about 18 m from the upper end of each plot. Float switches were initially set to schedule irrigation to maintain the field water table about 0.5 m below the top of the plant row. When the water table dropped below 0.5 m, the microswitch closed, providing power to the solenoid valve for irrigation. When the water table rose above 0.5 m, the microswitch opened, and irrigation was stopped. Actually, the switches were set with a 1.2-cm lag between turn-on and turn-off to prevent the irrigation system from cycling excessively, while maintaining adequate soil water levels for plant growth. Buffer areas were irrigated at the same times as the adjacent

treatment plot. In stages during the season, threshold water table levels were re-set to lower values.

Irrigation water was chemically treated and filtered to prevent clogging of the drip emitters. The filtration system consisted of an Y-strainer, media filters and screen filters at the well, and disk filters at each field plot. Flushing of each lateral occurred automatically each time the irrigation system operated, while manifold and main pipelines were manually flushed each week. A commercially-available irrigation line treatment chemical ('DiSolv', Flo-Tec, Inc.) was used for chemical water treatment. It was continuously injected into the irrigation water at an average of about 4 ppm to prevent emitter plugging by preventing chemical precipitates and biological growths. Reductions in emitter flow rates were observed whenever irrigation was interrupted for extended periods; however, flow rates recovered within days of the resumption of regular irrigation and chemical water treatment (Smajstrla et al., 1998).

Irrigation volumes applied were monitored with totalizing flow meters at the irrigation pump, at the inlet to each field plot, and at the flush valves. Irrigation occurrences and durations were recorded with event counters and timers. Data were recorded from the beginning of irrigation at plant emergence until irrigation was discontinued about one week before plant harvest each year.

Runoff Measurement

Runoff from one water furrow in each of the experimental plots was measured throughout the growing season. A sump was installed at the outlet in each water furrow and water was collected in the sumps by gravity flow. Water was pumped out of the

sumps using sump pumps, and volumes were measured using flow meters. Timers and event counters also were installed to measure time of pumping and number of events.

Soil Hydraulic Characteristics

Soil Water Retention Curve

Soil water retention curves were developed using published data (Carlisle et al., 1989). The soil at the experimental area is sometimes classified as Ellzey Fine Sand, but a coring at the field showed more approximation with the profile description of Placid Fine Sand. Both soils are very closely associated, consisting of very poorly drained, nearly level soil that was formed in thick beds of sandy marine sediments (USDA-SCS, 1983).

The retention curves for the first 5 layers are shown in Figure 5-2. An equivalent curve (average of the 5 layers) is shown in Figure 5-3, plotted against the fitted curve using van Genuchten equation (2.12). The resulting parameters for the fitting are tabulated in Table 5-1.

Table 5-1: Parameters used in van Genuchten's equation to describe the soil hydraulic properties of Placid Fine Sand.

Parameter	Value
α	0.0188
n	3.9941
m	0.7496
θ_s	0.430
θ_r	0.030

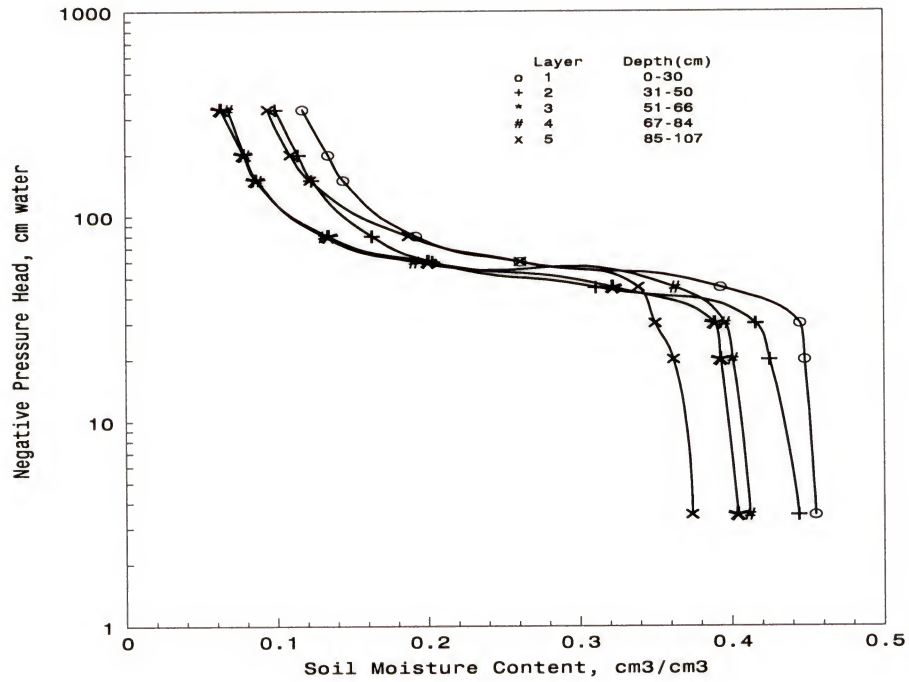


Figure 5-2: Soil moisture curve for Placid Fine Sand.

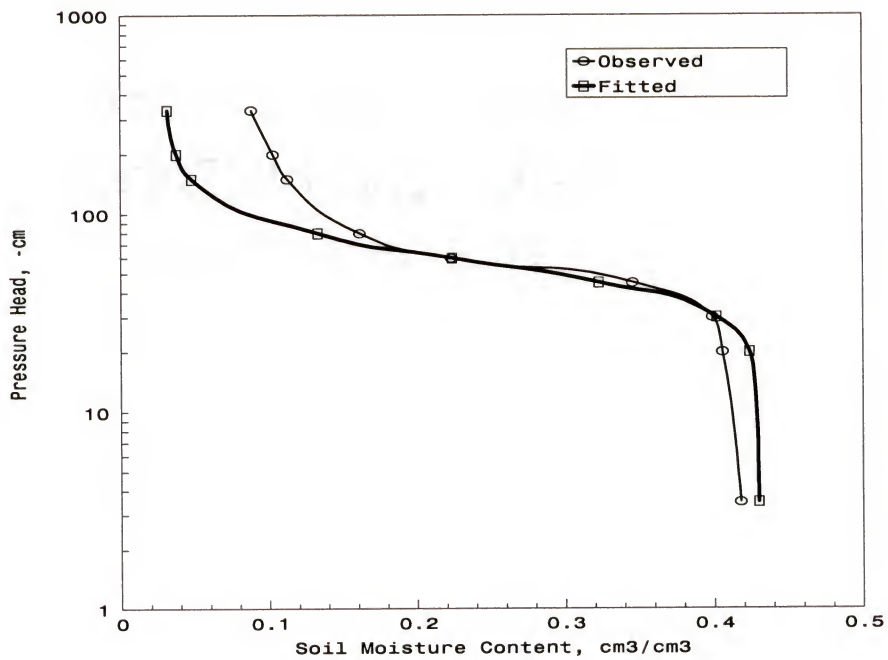


Figure 5-3: Fitted and observed soil moisture retention curves for one equivalent layer of Placid Fine Sand.

Saturated Hydraulic Conductivity

Saturated hydraulic conductivity (K_s) was determined with a field method. Although laboratory data were available, they were not directly used because they often show little or no correlation with field values (FAO, 1980). Kanwar et al. (1989) found that K_s values determined in the laboratory were about 10 to 800 times higher than mean K_s values determined by field methods. They suggested that macropores (cracks, wormholes, wall effects, etc.) could lead to pipe flow where continuous macropores essentially connect one end of the core to the other. Because of macropore flow and near-complete saturation of samples in the laboratory, higher K_s values could be anticipated.

There is a wide range of methods for determining K_s "in situ" where a water table is present, such as the single- and two-auger hole, piezometer, and multiple-well methods. Several methods also are available to measure K_s in the absence of a water table, such as the air-entry permeameter, double-tube method, ring infiltrometer, and well-permeameter methods. Some of these methods have been improved for rapid measurements of K_s , and most of them have been used with various degrees of success. However, limitations of such methods include measurement times of several hours or even days, large water requirements, and the need for two or more operators in order to conduct the tests. The methods are classified as small-scale because they determine the K_s value in a relatively small soil body near the well. Methods for measuring hydraulic conductivity in the field have been reviewed by Boersma (1965a, 1965b) and Amoozegar and Warrick (1986).

K_s of a soil profile can be highly variable from site to site (spatial variability), and also can vary at different depths. Not only can different soil layers have different K_s , but

K_s also can vary even within a soil layer. To eliminate the problem of variation as much as possible, large-scale methods have been designed to obtain a representative K_s for a large soil body. An advantage of large-scale methods is that the flow paths of the groundwater and the natural irregularities of the K_s -values along these paths are integrated in the overall K_s value. Thus it is not necessary to determine the variations in horizontal and vertical directions (Oosterban and Nijland, 1994). These methods generally use observations of the discharges from parallel drains, along with corresponding elevations of the water table at various distances from the drains. The methods are more expensive and time-consuming than small-scale methods, but also are more reliable.

Extraction methods, such as the auger-hole method, may suffer additionally the problem of instability in sandy soils. If filters are used to stabilize the auger hole, there is still the risk that sand will penetrate into the hole from below the filter (if the hole is not lined), or that sand particles will block the filter.

Values of K_s may differ as much as 100% between sites only a few feet apart in soil classified as a single type (Boersma, 1965a). Because of such differences, it is more appropriate to take approximate readings at a large number of sites than to take precise measurements at only one or two sites. Thus, low-cost and rapid measurement methods are necessary.

Rosa and Smajstrla (1999) presented a low-cost and easy-to-use device for measuring saturated hydraulic conductivity with the auger-hole method. They tested filtered and non-filtered wells and compared results with those from the parallel-drain method. The authors found that filtered wells produced data in very close agreement with

the drain method, and should be used to avoid the problem of clogging the well during the measurements in this type of soil.

The estimated overall value of K_s for the experimental area was about 7.8 cm hr^{-1} . This value was used in this work. K_s -values for disturbed soil samples taken at the same site were measured by Rankin and Smajstrla (data not published) using the constant head permeameter method. The overall average K_s -value was approximately 60 cm hr^{-1} , a very high value compared to the field results. The primary reasons for this discrepancy are first, the samples were taken from the top layer in the profile, usually a soil material with higher saturated hydraulic conductivity, and second, disturbed samples that inadequately represented actual field conditions were used. Because of the poor correlation between laboratory and field data, the use of laboratory tests should be limited to cases where no better alternative is at hand, and a model calibration involving other soil hydraulic parameters must be performed to compensate the use of this kind of data.

Climate Data

To estimate potential evapotranspiration and record rainfall a weather station was installed and climate data were measured. At the field site, rainfall, maximum and minimum temperatures, and wind speed were measured. Solar radiation was measured at the Hastings Research and Education Center headquarters building, approximately five miles from the field research site.

To ensure enough accuracy and to prevent the loss of data, rainfall was measured with both manual and recording rain gauges. Rainfall amounts and distributions for the simulated periods are discussed in the next chapters.

Potential evapotranspiration for each simulated season was calculated from the Penman equation, using daily values of solar radiation, temperature and wind speed. Seasonal and daily ET distributions are discussed in the next chapters.

CHAPTER 6 NUMERICAL SOLUTION: CALIBRATION

Data from the Hastings field research project were used during model development, for initial evaluation of the model and for calibration of some parameters.

The calibration of the model was done using data from February to May 1996, the length of the irrigated potato season. Irrigation and runoff volumes and water table elevations were the data used in model evaluation. Data from one irrigated plot were used for model calibration because in this season only one device for measuring runoff was installed. Water table elevation was taken from the well where the float switch to control irrigation was installed.

Soil Hydraulic Properties

The most important calibration was of the soil hydraulic parameters used in the van Genuchten equation. When the model was tested with the parameters obtained by fitting the original soil water characteristics curves (Table 5-1) the results were very different from the observed data, implying some problem with the original water characteristics curves. The correspondence between field- and laboratory-measured retention data was poor due to inability of undisturbed cores to sufficiently represent macroporosity in the field. The alternative was to calibrate a soil with new parameters, maintaining only the saturated and residual water contents already obtained. This procedure resulted in a set of parameters that can be used in both wetting and drying cycles, ignoring hysteresis. The calibration was performed looking for a better overall

fitting of the water table position when irrigation or precipitation occurred (wetting) and also when the soil was draining.

The calibrated parameters for the van Genuchten equation that fitted better are presented in Table 6-1, and compared with the previously fitted parameters. The characteristic curves obtained with both sets of parameters are shown in Fig. 6-1.

Recall from Chapter 2 (eq. 2.12) that α , n , and m are empirical constants, whose values depend upon the soil properties. The parameter α is, in part, a measure of the first moment of the pore-size-density function (L^{-1}) (as α increases, so does the first moment); n is an inverse measure of the second moment of the pore-size-density function (as n increases, the pore-size-density function becomes narrower) (Wise, 1991).

From Table 6-1, the larger difference between the values of the parameters is for the parameter n (the difference in m -values is due to the relation $m=1-1/n$). When the value of n is reduced from 3.9941 to 1.2800, it means that the relative abundance of smaller pores (in comparison to the mean pore size) increases in the porous medium. These smaller pores are difficult to drain, due to their larger viscous effects and their higher affinity for water (Wise et al., 1994). Consequently, in Fig. 6-1, for smaller values of n , more water is retained and, in the field, more water remains in the vadose zone (region of the soil system above the water table).

Table 6-1: Parameters in van Genuchten's equation determined using original and calibrated soil water retention curves for Placid Fine Sand.

Parameter	Calibrated	Original
α	0.0175	0.0188
n	1.2800	3.9941
m	0.2187	0.7496
θ_s	0.430	0.430
θ_r	0.030	0.030

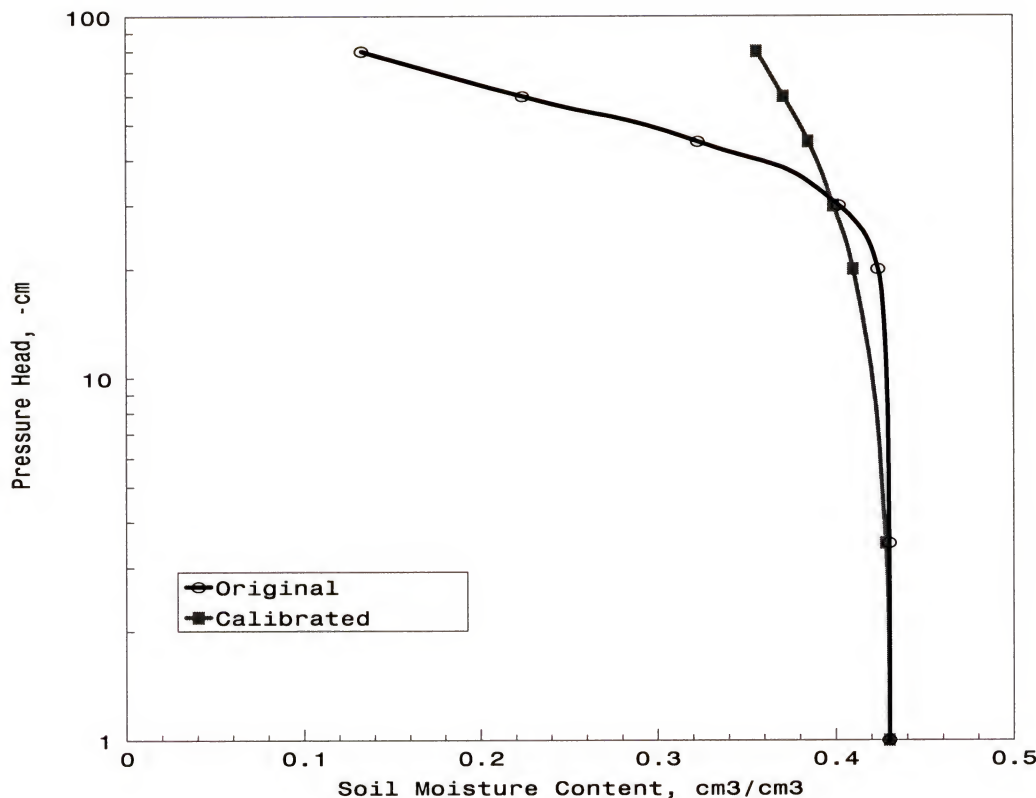


Figure 6-1: Soil moisture retention curves with original and calibrated parameters.

In fact, visual observations of the soil moisture in the field, several days after rain, showed the presence of wetness in the vadose zone. This was the main reason that irrigation usually was not turned on when the water table reached the control point after the rain, and a delay in irrigation of several days was allowed (discussion in a later section).

The hydraulic conductivity obtained with the calibrated parameters is presented in Fig. 6-2. Mualem's (1976) relative hydraulic conductivity, subject to van Genuchten 's (1980) parameterization (eq. 2.13) is a function of n . The larger pores, which have less resistance to fluid transmission, tend to be drained first, constraining water to flow

through the remaining (smaller) pores. Hence, as the value of n decreases, the hydraulic conductivity of the unsaturated zone decreases more rapidly with decreasing water content, which decreases the net drainage rate in the unsaturated zone.

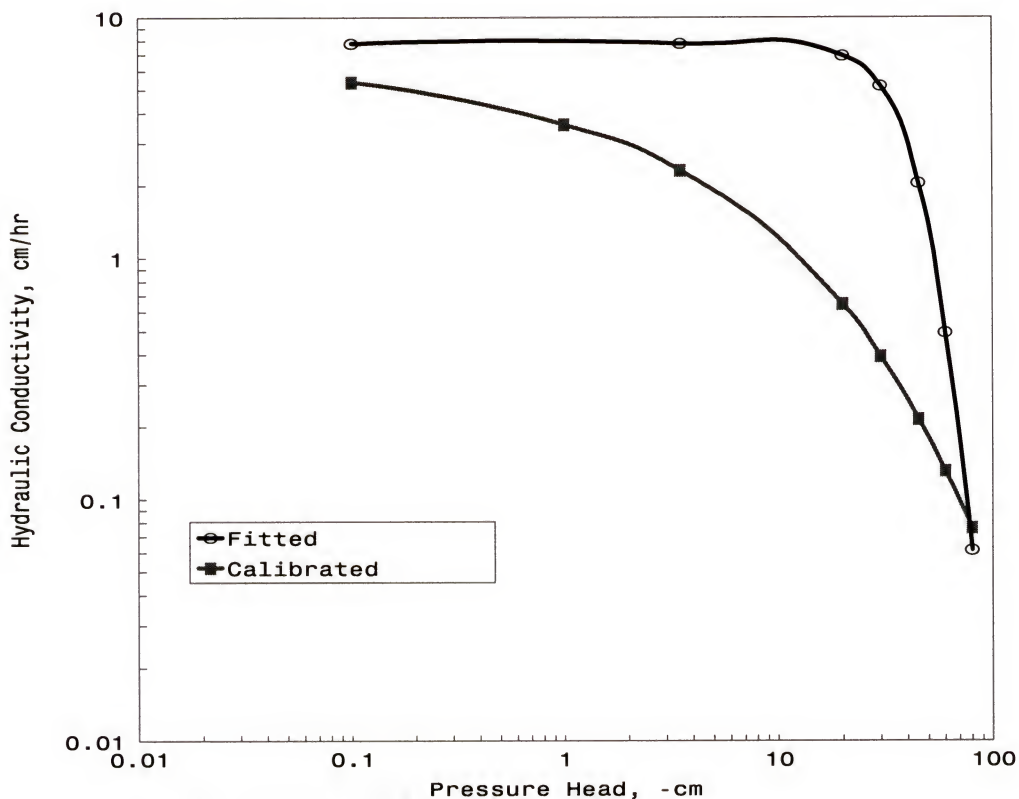


Figure 6-2: Predicted hydraulic conductivity with original and calibrated parameters.

Estimated Daily ET

Daily potential evapotranspiration, ET , was a component of the extraction function and was estimated independently by the use of the Penman equation. Estimates of surface albedo (α) are required for applying the Penman equation to calculate ET . This term is not constant and varies with ground cover, soil type, and crop stage of growth. Because of the difficulty in estimating seasonal changes in surface albedo, one approach

for applying the Penman method is to use an albedo for a free water surface ($\alpha=0.05$) to estimate potential evaporation rate for a free surface, and then multiply that estimate by an empirical constant (k_I) to estimate ET . Jones et al. (1984) recommended the use of $k_I = 0.70$ for Florida conditions.

As discussed in Chapter 3, the evapotranspiration rate, ET_r , was calculated by distributing the daily potential evapotranspiration over a 24-hr period by using a sinusoidal type distribution (eq. 3.42).

Figure 6-3 presents the shape of equation (3.42) for a hypothetical potential $ET = 10$ mm/day, $T_{cycle} = 24$ hr, with the cycle beginning at 2:00 am. The maximum ET_r occurs at $T_{cycle}/2$, or 14:00 hr for this example. Vellidis (1989) found that this kind of distribution most accurately simulated the ET rates observed in lysimeters used in his study.

The effect of both crop transpiration and soil evaporation were integrated into a single crop coefficient. The K_c coefficient incorporates crop characteristics and averaged effects of evaporation from the soil. For most hydrologic water balance studies, average crop coefficients are relevant and more convenient than the K_c computed on a daily time step using a separate crop and soil coefficient.

The procedure for calculating crop evapotranspiration (ET_c) consisted of identifying the crop growth stages, their lengths, and selecting the corresponding crop coefficients (K_c). ET_c was obtained by multiplying the evapotranspiration rate (ET_r) by the appropriate crop coefficient. Crop coefficients for potato development stages were taken from FAO Irrigation and Drainage Paper 56 (Allen et al., 1998).

The crop coefficient was maintained constant at the initial stage that ran from planting date to approximately 10% ground cover. During the initial stage, the leaf area

was small, and evapotranspiration was predominantly in the form of soil evaporation. The crop development stage ran from 10% ground cover to effective full cover when plants reached nearly full size. As the crop developed and shaded more and more of the ground, evaporation becomes more restricted and transpiration gradually became the major process. The mid-season stage ran from effective full cover to the start of maturity, indicated by the beginning of the senescence of leaves; at this stage the K_c reached its maximum value and was relatively constant, as occur for most growing and cultural conditions. Finally, the late season stage ran from the start of maturity to harvest. The K_c at the end of the late season stage ($K_{c\ end}$) was generally high because the crop was irrigated until near harvest.

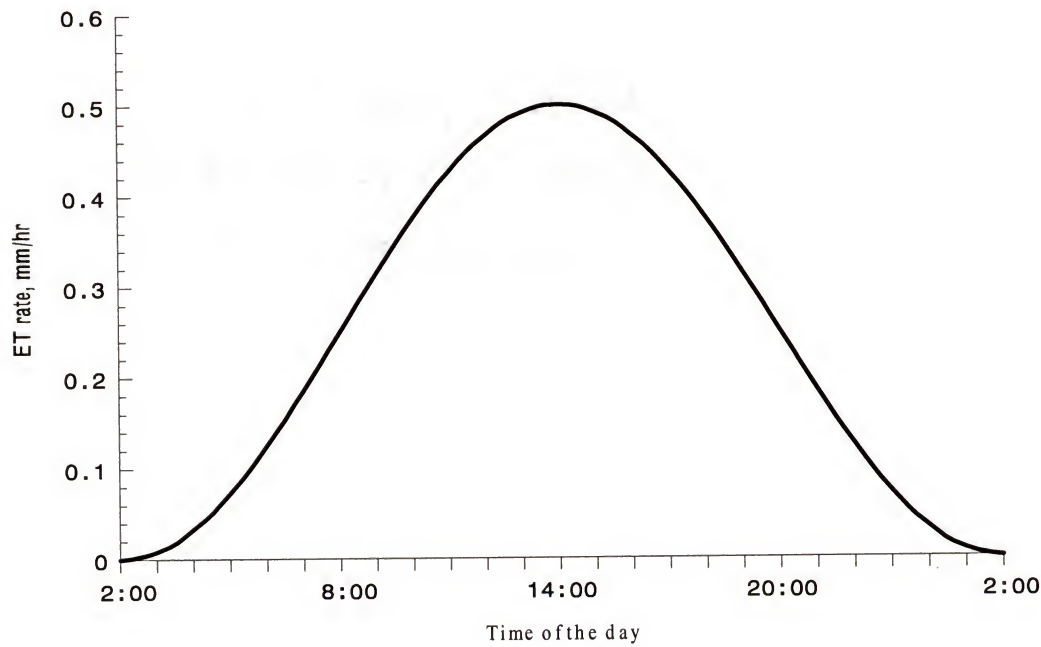


Figure 6-3: Simulated distribution of the daily ET over a 24-hr cycle.

The crop coefficients and lengths of the development stages used in this work are presented in Table 6-2 and the crop coefficient curve is shown in Figure 6-4.

Table 6-2: Lengths of the stages and crop coefficients for potato used in this work.

Stage	Length (days)	K _c
Initial	L _{ini} = 22	K _c ini = 0.3
Development	L _{dev} = 27	K _c dev = Variable
Mid	L _{mid} = 38	K _c mid = 1.15
Late	L _{late} = 20	K _c late = Variable
End	-	K _c end = 0.75

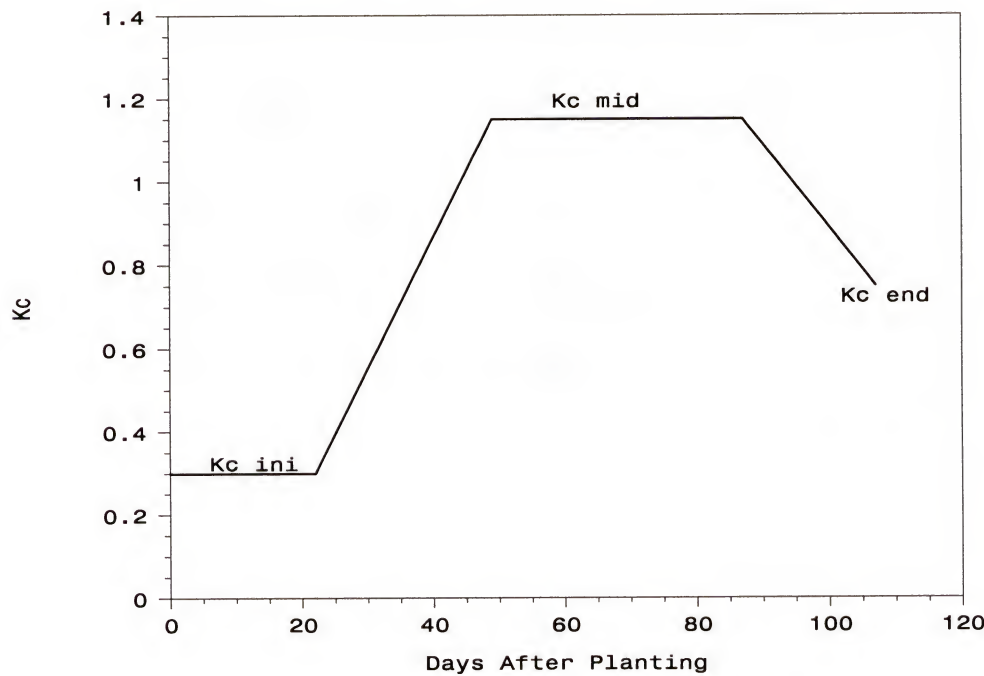


Figure 6-4: Crop coefficient curve for potato used in this study.

The crop coefficients for the development and late stages were calculated by the following equations

$$Kc_{dev} = Kc_{ini} + \frac{DAP - DBD}{L_{dev}} (Kc_{mid} - Kc_{ini}) \quad (6.1)$$

and

$$Kc_{late} = Kc_{mid} + \frac{DAP - DBL}{L_{late}} (Kc_{end} - Kc_{mid}) \quad (6.2)$$

where

DAP = days after planting, or current Julian day of simulation,

DBD = Julian day of beginning of development stage,

DBL = Julian day of beginning of late stage.

Figure 6-5 presents potential *ET* and calculated crop *ET_c* for the period of model calibration. The difference between the curves reflects the changes in crop coefficients along the crop growing season. During most of the simulated period *ET_c* was higher than the potential *ET*. Deviation of the *K_c* from the reference value '1' was primarily due to differences in crop height and resistance between the grass reference and the potato, and the weather conditions. During this period the soil nearly continuously was wetted due to the precipitation and irrigation, providing excellent conditions for the development of the crop. Also, the high value of *K_c* at the end of the late season growth stage reflects the water management practices specific to this crop, when irrigation was applied until near date of harvest.

Deep Percolation

As described in Chapter 3, the vertical drainage across the lower boundary of the soil profile was approximated by a flux that depended on the position of the water table level (eq. 3.21).

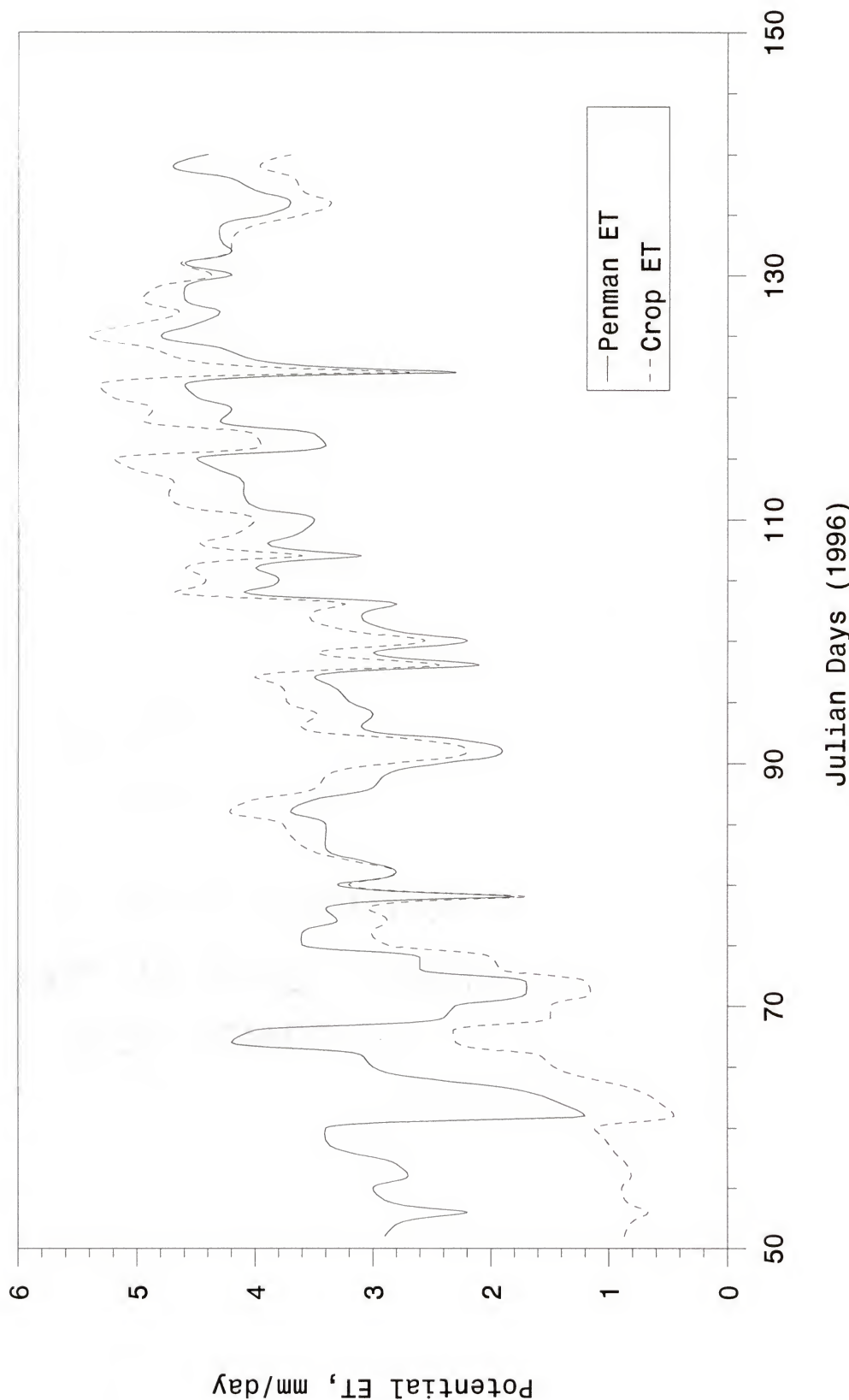


Figure 6-5: Daily values of potential evapotranspiration (Penman) and crop ET for the 1996 simulated period.

First, an exponential equation was fitted with field data from a specific period of drainage to describe the position of the water table level with time. Then, a second approximation was taken to relate the drop of the water table with the hydraulic head at the bottom of the profile. Finally, a multiplication factor was calibrated to represent the flux at the bottom. The final expression that calculates the flux at the bottom of the profile is given by

$$QB(h) = 0.001 \exp(0.0173h) \quad (6.3)$$

where

$QB(h)$ = flux at the bottom of each column in the grid (cm/hr), and

h = hydraulic head at the bottom of each column (cm).

The same equation can be expressed in terms of depth of water table level:

$$QB(h) = 0.008 \exp(0.0173wtdepth) \quad (6.4)$$

where $wtdepth$ is water table depth (cm), negative with relation to the soil surface.

The relationship between flux and hydraulic head at the bottom of the grid is shown in Figure 6-6. There were no field data of deep percolation to compare with the simulated results and this term was used only to complete the total mass balance. The use of this kind of relationship is preferable to maintaining a constant value for deep percolation or neglecting it.

Water Table Levels

Water table position prediction was the goal of the model. All the efforts in the calibration process were done to improve the model representation of the drainage and wetting (precipitation and irrigation) phases.

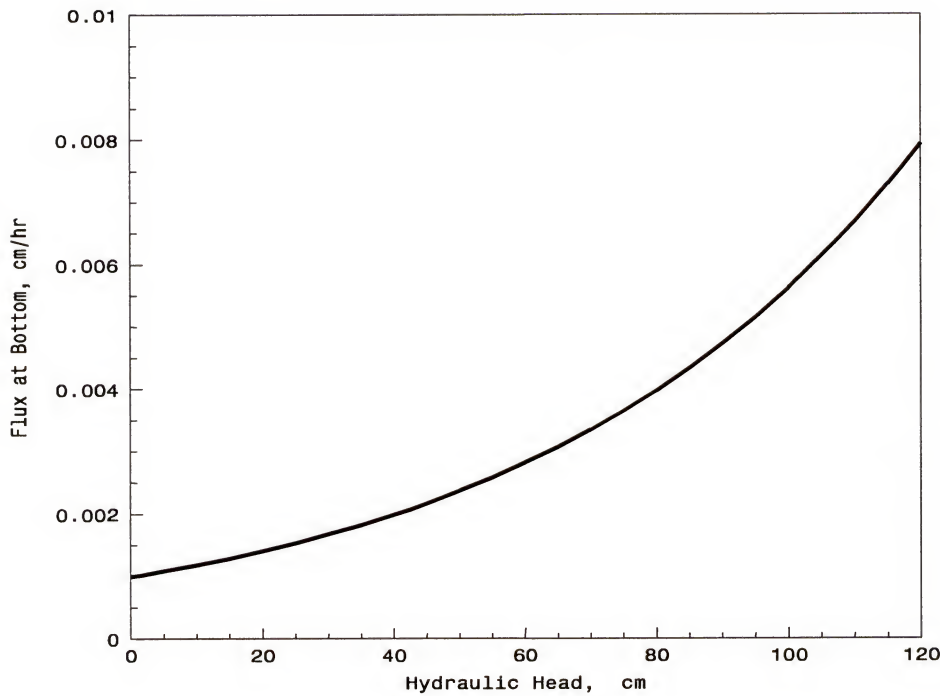


Figure 6-6: Relationship between flux and hydraulic head at the bottom of the soil profile.

As discussed earlier, the soil hydraulic characteristics constituted a very important role in simulating the water table position, with the deep percolation term playing a minor role. Modifications at the right (seepage) and the top (surface runoff) boundaries also contributed to the water table level calibration.

The potato crop was planted on February 6 (Julian day 37) and harvested on May 20 (Julian day 141). The calibration period ran from February 20 (Julian day 51) to May 19 (Julian day 140) in the year 1996. From the field data, one plot (DRIP 1 in Fig. 5-1) was chosen to provide the data for calibration because the device for measuring runoff was installed at that plot. Data for field water table levels were taken from the well installed at the north position of the plot because the irrigation was controlled at this position; simulated water tables were taken from the grid corresponding to the position of

the well at the field (approximately halfway between irrigation lines). Field water table data were recorded continuously but transferred to a spreadsheet on a 4-hr interval, so the simulated water table was printed on a 4-hr interval to permit direct comparison with field data.

The continuous field and simulated water tables for the simulation period are shown in Figure 6-7. The figure also shows daily rainfall events as a bar graph overlay. The peaks in the simulated water table were more pronounced than in the observed water table, especially for the last storm, when the simulated water table response was faster than the observed water table. It seems that when the antecedent water table was high and the soil profile was practically saturated, the soil hydraulic properties better represented the real conditions in the field. On the other hand, if the water table was low, the soil hydraulic properties did not represent the field conditions very well, and the response to precipitation and irrigation was not adequate, a consequence of the rapid decrease in hydraulic conductivity with the decrease in water content.

Runoff

As discussed in Chapter 3 runoff was calculated considering its occurrence at the surface and at the edge of the water furrow (seepage). In fact, the term surface runoff is not totally appropriate in this case because of the modification in the grid to avoid the irregularities due to crop beds. The actual "surface runoff" in the model occurred below the top of the grid.

Runoff from flat, sandy soils is not produced by the common concept of an infiltration limiting "rainfall excess". Runoff is more likely a result of rainfall on

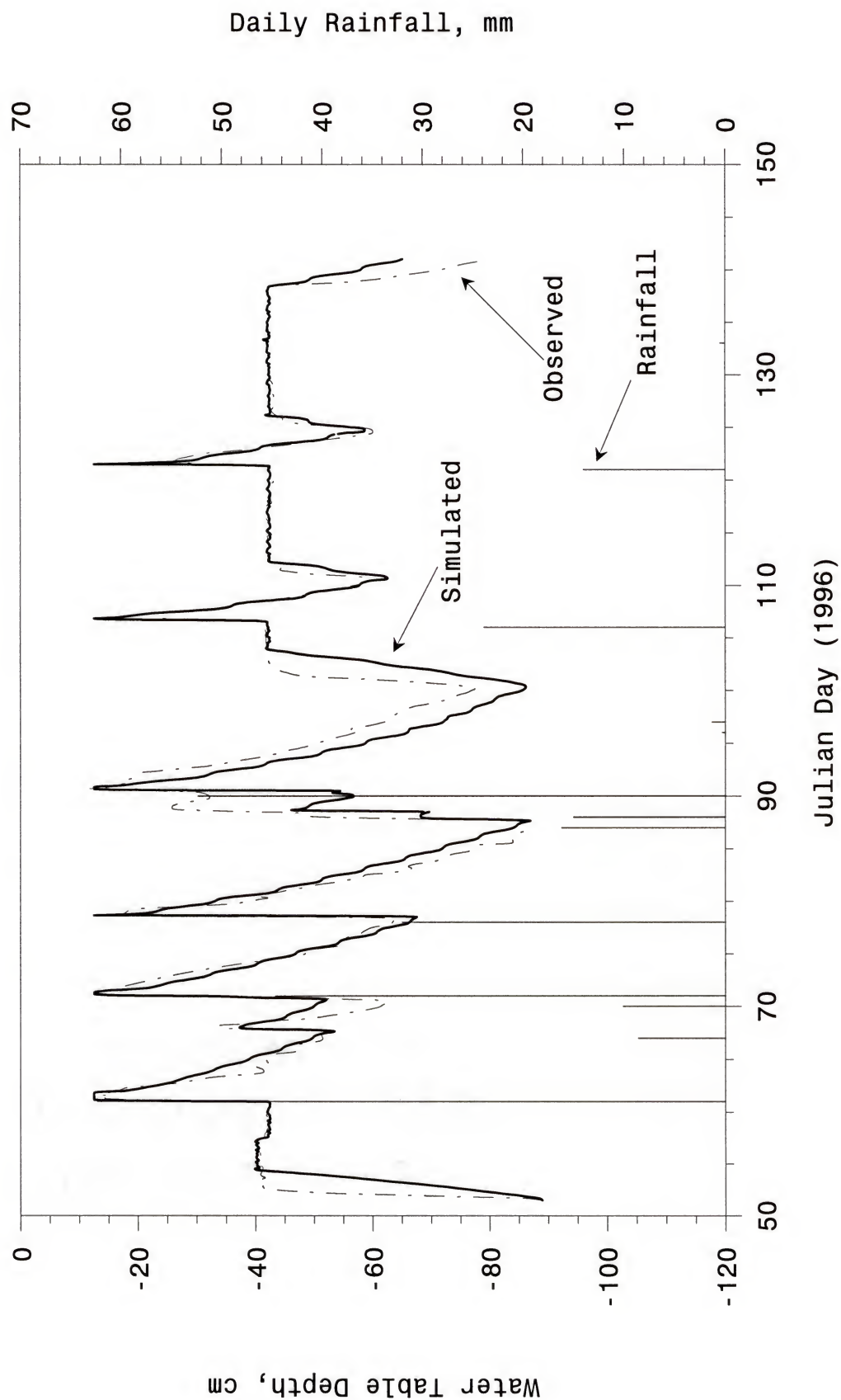


Figure 6-7: Observed and simulated water table in the 1996 season.

saturated areas and subsurface flow to ditches and drainage ways during and following a storm.

The principal calibration in terms of runoff was done at the seepage face. Early simulations showed an excess of drainage at this boundary, with a very rapid decrease in water table levels when water was not allowed to remain in the water furrow (surface retention) during rainfall events. The alternative was to permit some water retention at the furrow, and after that, the process of runoff was initiated. As a matter of fact, visual observations at the field showed that runoff did not begin immediately when the water table level reached the water furrow, firstly because of the hydraulic roughness of the surface as influenced by micro-relief, and secondly because of the macro-slope (slope not uniform). At the end of the storm, this water would infiltrate into the soil profile. These observations corroborated the modification at this boundary of the grid, leading to a better handling of the seepage term.

In the first year of simulation (used for calibration) a device to measure surface runoff was installed at the end of the irrigated plot. There was no flow meter installed, the first year volume was estimated by the time of the pump operation. A calibration had been performed at the laboratory and the flow of the pump measured at about $0.360 \text{ m}^3 \text{ min}^{-1}$. However, the calibration was performed with clean water, and the runoff water was usually very dirty, affecting the real volume that was pumped from the field. Even with the installation of screen filters at the device, a variation in the flow was expected, and affected the accuracy of the runoff measurements during this year.

Runoff from three major storms were measured in the field. Table 6-3 presents the total precipitation for the events, and a comparison between measured and simulated

runoff. The simulated runoff is a summation of the seepage and the surface runoff calculated by the model. The larger difference between the data is observed in the first event after the installation of the measuring device, around Julian day 90. The main reason for this discrepancy can be explained by the difference in water table levels measured and simulated during that period of time (Fig. 6-7). The field and observed water tables were very low when the first storms occurred, and the field water table response was much more rapid than the simulated water table. For the next two storms the water table was already high due to irrigation when precipitation began and the differences between simulated and observed runoff are lower.

Table 6-3: Measured and simulated runoff for three storm events in 1996.

Date of the Storm (Julian Day)	Precipitation (mm)	Observed Runoff (mm)	Simulated Runoff (mm)
90	52.4	62.1	33.9
106	23.9	10.1	14.4
121	14.0	4.7	4.7

Irrigation

Irrigation was an important parameter to be considered in the calibration of the model, since the objective of the field research project was to study the performance of the subsurface drip irrigation in maintaining a desired depth of the water table. Data from one irrigated plot was used for comparison with the simulated data. The description of the irrigation system was presented in Chapter 5.

The necessary inputs for simulating irrigation were the rate of water application and its distribution during the season. As presented in Chapter 3, two line sources, one at the line of symmetry and another at the middle of the grid were simulated because only half of the field plot was being simulated. Each line source, of strength $Q = 28.96 \text{ cm}^2/\text{hr}$, was considered to apply the water directly at the source cells, and the application rate was calculated as $Q_{IRRI} = 1.16 \text{ cm/hr}$ (strength Q divided by cell's width, 25 cm is this case). Only half of the volume applied by the first line source was considered to enter in the grid (because of the symmetry). This information was used to convert the simulated irrigation volume to values to be compared with the field values.

Regarding the distribution of irrigation during the season, it was necessary to determine the periods when field irrigation was turned on to give this input to the model. An analysis of the field data in terms of water table depth was used to determine with good precision when the irrigation system was turned on and off. This procedure was necessary because the irrigation system was manually turned off when storms occurred (sometimes before the storms began) and, again, manually turned on when irrigation was necessary. In the last case, a delay of several days always was permitted due to the moisture remaining in the soil profile.

Field irrigation and the simulation were begun on Julian day 51 (Fig. 6-7). The effect of irrigation was shown as the rapid rise in water table from about -90 cm to near -40 cm. The irrigation continued for approximately 9 days before interruptions occurred due to rainfall. It can be seen that the rise in the field water table was faster than in the simulated water table. At the beginning of the simulation the soil profile was very dry, even considering the water content in the profile being in equilibrium with the water

table. If one looks at the relationship hydraulic conductivity-pressure head (Fig. 6-2), the value of this soil hydraulic property decreased very rapidly with the increase in negative pressure head. Consequently, the transmission of water from the irrigation source cell to the lower layers was slow, and the simulated water table reached the depth-control approximately 40 hours after the field water table. The same behavior was observed for the second irrigation, and to a lesser extent for the third irrigation, when the preceding water table depth was not too low. For the last irrigation, there was a very good agreement between the water table curves.

One alternative to improve the response of the simulated water table to irrigation was to change the soil hydraulic parameters in van Genuchten equation. However, the attempt to better fit the irrigation response caused the drainage curves to deviate very much from the observed data. A sensitivity analysis in soil hydraulic properties is discussed in Chapter 7.

More than 60-mm of rain occurred around Julian day 61, raising the water tables to about -12.5 cm. After the occurrence of this storm, when the water table was dropping and reached the depth-control there was some irrigation even with the soil still wet. The reason for that irrigation was that the storm occurred during a weekend and the irrigation system was not turned off manually, then the automatic irrigation control system turned the irrigation on when the depth-control was reached.

For the next 6 weeks, large uniformly distributed rains occurred, so that no irrigation was required until Julian day 100. During this period the water table often dropped below the depth-control, however, unsaturated soil moisture was adequate to prevent irrigation until the next rain. As a result, rainfall was highly effective during this

rainy period. During this time, a few tensiometers and visual inspection of the plants and soil were used to monitor soil moisture and determine when to re-start irrigation.

Except for one rainy event (around Julian day 90) the simulated water table followed very closely the observed water table. When the first rain occurred in this event the water table was very low and, similar to irrigation, the simulated response was not quick enough. Also, after this storm, the drainage was faster for the simulated curve, with the water table dropping lower than the observed water table.

After Julian day 100 irrigation occurred almost continuously except for two rainfall events. The first was a 24-mm rain that occurred on Julian day 106 and delayed irrigation until Julian day 110. The second was a 14-mm rain that occurred on Julian day 121 and delayed irrigation until Julian day 124. Both of these events were highly effective, delaying irrigation for 3 days or more. Cumulative irrigation applications and daily rainfall are shown in Figure 6-8. Flat portions of the curves show periods of no irrigation while steeper portions show periods of irrigation. The total hours of irrigation were approximately 509 hr for the simulation and 527 hr for the observed data. The applied irrigation amounts were 253 mm and 255 mm, respectively for the simulation and field. These results can be considered excellent in terms of prediction of the amount of irrigation required in the entire season.

The average depths of the simulated and the observed water tables were practically the same during the irrigation periods. To avoid excessive irrigation cycles during the irrigation period, a range of about 0.5 cm was introduced, also reflecting the variation in the field data where a similar range was used. The simulated and observed water tables during part of the irrigation period near the end of the growing season are

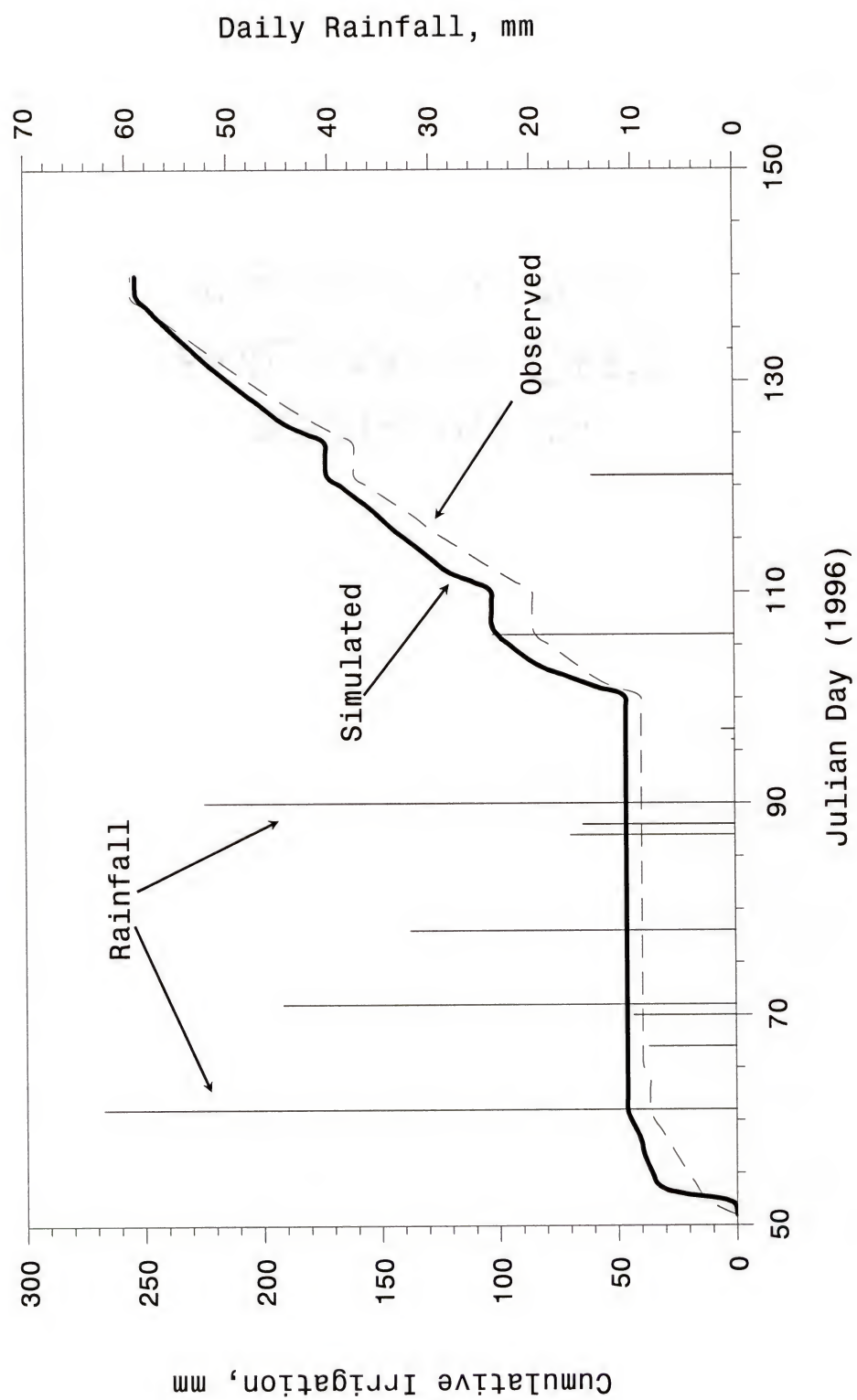


Figure 6-8: Cumulative observed and simulated irrigation in the 1996 growing season.

shown in Figure 6-9. Each daily cycle is clearly seen in this figure, showing the effect of the sinusoidal distribution of the evapotranspiration. One higher spike in the simulated curve was due to a rain of 0.5 mm that apparently did not affect the observed water table. Also in the Figure 6-7 the effect of the sinusoidal distribution of *ET* was clearly seen as little bumps during drainage periods (the bumps work as drainage reducers during the nocturnal hours).

Water Balance

The components of the simulated water balance are presented in Table 6-4. The simulation time for the 88.5 days of the simulated period was approximately 32 hours, with an average time step of 0.005 hr (18 sec), running on a Pentium 450 MHz with 128 Mb of memory. The mass balance final error was very good, around 0.03%.

Table 6-4: Water Balance for the 1996-simulation period.

Mass Balance Term	Value (mm)
Initial Storage	478
Precipitation	281
Irrigation	253
Deep Percolation	78
Crop Evapotranspiration	284
Total Runoff	155
Final Storage	495

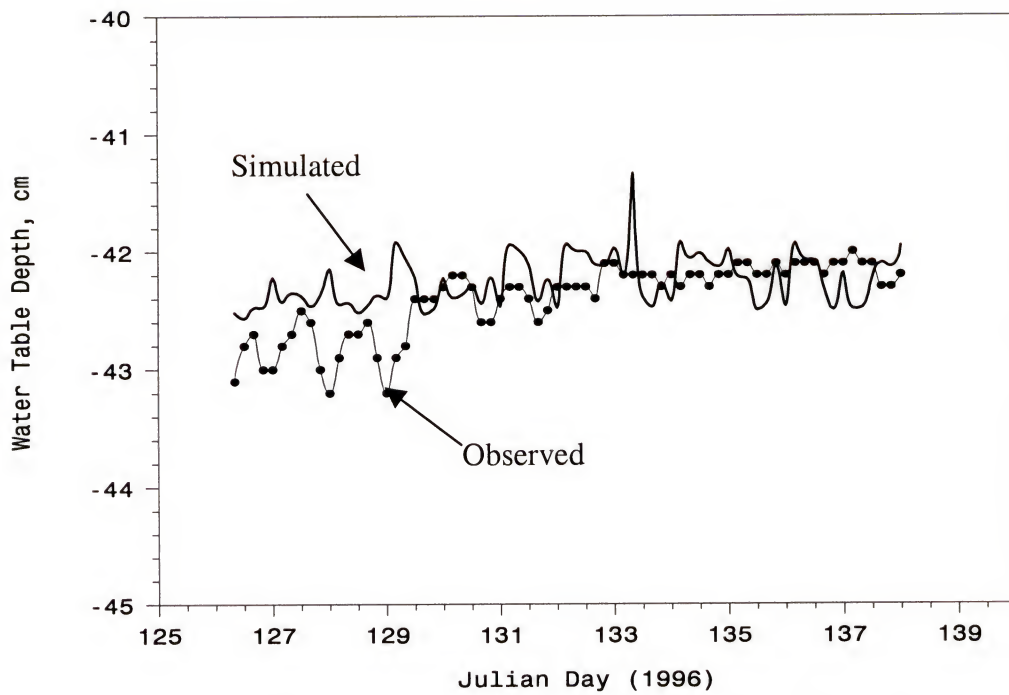


Figure 6-9: Simulated and observed water tables during a period of irrigation late in the 1996 growing season.

CHAPTER 7

MODEL VERIFICATION AND SENSITIVITY ANALYSIS

Model Verification

The verification of the model was done using data from late February to May 1997, the length of the irrigated potato season in that year. Irrigation and runoff volumes, and water table elevations from the same irrigated plot used in model calibration were the data used in model verification.

Estimated Daily ET

Again, daily potential evapotranspiration, ET , was a component of the extraction function and was estimated independently by the use of the Penman equation. The evapotranspiration rate, ET_r , was calculated by distributing ET over a 24-hr period by using a sinusoidal type distribution. The same crop coefficient curve (Fig. 6-4) was used to calculate crop evapotranspiration in the verification of the model.

Figure 7-1 presents potential ET and calculated crop ET_c for the period of model verification. The high peaks in a downward direction for both evapotranspirations coincide with the occurrence of rainstorms, when the climate conditions were not favorable to evaporation and crop transpiration.

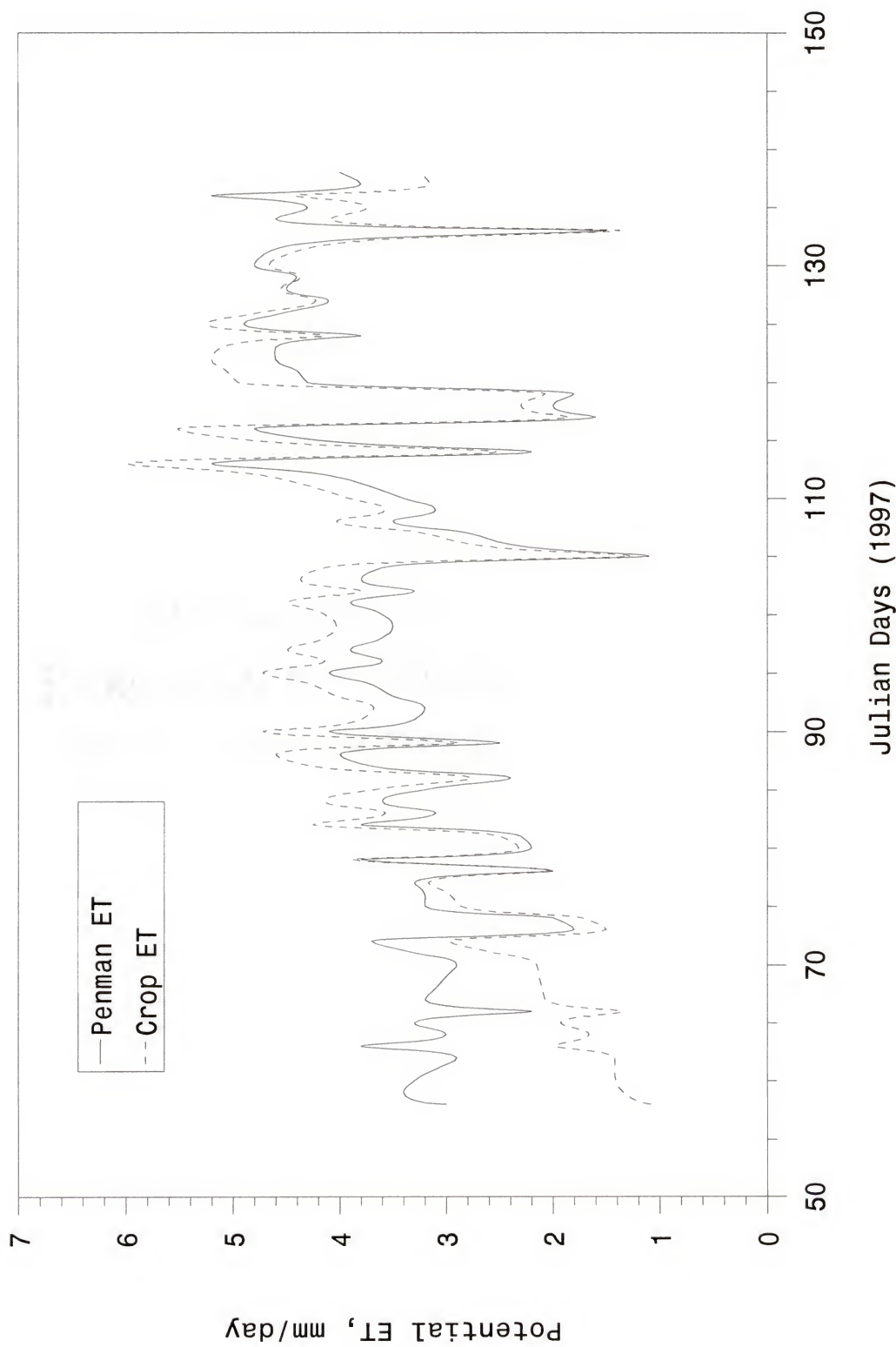


Figure 7-1: Daily values of potential evapotranspiration (Penman) and crop ET for the 1997 simulated period.

Water Table Levels

The potato crop was planted on February 3 (Julian day 34) and harvested on May 20 (Julian day 140). The verification period ran from February 27 (Julian day 58) to May 18 (Julian day 138) in 1997. Data from one field plot (DRIP 1) were used for comparison with simulated results. The field and simulated water table elevations are shown in Figure 7-2. At the beginning of the simulation the water table was very low as a result of the relatively dry month of February. At that time, irrigation was initiated.

A good agreement between field and simulated water table levels was observed during most of the simulated period. Near the end of the period of simulation, the observed water table does not drop as much as the simulation. The direct comparison between simulated and recorded water table depths is shown in Figure 7-3. The points below the diagonal show the occurrence of the simulated water table lower than the observed water table. Most of the close agreement between the data (near the diagonal) was observed during irrigation periods. The simulated results are discussed more particularly in the next sections.

Irrigation

At the beginning of the season, irrigation continued for approximately two weeks before interruptions occurred due to rainfall on Julian days 72 and 73. It was observed during this initial irrigation period that there was a change in water table depth control, because it was observed that the moisture was not adequate in the root zone. Later in the growing season, as the plant root zone increased and the field plot appeared to be wetter than desired, the control depth was reset to a lower position (around Julian day 93).

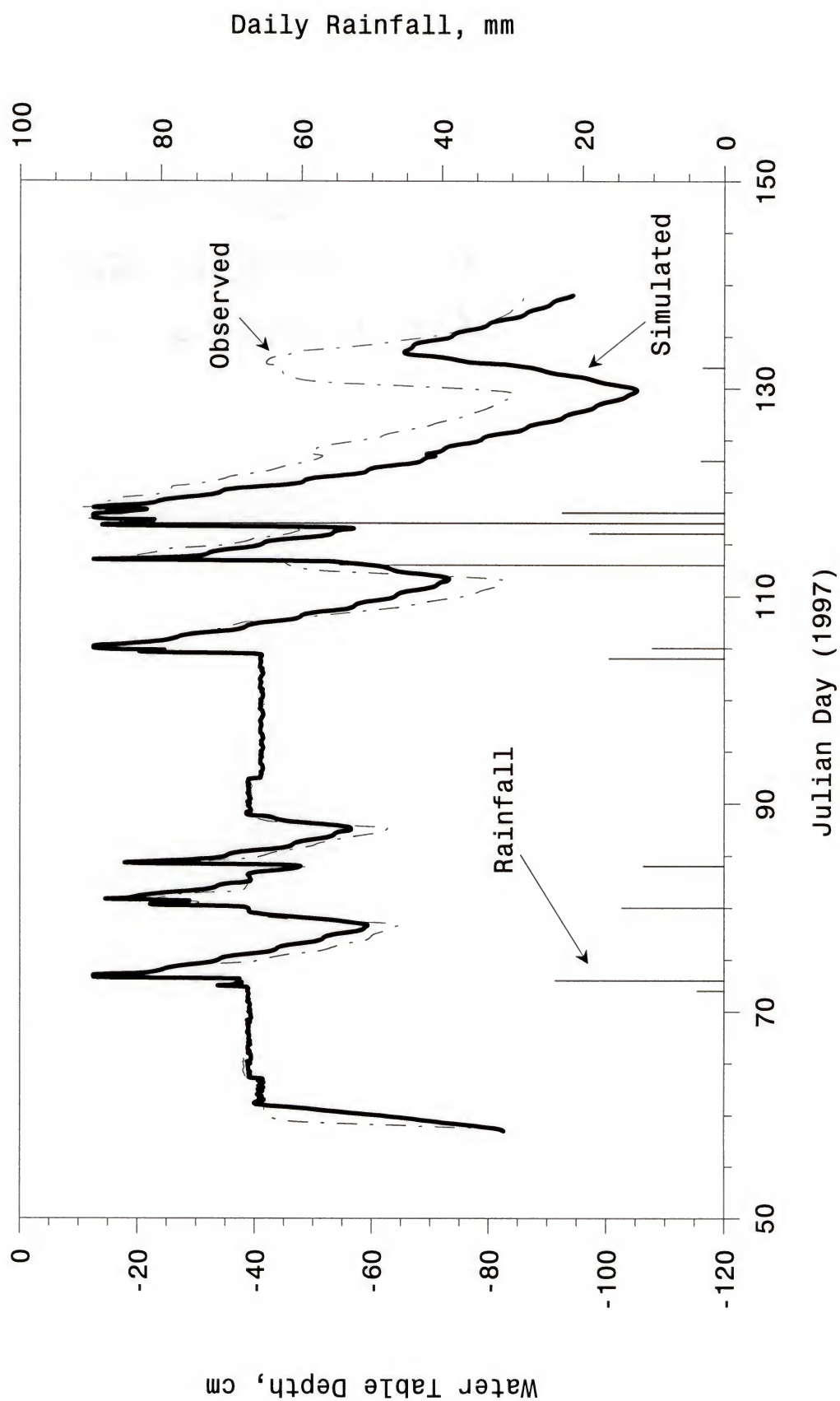


Figure 7-2: Observed and simulated water table in the 1997 growing season.

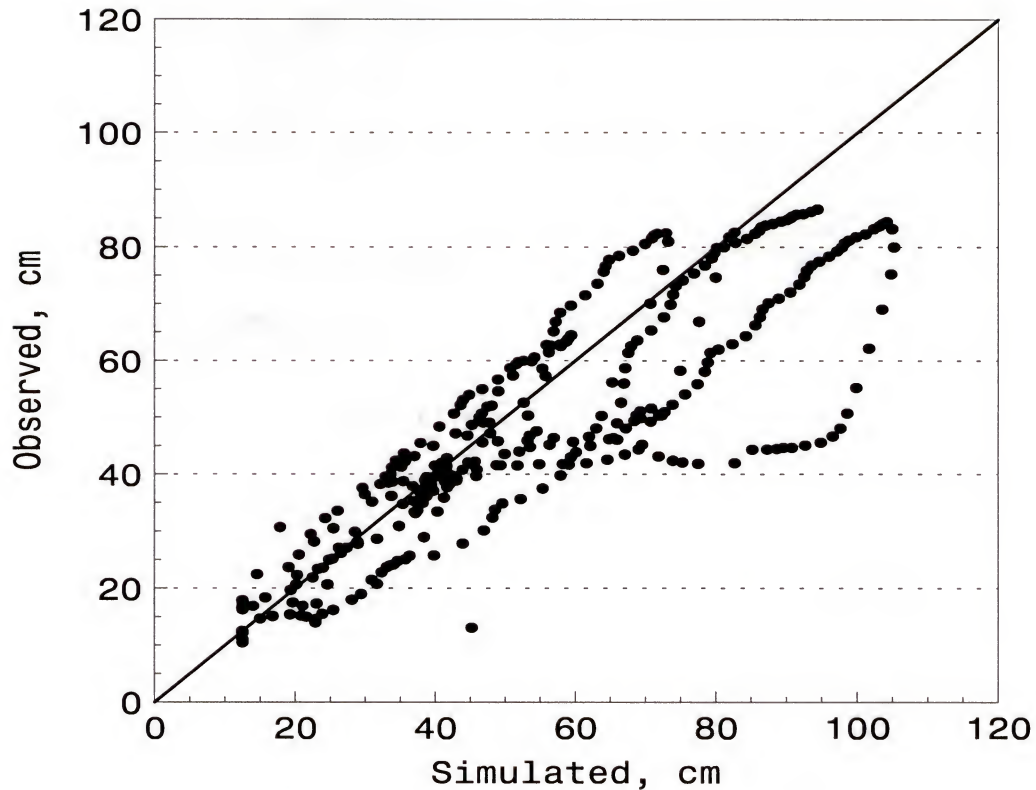


Figure 7-3: Scattergram of observed and simulated water table depth (taken positive downward) in the 1997 simulation.

Sustained irrigation was initiated on Julian day 87 and continued until rain occurred on Julian days 104 and 105. Irrigation occurred only very briefly between rains at other times during the season. Rainfall was highly effective during the 1997 simulation period, as irrigation was required on only 43 days during the 107-day total growing season. Cumulative irrigation applications and daily rainfall are shown in Figure 7-4. The curves are very close most of the time, and differ at the end of the season due to the deeper simulated water table depth at that time.

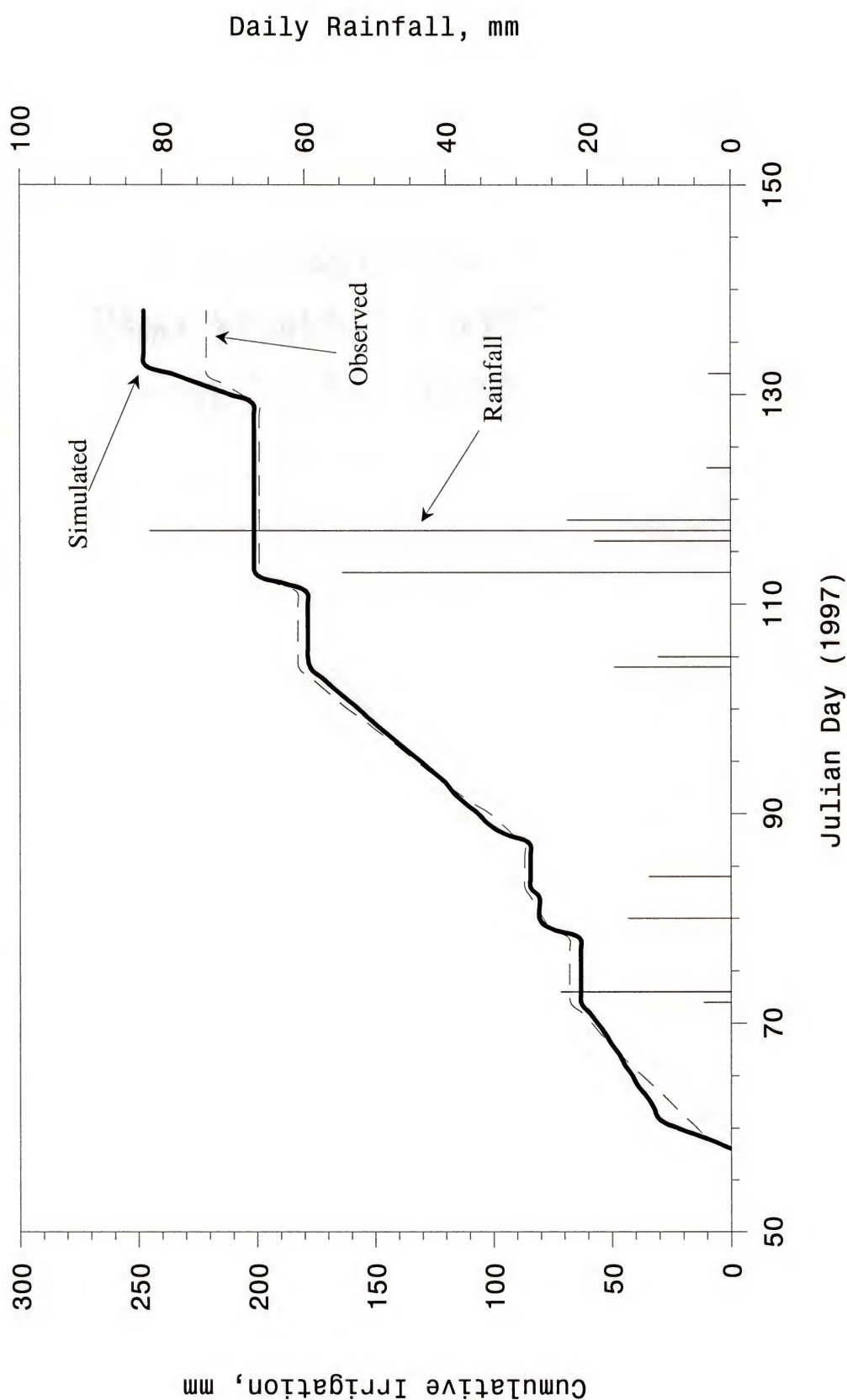


Figure 7-4: Cumulative observed and simulated irrigation in the 1997 growing season.

The total hours of irrigation were approximately 490 hr for the simulation and 439 hr for the observed data. The applied irrigation amounts were 247 mm and 221 mm, respectively, for the simulation and field data. These results were very reasonable in terms of prediction of the amount of irrigation required for the entire season, considering that the model assumed a uniform rate of application throughout the season. Field observations showed a variation in flow rate due to partial clogging of the emitters, and weekly flushing of the pipelines and filters was necessary. Due to this intensive clogging control, calibrations during the crop growth period showed that the irrigation application rate was slightly higher than the designed application rate, and a different irrigation rate from the first year of simulation was used in this season ($QIRRI = 1.179 \text{ cm/hr}$).

The large difference in irrigation volume during the late part of the season in the simulation occurred because the antecedent water table depth was very low. The simulated irrigation in that period did not raise the water table to the desired depth since the irrigation was turned off before the water table reached the depth control. As discussed in the previous chapter, this problem was caused by the unsaturated conditions estimated by the model. Also, the crop evapotranspiration during the late season could be overestimated, contributing to the excessive drainage.

It was interesting to observe the irrigation profile along the field. Figure 7-5 shows the irrigation profile at the simulated grid in two distinct periods, early (Julian day 65) and mid irrigated seasons (Julian day 100). The difference between the profiles was due, first to the different irrigation applied control depths, and second to the different magnitudes of crop evapotranspiration (ET_c) between the two periods (data taken at noon). As expected, the water table was always higher near the irrigation lines. No field

profile measurements were made at those times, but observations done on different occasions showed the same profile shape. The influence of the daily sinusoidal distribution of ET_c in the irrigation profile is shown in Figure 7-6 for 0 hr and 12 hr of the same day (Julian day 100). At 0 hr, the shape of the water table profile was practically a straight line because the evapotranspiration was so small that the entire water table profile was maintained at the control depth (the irrigation was minimum). At noon, with the influence of the crop evapotranspiration, the irrigation was practically continuous and the shape of the curve is an ellipse in which the lowest point is at the midpoint between the irrigation lines.

Runoff

Runoff from the same experimental plot was continuously measured throughout the growing season. A sump was installed in the water furrow and water was collected in the sump by gravity flow. Water was pumped out using a sump pump, and volumes were measured using a timer, event recorder and flow meter (installed for this season).

Figure 7-7 shows rainfall and the cumulative simulated and observed runoff throughout the season. The data were very consistent throughout the season, with runoff patterns very similar following large rainfall events. More runoff occurred for the first two events in the simulation and the opposite occurred for the rest of the events. The greatest deviation between the observed and simulated runoff amounts occurred as a result of the very large (124 mm) rainfall that occurred on Julian day 116-118. During this event, the entire research area was flooded and it was likely that runoff from surrounding roadways and an adjacent pine plantation may have contributed to the

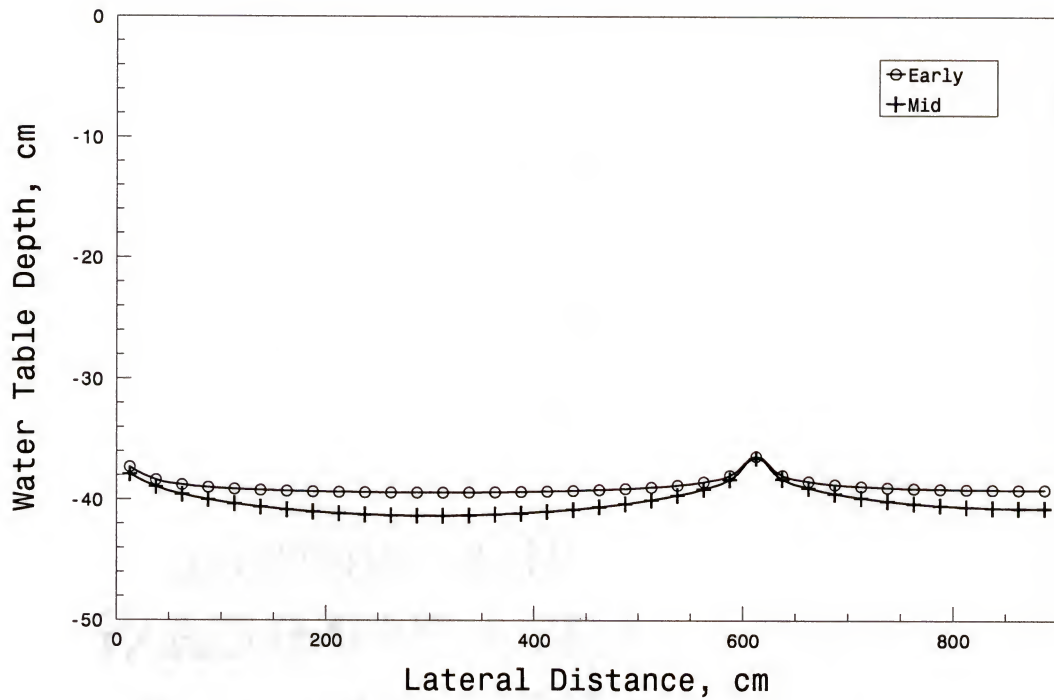


Figure 7-5: Water table profile during irrigation in the early and mid seasons.

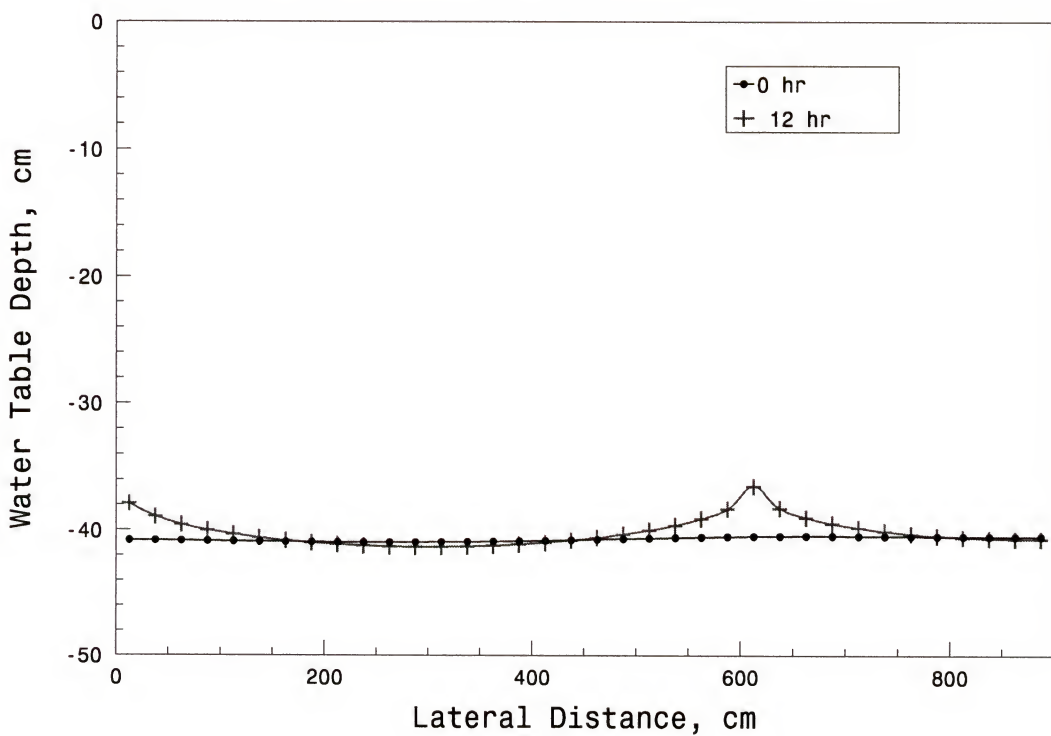


Figure 7-6: Water table profile during irrigation in the early and mid hours of the day.

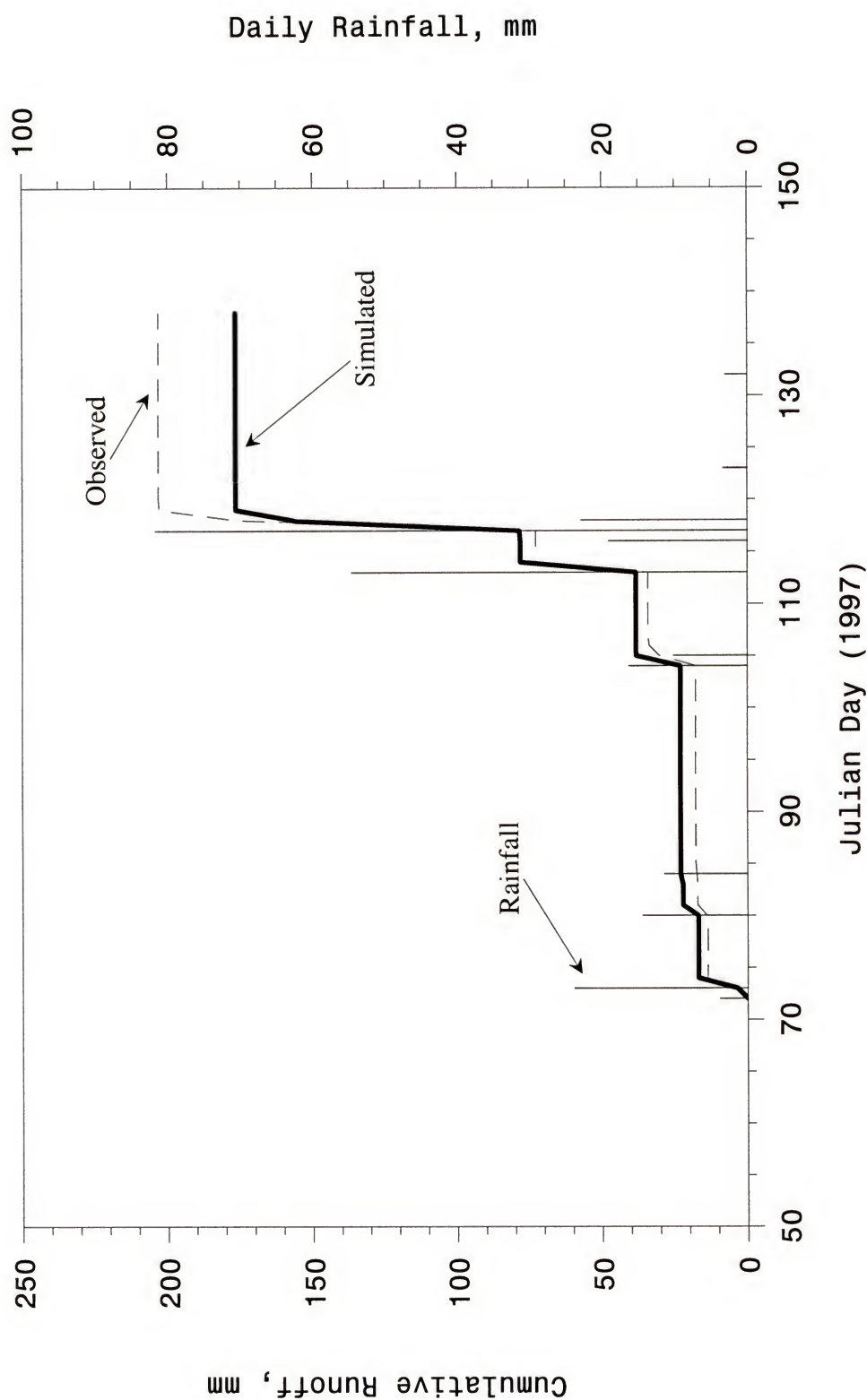


Figure 7-7: Cumulative observed and simulated runoff in the 1997 growing season.

discrepancy observed. Also, the soil profile was already well saturated from the previous rain, contributing to the excess of runoff.

Because the amount of runoff that occurs from a given rainstorm depends on both the amount of rain and the amount of moisture that was in the soil profile when the rain occurs, usually it was difficult to predict runoff as a simple function of rainfall. Considerable work has been done on this subject, especially in recent years in Florida where problems associated with runoff of nutrients into south Florida watersheds have received much attention. Heatwole et al. (1987) modified the CREAMS (Knisel, 1980) water quality model to improve its prediction of runoff for typical flat sandy, high water table watersheds in south Florida. Capece et al. (1987, 1988) evaluated various models for estimating runoff volumes and peak runoff rates for typical Florida flatwoods watersheds. After comparing seven different modifications of the model, they found that several forms of the SCS runoff equation worked well for Florida conditions. They found best agreement when the form of the model that was used included a means of measuring antecedent moisture conditions that exist when rain occurs.

The SCS runoff equation is given as

$$Runoff = \frac{(Rain - 0.2 * S)^2}{Rain + 0.8 * S} \quad (7.1)$$

where *Runoff* and *Rain* are given in units of depth (L) or volume per unit land ($L^3 L^{-2}$) and *S* is the watershed storage factor, given in the same units.

Effective rainfall is that portion of rainfall that reduces the amount of water that otherwise must be provided to meet the crop water requirement. As a matter of fact, effective rainfall also includes water lost to deep percolation and lateral flow (interflow) that occurs as the water table is maintained high during subirrigation.

Smajstrla et al. (1998) developed a numerical model for the estimation of runoff and effective rainfall using data from the field site used in this work. They used the SCS equation, with S being calculated as the water table response to rainfall. They found that the watershed storage factor was zero when the water table reached the bottom of the beds because, at this level, surface water drained from the alleyways between the plant rows. This is in perfect accordance with the way that surface runoff was treated in our model. Their results were very similar to those obtained in this work.

The model used in this work could predict runoff very well as a function of rain, as can be seen in Figure 7-8, where a straight line can be traced uniting the simulated points. It seems that the model handled correctly the available storage capacity that was primarily a function of the water table depth when the rain occurs. The discrepancy between simulated and observed runoff data for the last storm can be observed in Figure 7-8, where the measured runoff was slightly higher than the amount of rainfall for that storm, corroborating the fact that surrounding areas contributed to the runoff. Also, the modification in the top surface boundary (flat surface instead of beds) and the handling of seepage at the face of the drain seem to have worked very well.

Deep Percolation

Since there is little specific data related to this pathway, its inclusion in the model was more empirical. A small amount of percolation was simulated, in part as a demonstration of the model. The model sensitivity to this parameter is discussed later in this chapter.

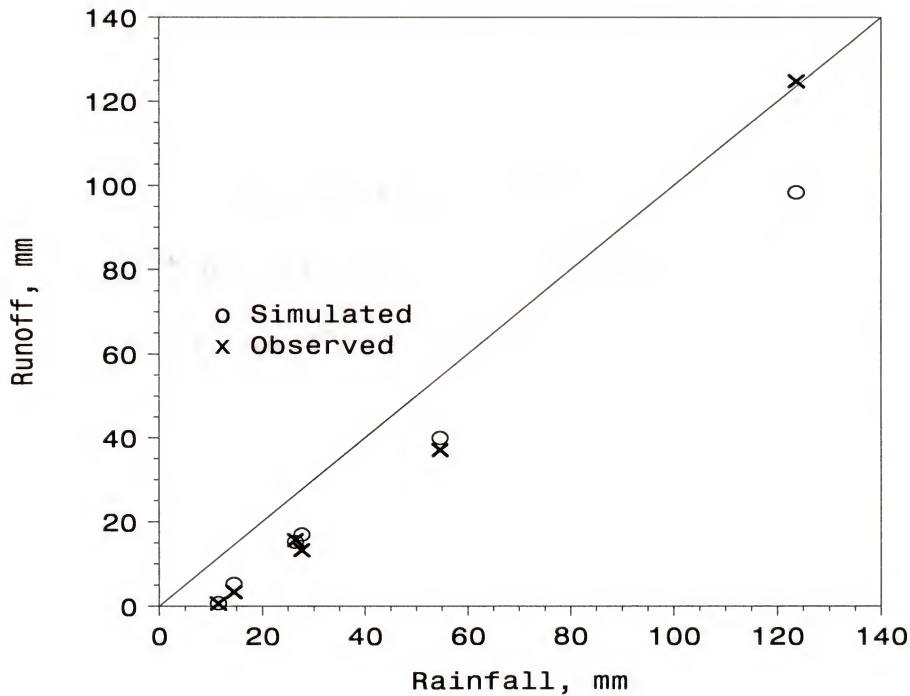


Figure 7-8: Measured rainfall versus simulated and observed runoff during the 1997 simulation period.

Water Balance

Water balance data for the 1997 period of verification showed that the rainfall and irrigation the system primarily by evapotranspiration, secondarily by runoff, and thirdly by deep percolation (Table 7-1). In a long-term simulation, the change in storage is practically negligible. Again the final mass balance error was very low, around 0.05%, running with an average time step of 0.005 hr.

Considering the above discussion, the model simulates the field site very well. Water table levels, irrigation, and runoff were predicted reasonably well, showing mainly that the modifications in the soil hydraulic properties were in the correct direction to represent adequately the field conditions.

Table 7-1: Water Balance for the 1997-simulation period.

Mass Balance Term	Value (mm)
Initial Storage	483
Precipitation	265
Irrigation	248
Deep Percolation	69
Crop Evapotranspiration	277
Total Runoff	177
Final Storage	473

Sensitivity Analysis

The 1997 simulation described above was used as the base simulation for the parameter sensitivity analysis. The effect of a parameter on model response may vary greatly between a wet and a dry year. Parameters chosen for analyses included soil characterization, climate data, deep percolation rate, and irrigation application rate.

Because the magnitudes and the range of variation of the various parameters may be greatly different, a standard percentage change in parameters was not used. Rather, parameters were varied from the base value according to the reasonable range of values for that parameter.

Coleman and DeCoursey (1976) presented a methodology for employing model sensitivity analysis to estimate the reduction in variance achieved by model modification; the achieved reduction in variance provides a basis for determining whether the modification is justified. The method defines sensitivity (S) as the derivative of model results (R) with respect to a parameter (P) of interest. Therefore,

$$S = \frac{\partial R}{\partial P} \quad (7.2)$$

Relative sensitivity (S_r) was defined as

$$S_r = \frac{\partial R}{\partial P} \frac{P}{R} \quad (7.3)$$

Relative sensitivity provides a consistent basis for comparing various parameters and concentrating research and data collection on the more sensitive. A value of zero means that a change in the parameter had no effect on the output. A value of one means the output changes by the same percentage the parameter is changed.

The results of the sensitivity analysis for the model used in this work are shown in Table 7-2. The actual values of the variables and the base simulation values have also been included in the table for reference.

The following observations were made:

1. The model had low sensitivity to changes in the saturated hydraulic conductivity values, at least within the range of variation in the sensitivity analysis.
2. The model was more sensitive to low values for the parameter n in the van Genuchten's equation than it was for higher values. Low values of n also resulted in a very poor mass balance, resulting from the effect of n on water flow. Low values of n have a choking effect on flow because of the very small pores which occur in a medium with a broad pore size distribution (Wise, 1991).
3. Changes in the parameter α in the van Genuchten's equation did not have much effect on the model's response.
4. The model was moderately sensitive to evapotranspiration as a daily input in both directions. Higher values of ET leave less water in the profile for runoff

and deep percolation, and require more irrigation. Because ET was an input it was not affected by any changes in the other parameters.

5. Runoff was very sensitive to changes in precipitation amounts but precipitation had very little effect on deep percolation and irrigation volumes. Some influence on irrigation would be expected if not only the total volume of precipitation but also the rainfall distribution were changed.
6. Total absence of percolation slightly increased the runoff amount and decreased the irrigation volume. Increasing the rate of deep percolation had the opposite effect. Note that doubling the rate of percolation means that the water table position drops faster but the amount of percolated water did not increase in the same proportion because of the relationship between water table position and rate of percolation.
7. Irrigation rate had little effect on runoff and percolation. The effect on runoff was due more to the existing profile of the water table during irrigation before the rains occurred. Irrigation volumes were not affected in the same proportion as the changes in the parameter because the number of hours of irrigation varied for each rate. For instance, reducing the rate of irrigation to half of the base-value resulted in the hours of irrigation system operation increasing 67% (data not shown in the table) but the irrigation volume was reduced about 17%.

Table 7-2: Sensitivity analysis of selected parameters for the 1997 simulation period.

Parameter (Base)	Param. Value	% of Base	Runoff (mm)	Percolation (mm)	ET (mm)	Irrigation Value (mm)
			Value	Sens.	Value	Sens.
BASE SIMULATION						
			172.35	69.09	276.53	247.98
K_s (cm hr ⁻¹) (7.80)	3.90 11.70 15.60	-50 +50 +100	165.84 172.82 172.40	0.076 0.006 0.000	69.45 69.02 69.02	-0.010 -0.002 -0.001
n (1.28)	1.024 1.536 2.560	-20 +20 +100	45.67 165.15 150.85	3.675 -0.209 -0.125	40.99 72.14 72.33	2.034 0.221 0.047
α (0.0175)	0.014 0.021 0.035	-20 +20 +100	176.98 168.14 154.09	-0.134 -0.122 -0.106	66.74 70.79 75.20	0.170 0.123 0.088
ET (mm)	-20 +20	184.97 161.76	-0.366 -0.307	72.47 66.31	-0.245 -0.201	221.22 331.84
Rain (mm)	-20 +20	124.67 220.62	1.383 1.400	68.31 69.41	0.056 0.023	276.53 276.53
Percolation Rate (cm hr ⁻¹)	-100 +100	188.35 158.05	-0.093 -0.083	0.00 131.81	1.000 0.908	276.53 276.53
Irrig. Rate (cm hr ⁻¹) (1.1788)	0.5894 1.7682	-50 +50	156.98 178.64	0.178 0.073	64.78 71.47	0.125 0.069

CHAPTER 8

SUMMARY, CONCLUSIONS AND RECOMMENDATIONS

Summary

In northeast Florida, potatoes are grown on beds in sandy soils that require irrigation even if they are subject to naturally occurring high water tables. Fully-enclosed subirrigation using buried microirrigation tubing is one of the methods feasible for irrigating potatoes under these conditions, with the advantage of reducing runoff and irrigation requirements as compared to conventional semi-closed seepage irrigation.

A two-dimensional finite difference model was developed to simulate the transient movement of water table during drainage, subirrigation, rainfall, and root extraction in a soil profile overlaying a shallow water table and irrigated with buried microirrigation line sources. As part of the model development, its various components were tested by comparing the simulated results with other published numerical solutions, including problems of infiltration, drainage and evapotranspiration. The results of the model and the examples were in very good agreement, which confirms that the model was suitable for application.

The model was calibrated and verified by comparing simulated results with experimental field observations on water table management research plots. The site used for this research was located near Hastings, FL. To describe the soil hydraulic properties, which are nonlinear functions in the model, the van Genuchten equation was used. Climatic inputs needed were rainfall and potential evapotranspiration.

The governing equation of the model is the two-dimensional Richards equation. The flow equation was written with pressure head as the dependent variable in a fully implicit block-centered backward difference finite difference scheme with explicit linearization of soil parameters. The resultant system of equations was solved by a Gaussian elimination method.

The model simulates water movement from a subsurface drip irrigation system with an automated controller for the water table level, and the response of the water table to precipitation, evapotranspiration, and deep percolation. The water uptake by plant roots was simulated by an extraction function with a root distribution term. Deep percolation was modeled with a water table-drainage flux relationship. Runoff was simulated at the surface and at the face of the water furrow located at the right boundary. The model results were in good agreement with the field data. A sensitivity analysis was performed on the model to observe the influence of some parameters on model response.

Conclusions

1. The model can give reasonable predictions of seasonal runoff, irrigation volume, and water table levels during crop growth.
2. The two-dimensional model can be used to investigate different irrigation strategies involving water table management control. Applications of the model include using it to optimize the depth of water table for each growth stage, and to optimize the duration, frequency, and rate of irrigation.

Recommendations for Future Research

The model was developed in a modular form to allow updating model components as improved methods are developed or the capabilities of existing ones are expanded. Such changes would include improvements to the treatment of soil hydraulic properties, root water extraction, runoff, deep percolation and irrigation control.

Research is needed into the incorporation of the model as the basis for a control strategy of a field water table management project. Such incorporation involves its use as a management tool and its eventual use as an automated controller in real time (expert system) of the water table, based on climate, soil, field, crop, and growth season.

Additional evaluation of the soil hydraulic properties is needed to clarify the parameter values appropriate for the field conditions. Other methods for the prediction of the soil hydraulic functions need to be tested. The model can be applied to study the effect of spatial variability of the soil hydraulic properties on drainage and subirrigation.

Future improvements of the model include the addition of subirrigation by seepage to expand the range of problems that may be simulated.

APPENDIX A MODEL ORGANIZATION

The computer model consists of a main program and 11 subroutines. The subroutines are stored and compiled separately and then linked together with the main program to form an executable program. Below is a list and brief descriptions of the source files and the associated subroutines.

Main program unit WATABLE_2D

This is the main program of the model. The unit controls execution of the model and determines the order that the subroutines are called.

Subroutine INPUT_2D

This unit is designed to read data from different input files. Table A-1 summarizes from which input file particular information is read.

Subroutine UPDATE_2D

This unit uses van Genuchten equation to compute the values of water content, soil water capacity, and hydraulic conductivity corresponding to a calculated water pressure at each time step.

Table A-1: Input files and type of information read.

Name of the File	Information Read from the File
SOIL.INP	Number and position in the profile of soil materials Hydraulic parameters
SELECTOR.INP	Time information Initial fluxes at the boundaries Initial position of water table Print information
INITHEAD.INP	Initial water pressures at each node (if this option is selected)
GRID.INP	Nodal information Boundary geometry information
PRECIP.INP	Hourly precipitation
ETO.INP	Daily potential evapotranspiration

Subroutine CONDUC_2D

This unit determines the internode hydraulic conductivity using a pre-determined method (geometric, arithmetic, etc.).

Subroutine ROOT_2D

This unit computes the root distribution for each cell in the profile, corresponding to the fraction of the evapotranspiration rate extracted from each cell.

Subroutine ETDIST_2D

This unit uses a sinusoidal function to compute the evapotranspiration rate for each cell at each time step using the root distribution term calculated in ROOT.

Subroutine WATFLOW_2D

This unit calculates the flow at each interior node and at the boundaries (runoff, seepage, deep percolation).

Subroutine TIME_2D

This unit determines the value of the time increment and updates the time-dependent variables.

Subroutine RESET_2D

This unit constructs the global matrix equation for water flow, including the right hand side vector.

Subroutine BANDSOLVE_2D

This unit solves the banded symmetric matrix equation for water flow by Gaussian elimination with row interchanges, followed by back substitution. This subroutine is called in the RESET_2d subroutine.

Subroutine MASSBAL_2D

This unit calculates the mass balance error at each time step by comparing the sum of inflows, outflows, initial water storage and final water storage in the profile.

Subroutine OUTPUT_2D

This unit is designed to print computed data in different output files at prescribed times. Table A-2 summarizes where particular data are printed.

Table A-2: Output files and type of data printed.

Name of the File	Information Printed to File
BALANCE.OUT	Basic information about the simulation Initial and boundary conditions Mass balance
HEADS.OUT	Water pressures at each node
WTDEPTH.OUT	Water table depth along the horizontal profile
FLUX.OUT	Flux and soil hydraulic data at a particular position in the profile.

A significant list of common variables is presented in Table A-3. Local variables are defined in each subroutine.

Table A-3: List of significant variables of the two-dimensional model.

Variable	Definition
Alpha	Alpha parameter in van Genuchten equation
Bottom	Depth of simulated soil profile, (L)
Cond	Unsaturated hydraulic conductivity, (LT^{-1})
Conds	Saturated hydraulic conductivity of each layer, (LT^{-1})
Controlprint	Interval to print outputs, (T)
Cum_time	Cumulative time of simulation, (T)
Depth(j,i)	Vertical distance from the surface to center of cells, (L)
DT	Time step, (T)
DTmax	Maximum size of time step, (T)
DTmin	Minimum size of time step, (T)
DX(i)	Grid size in the horizontal (x) direction, (L)
DZ(j)	Grid size in the vertical (z) direction, (L)
DY	Grid size in the y-dimension (L)
D1(j)	Distance between nodes at (J,I) and (J-1,I), (L)
D2(j)	Distance between nodes at (J,I) and (J+1,I), (L)
D3(i)	Distance between nodes at (J,I) and (J,I-1), (L)
D4(i)	Distance between nodes at (J,I) and (J,I+1), (L)
ETP	Daily predetermined potential evapotranspiration (LT^{-1})
ETRate	Hourly evapotranspiration rate (LT^{-1})
H(j,i)	Soil water pressure at each cell (L)
I	Counter in the horizontal (x) direction
IDAY	Current Julian day of the simulation
IENDAY	Julian day that simulation ends
IX	Number of cells in the horizontal direction
J	Counter in the vertical direction (z)
JZ	Number of nodes in the vertical(z) direction
K1(j,i)	Hydraulic conductivity at the top surface of a cell (LT^{-1})
K2(j,i)	Hydraulic conductivity at the bottom surface of a cell (LT^{-1})
K3(j,i)	Hydraulic conductivity at the left surface of a cell (LT^{-1})
K4(j,i)	Hydraulic conductivity at the right surface of a cell (LT^{-1})
LAH	Annual hour (T)
Length	Length of the soil profile in the y-direction (L)
Precip	Hourly precipitation (LT^{-1})
QB(i)	Flux across the bottom boundary (LT^{-1})
Qirri	Irrigation rate (LT^{-1})
QL(j)	Flux across the left boundary (LT^{-1})
QR(j)	Flux across the right boundary (LT^{-1})
QS(i)	Flux across the top boundary (LT^{-1})
Q1(j,i)	Flux across the top surface of a cell (LT^{-1})
Q2(j,i)	Flux across the bottom surface of a cell (LT^{-1})
Q3(j,i)	Flux across the left surface of a cell (LT^{-1})

Table A-3--continued

Variable	Definition
Q4(j,i)	Flux across the right surface of a cell (LT^{-1})
S(j,i)	Soil water extraction in the cell (T^{-1})
Sink(j,i)	Sink term in the cell (T^{-1}) (if exists)
Time_of_irrigation	Cumulative time of irrigation during simulation (T)
SWC(j,i)	Soil water capacity (L^{-1})
TAREA	Total surface of the soil profile (L^2)
Time24	24 hr time counter (T)
VN	<i>n</i> parameter in van Genuchten equation
WC(j,i)	Water content of a cell (L^3L^{-3})
WCR	Residual water content of the soil in each layer (L^3L^{-3})
WCFC	Water content of the soil at field capacity in each layer (L^3L^{-3})
WCS	Saturated water content in each layer (L^3L^{-3})
WCWP	Water content at wilting point in each layer (L^3L^{-3})
Width	Width of the soil profile in the horizontal (x) direction (L)
WF_depth	Depth of the water furrow (L)
WTdepth	Depth of the water table in each grid I (L)

APPENDIX B
NUMERICAL MODEL PROGRAM LISTING

```
*****
*          WATABLE_2D
*
*  NUMERICAL MODEL OF TWO-DIMENSIONAL FLOW IN A VARIABLY
*  SATURATED POROUS MEDIUM CONFIGURED TO SIMULATE SOIL
*  WATER INFILTRATION, REDISTRIBUTION, AND ROOT EXTRACTION,
*  SUBSURFACE DRIP IRRIGATION AND HIGH WATER TABLE
*
*  DEVELOPED BY JADIR ROSA
*****
PROGRAM WATABLE_2D
```

PARAMETER(

```
.IS=90, ! Maximum number of internal nodes in the x-direction
.JS=40, ! Maximum number of internal nodes in the z-direction
.LD=365) ! Number of days in which the simulation was performed
```

```
IMPLICIT DOUBLE PRECISION(A-H,K,O-Z)
DOUBLE PRECISION LAH
```

CHARACTER*15 DYN

CHARACTER*20 SOIL_ID

CHARACTER*10 IRRICONTROL

CHARACTER*15 CONTROLPRINT

CHARACTER*15 SURFRUN, SEEP

CHARACTER*15 HYSTERESIS

DIMENSION

```
.S(JS,IS),QB(IS),QL(JS),QR(JS),QS(IS),DX(IS),DZ(JS),DEPTH(JS),
.RADIUS(IS),H(JS,IS),OLDH(JS,IS),K1(JS,IS),K2(JS,IS),K3(JS,IS),
.K4(JS,IS),COND(JS,IS),SWC(JS,IS),WC(JS,IS),ETP(LD),RDT(JS,IS),
.PRECIP(LD,0:23),WTDEPTH(is),NBeginRow(8),NEndRow(8),ThickLayer(8),
.VN(8),ALPHA(8),COND(8),WCR(8),WCS(8),WCFC(8),WCWP(8),KS(JS),
.Deltaflux(js,is),SINK(JS,IS),Q1(JS,IS),Q2(JS,IS),Q3(JS,IS),
.Q4(JS,IS),fluxdelta(js,is),D1(JS),D2(JS),D3(IS),D4(IS),
.QSRUNOFF(IS),SEEP(JS)
```

```
OPEN (UNIT=7, FILE='Balance.out',STATUS='UNKNOWN')
OPEN (UNIT=8, FILE='HEADS.OUT',STATUS='UNKNOWN')
OPEN (UNIT=11, FILE='WTDEPTH.OUT',STATUS='UNKNOWN')
OPEN (UNIT=12, FILE='FLUX2D.OUT',STATUS='UNKNOWN')
```

```
***** READING THE INPUT FILES AND INITIALIZING VARIABLES **
```

Call Getdat(i,i,iday)

Call Gettim(ihours,mins,isecs,i)

Rt0 = iday*24.*60.+ihours*60.+mins+isecs/60.

DYN = 'INITIAL'

```
CALL INPUT_2D(
.SOIL_ID,NLayers,VN,ALPHA,COND,WCR,WCS,WCFC,WCWP,PRINTCONTROL,
.ITERMAX,IDAY,IENDAY,Time_Begin_Sim,Time_End_Sim,DTMIN,DTMAX,
.DY,TAREA,JZ,IX,TSTART,TEND,SINIT,DX,DZ,DEPTH,RADIUS,H,
.ETP,PRECIP,QIRRI,BOTTOM,WIDTH,WT_Initial,jwt,D1,D2,D3,D4,
.NBeginRow,NEndRow,ThickLayer,WF_depth,NWFZ,NWFX,IL1,IL2,JL,IC,
.INTERNODE_K)
```

```

CALL UPDATE_2D(
.NLayers,ALPHA,VN,WCS,WCR,COND$,$IX,$JZ,$H,OLDH,DZ,WC,SWC,COND,KS,
.Depth,Drain,DX,DY,WTDEPTH,jwt,NBeginRow, NEndRow,Bottom,NWFX,
.precip,l$dd,lhh,RAIN,HYSTERESIS,wta)

CALL CONDUC_2D(
.DYN,H,IX,JZ,NWFX,NWFZ,COND,precip,K1,K2,K3,K4,INTERNODE_K)

CALL MASSBAL_2D(
.DYN,IX,JZ,DX,DZ,DY,TAREA,BOTTOM,QB,QL,QS,QR,S,WC,WCS,IRRICONTROL,
.QIRRRI,DT,Drain,Delta_mass,Error_mass,Porc_mass,Storage,QRUNOFF,
.Sim_mass,Storage_initial,Storage_maximum,Runoff, SINK,NWFZ,
.Root_extraction,Cum_perc,Cum_irrig,Water_in,Old_storage,
.Actual_balance,NLayers,QBWF,H,b,Cum_precip,SURFRUN,Seepage,
.PRECIP, LDD, LHH,EXCESS,IL1,IL2,JL)

CALL ROOT_2D (IX,JZ,DX,NWFX,RDT)

CALL TIME_2D(
.DYN,IX,JZ,S,DX,DZ,fluxdelta,DTMAX,DTMIN,SINK,precip,H,
.Time_Begin_Sim,Cum_Time,TIME24,IDAD,DT,HOUR,LDD,LHH,LAH,DEPTH,
.Time_End_Sim,q1,q2,q3,Q4,a,b,wc,SWC,COND,CONTROLPRINT,
.PRINTCONTROL,Time_of_irrigation)

CALL WATFLOW_2D(
.DYN,IX,JZ,QSINIT,QBINIT,QLINIT,QRINIT,DX,DZ,K1,K2,K3,K4,H,TIME24,
.Cum_time,Time_End_Sim,Hour,LDD,LHH,Depth,WC,SWC,Precip,QS,QB,QL,
.QR,fluxdelta,NWFZ,NWFX,COND,SINK,Q1,Q2,Q3,Q4,QBWF,wf_depth,a,IDAD,
.oldh,QIRRRI,wtdepth,COND$,$D1,$D2,$D3,$D4,Time_Begin_Sim,KS,
.bottom,CONTROLPRINT,SURFRUN,LAH,QRUNOFF,IL1,IL2,JL,IC,
.SEEP)

CALL OUTPUT_2D(
.DYN,SOIL_ID,JZ,IX,IDAD,Cum_Time,Time_End_Sim,IENDAY,TIME24,DT,
.Storage_initial,Storage,Actual_balance,Water_in,Time_Begin_Sim,
.Root_extraction,Cum_irrig,Cum_perc,Sim_mass,QS,LAH,B,Seepage,
.Porc_mass,Runoff,QB,QIRRRI,PRECIP,LDD,LHH,RADIUS,BOTTOM,NITER,
.DEPTH,H,WTDEPTH,WT_Initial,Q1,Q2,Q3,Q4,SINK,Cum_precip,
.Time_of_irrigation,Kc)

***** Beginning of simulation loop *****

DYN = 'INTEG'

NITER = 0
ICOUNT = 0

100 CALL ETDIST_2D(
.DYN,TEND,TSTART,TIME24,IDAD,JZ,IX,TAREA,WCWP,WCFC,DY,NLayers,
.NBeginRow,NEndRow,WC,ETP,RDT,DZ,DX,SINIT,S,Smax,LAH,Kc)

400 CALL WATFLOW_2D(
.DYN,IX,JZ,QSINIT,QBINIT,QLINIT,QRINIT,DX,DZ,K1,K2,K3,K4,H,TIME24,
.Cum_time,Time_End_Sim,Hour,LDD,LHH,Depth,WC,SWC,Precip,QS,QB,QL,

```

```

.QR,fluxdelta,NWFZ,NWFX,COND,SINK,Q1,Q2,Q3,Q4,QBWF,wf_depth,a,IDAY,
.oldh,QIRRI,wtdepth,COND$,$D1,D2,D3,D4,Time_Begin_Sim,KS,
.bottom,CONTROLPRINT,SURFRUN,LAH,QSRUNOFF,IL1,IL2,JL,IC,
.SEEP)

500 CALL TIME_2D(
.DYN,IX,JZ,S,DX,DZ,fluxdelta,DTMAX,DTMIN,SINK,precip,H,
.Time_Begin_Sim,Cum_Time,TIME24,IDAD,DT,HOUR,LDL,LHH,LAH,DEPTH,
.Time_End_Sim,q1,q2,q3,Q4,a,b,wc,SWC,COND,CONTROLPRINT,
.PRINTCONTROL,Time_of_irrigation)

600 CALL RESET_2D(
.IX,JZ,NWFZ,IRRICONTROL,DT,DZ,DX,K1,K2,K3,K4,QS,QB,QR,QL,QBWF,SWC,
.S,SINK,H,DEPTH,WF_DEPTH,OLDH,WTDEPTH,QIRRI,D1,D2,D3,D4,
.SURFRUN,SEEP,LAH,Time_of_irrigation,IL1,IL2,JL,IC,NWFX,KS,COND,WTA)

700 CALL UPDATE_2D(
.NLayers,ALPHA,VN,WCS,WCR,COND$,$IX,JZ,H,OLDH,DZ,WC,SWC,COND,KS,
.Depth,Drain,DX,DY,WTDEPTH,jwt,NBeginRow,NEndRow,Bottom,NWFX,
.precip,ldd,ldh,RAIN,HYSTERESIS,wta)

800 CALL CONDUC_2D(
.DYN,H,IX,JZ,NWFX,NWFZ,COND,precip,K1,K2,K3,K4,INTERNODE_K)

900 CALL MASSBAL_2D(
.DYN,IX,JZ,DX,DZ,DY,TAREA,BOTTOM,QB,QL,QS,QR,S,WC,WCS,IRRICONTROL,
.QIRRI,DT,Drain,Delta_mass,Error_mass,Porc_mass,Storage,QSRUNOFF,
.Sim_mass,Storage_initial,Storage_maximum,Runoff,SINK,NWFZ,
.Root_extraction,Cum_perc,Cum_irrig,Water_in,Old_storage,
.Actual_balance,NLayers,QBWF,H,b,Cum_precip,SURFRUN,Seepage,
.PRECIP,LDL,LHH,EXCESS,IL1,IL2,JL)

```

! Count the number of iterations

```

NITER = NITER + 1
ICOUNT = ICOUNT + 1

IF (CONTROLPRINT == 'TRUE' .OR. Cum_Time == 0.0d00) THEN
  WRITE(6,950) TIME24,IDAD,Cum_Time,DT,LAH
950 FORMAT('Time =',F11.5,' hr',2x,'Day =',I3,6X,
  .' Cumulative Time =',F12.5,' hrs',/,
  .' Time Step =',F10.5,' hr',17X,'Annual hour = ',F10.0,/)
  WRITE(6,*)

```

```

CALL OUTPUT_2D(
.DYN,SOIL_ID,JZ,IX,IDAD,Cum_Time,Time_End_Sim,IENDAY,TIME24,DT,
.Storage_initial,Storage,Actual_balance,Water_in,Time_Begin_Sim,
.Root_extraction,Cum_irrig,Cum_perc,Sim_mass,QS,LAH,B,Seepage,
.Porc_mass,Runoff,QB,QIRRI,PRECIP,LDL,LHH,RADIUS,BOTTOM,NITER,
DEPTH,H,WTDEPTH,WT_Initial,Q1,Q2,Q3,Q4,SINK,Cum_precip,
.Time_of_irrigation,Kc)

```

END IF

```

IF(TIME24 >= TIME_END_SIM .AND. IDAY >= IENDAY) THEN

```

```
GO TO 1000
ELSE
GO TO 100
END IF

1000 Call Getdat(i,i,iday)
Call Gettim(ihours,mins,isecs,i)
Rtime = iday*24.*60.+ihours*60.+mins+isecs/60.
Write(6,*) 'Real time [min] = ',Rtime-Rt0
Write(7,*) 'Real time [min] = ',Rtime-Rt0
WRITE(6,1100)
1100 FORMAT('END OF THE SIMULATION')

1500 STOP
CLOSE(7)
CLOSE(8)
CLOSE(11)
CLOSE(12)
END
```

```
*****
*          INPUT_2D
* This subroutine READs in the input and initial values of the variables fro
* the files SELECTOR.INP, GRID.INP AND SOIL.INP. Hourly precipitatio
* is read from PRECIP*.INP and daily potential evapotranspiration from
* ETo*.INP (* means the year being simulated).
* INITHEAD.INP is used if input initial pressure heads (h) when a non-
* uniform initial conditions are desired.
*****
```

```
SUBROUTINE INPUT_2D (
  .SOIL_ID,NLayers,VN,ALPHA,CONDS,WCR,WCS,WCFC,WCWP,PRINTCONTROL,
  .ITERMAX,IDAD,IENDAY,Time_Begin_Sim,Time_End_Sim,DTMIN,DTMAX,
  .DY,TAREA,JZ,IX,TSTART,TEND,SINIT,DX,DZ,DEPTH,RADIUS,H,
  .ETP,PRECIP,QIRRI,BOTTOM,WIDTH,WT_Initial,jwt,D1,D2,D3,D4,
  .NBeginRow,NEndRow,ThickLayer,WF_depth,NWFZ,NWFX,IL1,IL2,JL,IC,
  .INTERNODE_K)
```

```
PARAMETER(IS=90,JS=40,LD=365)
IMPLICIT DOUBLE PRECISION(A-H, O-Z)
```

```
CHARACTER*20 SOIL_ID
```

```
DIMENSION
  .DX(IS),DZ(JS),DEPTH(JS),RADIUS(IS),H(JS,IS),ETP(LD),D4(IS),
  .PRECIP(LD,0:23),VN(8),ALPHA(8),CONDS(8),WCR(8),WCS(8),WCFC(8),
  .WCWP(8),NBeginRow(8),NEndRow(8),ThickLayer(8),D1(JS),D2(JS),
  .D3(IS),rainday(ld)
```

! Input the soil type and then open the appropriate soils' data
! file and read the soil hydraulic properties.

```
OPEN (UNIT=1,FILE='SOIL.INP', STATUS='OLD')
OPEN (UNIT=3,FILE='grid.INP', STATUS='OLD')
OPEN (UNIT=4,FILE='INITHEAD.INP', STATUS='OLD')
```

! OPEN (UNIT=2,FILE='SELECTOR96.INP', STATUS='OLD')
! OPEN (UNIT=5,FILE='ET_o_96.INP', STATUS='OLD')
! OPEN (UNIT=9, FILE ='PRECIP96.INP', STATUS='OLD')

```
OPEN (UNIT=2,FILE='SELECTOR97.INP', STATUS='OLD')
OPEN (UNIT=5,FILE='ETo_97.INP', STATUS='OLD')
OPEN (UNIT=9, FILE ='PRECIP97.INP', STATUS='OLD')
```

! Read the soil parameters for the selected soil from the appropriate data file. These parameters
! will be used in the subroutine UPDATE to compute values of water content, specific water
! capacity and hydraulic conductivity to a given pressure head.

```
READ(1,100) SOIL_ID,NLayers
100 FORMAT(10X,A,/,20X,I3,/)
! Read soil hydraulic parameters for each layer.
DO I=1,NLayers
  READ(1,110) NBeginRow(i),NEndRow(i),ThickLayer(i),VN(i), ALPHA(i),
  . CONDS(i),WCR(i), WCS(i),WCFC(i),WCWP(i)
110 FORMAT(8X,2(I10),F10.1,7(f10.5))
  END DO
```

```

!  Read the number of iterations (ITERMAX)
  READ(2,120) ITERMAX
120 FORMAT(59X, I5)

!  Read the simulation beginning day (IDAY) and the simulation ending
!  day (IENDAY)
  READ(2,130) IDAY,IENDAY
130 FORMAT(59X,I5/,59X,I5)

!  Read the simulation beginning and ending times
  READ(2,140) Time_Begin_Sim, Time_End_Sim
140 FORMAT (59X,D15.6/59X,D15.6)

!  Read in the minimum and maximum allowable timesteps (DTMIN, DTMAX)
  READ(2,150) DTMIN, DTMAX
150 FORMAT(59X,D15.6/59X,D15.6)

!  Read the weighting method for calculating internode hydraulic conductivity
!  1=arithmetic ; 2=geometric
  READ(2,155) INTERNODE_K
155 FORMAT(59X, I5)

!  Read in the initial flux across top, bottom, left and right boundary conditions
  READ(2,160) QSINIT,QBINIT,QLINIT,QRINIT
160 FORMAT(3(59X,F15.6/),59X,F15.6)

!  Read QIRRI (cm/hr), the application rate of a buried line source irrigation.
  READ(2,170) QIRRI
170 FORMAT(59X,F15.6)

!  Read in the initial constant extraction rate, SINIT, in units of 1/hr.
  READ(2,180) SINIT
180 FORMAT(59X,F15.6)

!  Read the number of cells in the z (vertical) and x (horizontal) directions.
  READ(3,200) JZ,IX
200 FORMAT(59X,I9/59X,I9)

!  Read the geometry of the water furrow
  READ(3,300) WF_depth,NWFZ,NWFX
300 FORMAT(59X,F9.2/59X,I5/59X,I5)

!  Read position of irrigation lines and control cell
  READ(3,305) IL1,IL2,JL,IC
305FORMAT(59x,I5/59x,I5/59x,I5/59x,I5,///)

!  Read the size of each row and column
  READ(3,*) (DX(I), I=1,IX)
  READ(3,*) (DZ(J), J=1,JZ)

!  CALCULATE WIDTH OF THE SIMULATED PROFILE
  WIDTH = 0.0D00
  DO I=1, IX-1
    WIDTH = WIDTH + DX(I)

```

```

END DO

! Calculate depth of the simulated profile
BOTTOM = 0.0D00
DO J=1, JZ
  BOTTOM = BOTTOM + DZ(J)
END DO

DY = 1.0D00 ! length of the profile simulated

TAREA = WIDTH * DY !TAREA = the total surface area of the profile

DO J=1,JZ-1
  D2(J) = (DZ(J) + DZ(J+1)) / 2.0
  IF (J > 1) D1(J) = (DZ(J) + DZ(J-1)) / 2.0
END DO
  DO I=1,IX-1
    D4(I) = (DX(I) + DX(I+1)) / 2.0
    IF(I > 1) D3(I) = (DX(I) + DX(I-1)) / 2.0
  END DO
  IF(J==JZ) D1(J) = (DZ(J) + DZ(J-1)) / 2.0
  IF(I==IX) D3(I) = (DX(I) + DX(I-1)) / 2.0

! Calculation of vertical distance from the surface to center of cells
DEPTH(1) = DZ(1)/2.0
DO J=2,JZ
  DEPTH(J) = DEPTH(J-1) + (DZ(J-1) + DZ(J))/2.0
END DO

! Calculation of horizontal distance from the origin
RADIUS(1) = DX(1)/2.0
DO I=2,IX
  RADIUS(I) = RADIUS(I-1) + (DX(I-1) + DX(I))/2.0
END DO

! Read the initial depth of water table and the row that corresponds to the depth of the water furrow.
READ(2,310) WT_Initial, jwt
310 FORMAT(59X,F5.6,/,59X,I5)

! Read initial condition for water pressure
READ(2,311) IHEAD
311 FORMAT(59X,I5)

IF(IHEAD) 315,320,350
*****
! Use this part for initializing a uniform soil water pressure.
315    Watpres= -10.0
      DO J=1, JZ
        DO I=1,IX-1
          H(J,I) = Watpres
        END DO
      END DO
      Go to 500
*****
! Read the initial water pressure from input file. In this case, the data can be original input or from

```

```

! previous simulation (there is an option to read Time_Begin_Sim and IDAY from this file).
320 READ(4,330) Time_Begin_Sim, IDAY
330 FORMAT(7X,F5.2,8X,I5)
  READ(4,*) 
  DO J=1,JZ
    READ(4,340) (H(J,I),I=1,IX)
340 FORMAT(6X,36F10.3)
  END DO
  Go to 500
*****
! The initial moisture profile is taken to be in equilibrium with the initial water table position.
350 DO J=1,JZ
  DO I=1,IX
    H(J,I) = Depth(j) - WT_Initial
  END DO
END DO
*****
500 DO J=1,NWFZ
  H(J,IX) = -1000.00D00
  END DO
  DO j=nwfz+1,jz
    IF(H(j,IX) > (depth(j) - nwfz*dz(j)) ) THEN
      h(j,ix) = depth(j) - nwfz*dz(j)
    END IF
  END DO
*****
! READ in the weather data, i.e. ETP, TSTART, TEND

  READ(5,560) TSTART,TEND,NDATA
560 FORMAT(//,8X,F8.2,/8X,F8.2,/,8X,I5,/)
  DO I=1,NDATA
    READ(5,570) M, ETP(M) ! evapotranspiration in mm/day
570 FORMAT(13X,I5,4X,F8.1)
  END DO
! go to 650 ! if using daily precipitation
*****
! If using hourly precipitation data
  READ(9,575) NDATA      ! number of precipitation data
575 FORMAT(//,8X,I5,/)
! Read daily precipitation values
  DO J=1,NDATA
580 READ(9,590) M,(PRECIP(M,I), I=0,23) ! precipitation in mm/hr

  590 FORMAT(I5,24F5.2)
  END DO

! Convert precipitation to cm/hr
600 DO J=IDAY,IENDAY
  DO I=0,23
    PRECIP(J,I) = PRECIP(J,I)/10.0
  END DO
END DO
go to 690
*****
* If using daily precipitation data:

```

```
650 READ(9,660) NDATA !NUMBER OF PRECIPITATION DATA
660 FORMAT(//,8X,I5,//)
  DO I=1,NDATA
    READ(9,670) M, RAINDAY(M) ! PRECIPITATION IN CM
  670 FORMAT(12X,I5,4X,F8.2)
  END DO
!      Distribute the daily rain uniformly over each day
  DO J=IDAY,IENDAY
    DO I=0,23
      PRECIP(J,I) = RAINDAY(J)/24.0
    END DO
  END DO
*****  

690 READ(2,700) PRINTCONTROL
700 FORMAT(59X,F9.2)

CLOSE (1)
CLOSE (2)
CLOSE (3)
CLOSE (4)
CLOSE (5)
CLOSE (9)

RETURN
END
```

```

* ****
*          UPDATE_2D
* This subroutine uses van Genuchten's equations to compute
* values of water content, WC, specific water capacity, SWC,
* and hydraulic conductivity, COND, corresponding to a given
* pressure head, h. Also, it calculates the water table depth at each
* time step.
* ****

SUBROUTINE UPDATE_2D(
  .NLayers,ALPHA,VN,WCS,WCR,COND$S,IX,JZ,H,OLDH,DZ,WC,SWC,COND,KS,
  .Depth,Drain,DX,DY,WTDEPTH,jwt,NBeginRow,NEndRow,Bottom,NWFX,
  .Precip,ldd,lhh,RAIN, HYSTERESIS, wta)

PARAMETER (IS=90, JS=40, LD=365)
IMPLICIT DOUBLE PRECISION(A-H,K, O-Z)
CHARACTER*15 HYSTERESIS
DIMENSION
  .DZ(JS),H(JS,IS),COND(JS,IS),SWC(JS,IS),WC(JS,IS),OLDH(JS,IS),
  .Depth(js),OldWC(js,is),DX(is),WTDEPTH(is),precip(ld,0:23),VM(8),
  .VN(8),ALPHA(8),COND$S(8),WCR(8),WCS(8),NBeginRow(8),NEndRow(8),
  .KS(JS)

***** ! Determine water table depth
wta=wtdepth(13) ! water table depth at the point control of irrigation
Do I=1,IX
Do J=1,JZ
If(H(J,I) <= 0.0D00 ) then
  Go to 3
Else
  WTDEPTH(I) = -( DEPTH(J) - H(J,I) )
  Go to 4
End if
3 End do
4 End do
***** 10 DO L=1, NLayers
  NBR = NBeginRow(L)
  NER = NEndRow(L)
  VM(L) = 1.0D00 - 1.0D00*VN(L)**-1.0D00 !m=1-1/n
  A = ALPHA(L)
  RN = VN(L)
  RM = VM(L)
  DELTAWC = (WCS(L) - WCR(L))
  DO J=NBR,NER
    KS(j) = COND$S(L)
    DO I=1,IX
      Head = ABS(H(j,i))
      B = 1.0d00 + (A*Head)**RN
      C = B**(-RM)
    
```

```
D= (A*HEAD)**(RN-1.0d00)
E= (1.0d00 - D*C)**2.0d00
F= B**(-RM*0.5d00)

IF (H(j,i) >= 0.00d00) THEN
  WC(j,i) = WCS(L)
  SWC(j,i) = 0.00d00
  Cond(j,i) = KS(j)

  ELSE
    WC(j,i) = WCR(L) + Deltawc * C
    SWC(j,i)=(A*RM*RN*DELTAWC) * (B**-1.0d00) *
      ( 1.0d00-(B**-1.0d00) )**RM
    COND(J,I) = (E*F)*KS(J)

  END IF

END DO
END DO

END DO

RETURN
END
```

```
*****
*          CONDUC_2D
*
*      This subroutine determines the conductivity at the four surfaces of
*      each cell, K1(top), K2(bottom), K3(left), K4(right), using arithmetic
*      or geometric averages.
*****
SUBROUTINE CONDUC_2D(
.DYN,H,IX,JZ,NWFX,NWFZ,COND,precip,K1,K2,K3,K4,INTERNODE_K)

PARAMETER (IS=90, JS=40,LD=365)
IMPLICIT DOUBLE PRECISION(A-H,K,O-Z)
INTEGER NWFX,NWFZ

CHARACTER*15 DYN

DIMENSION COND(JS,IS),K1(JS,IS),K2(JS,IS),K3(JS,IS),K4(JS,IS),
.H(JS,IS),precip(Id,0:23)

! Initialize hydraulic conductivities of the imaginary cells on the drain.

IF(DYN == 'INITIAL') THEN
  I=IX
  DO J=1, JZ
    K1(J,I)=0.0d00; K2(J,I)=0.0d00; K3(J,I)=0.0d00; K4(J,I)=0.0d00
  END DO
  END IF

! Update hydraulic conductivities at each time step

IF(INTERNODE_K == 2) GO TO 1000 ! GEOMETRIC WEIGHTING
*****
! USING ARITHMETIC WEIGHTING

DO J=1,JZ
DO I=1,IX-1

  IF (J == 1) THEN
    K1(J,I) = 0.0d00
  ELSE
    K1(J,I) = (COND(J,I) + COND(J-1,I))/2.0D+00
  ENDIF

  IF (I == 1) THEN
    K3(J,I) = 0.0d00
  ELSE
    K3(J,I) = (COND(J,I) + COND(J,I-1))/2.0
  ENDIF

  IF(I == IX-1) THEN
    K4(J,I) = 0.0d00
  ELSE
    K4(J,I) = (COND(J,I+1) + COND(J,I))/2.0
  END IF
```

```

IF(J == JZ) THEN
  K2(J,I) = COND(J,I)
ELSE
  K2(J,I) = (COND(J,I) + COND(J+1,I))/2.0
ENDIF

END DO
END DO

I=IX-1
DO J=NWFZ+1,JZ
  IF ( H(J,I) >= 0.0 ) K4(J,I) = COND(j,i)
END DO
*****
!* USING GEOMETRIC WEIGHTING
1000  DO J=1,JZ
  DO I=1,IX-1

    IF (J == 1) THEN
      K1(J,I) = 0.0d00
    ELSE
      K1(J,I) = (COND(J,I)*COND(J-1,I))**0.5
    ENDIF

    IF (I == 1) THEN
      K3(J,I) = 0.0d00
    ELSE
      K3(J,I) = (COND(J,I)*COND(J,I-1))**0.5
    ENDIF

    IF(I == IX-1) THEN
      K4(J,I) = 0.0d00
    ELSE
      K4(J,I) = (COND(J,I+1) * COND(J,I))**0.5
    END IF

    IF(J == JZ) THEN
      K2(J,I) = COND(J,I)
    ELSE
      K2(J,I) = (COND(J,I) * COND(J+1,I))**0.5
    ENDIF

  END DO
END DO

I=IX-1
DO J=1,JZ
  IF ( H(J,I) >= 0.0 ) K4(J,I) = COND(j,i)
END DO

RETURN
END

```

```
*****
*          ROOT_2D
*
*      This subroutine computes the root distribution term, RDT,
*      for each cell in the profile. The RDT corresponds to the
*      fraction of the evapotranspiration rate, ETRATE, extracted
*      from each cell.
** *****

SUBROUTINE ROOT_2D (IX,JZ,DX,NWFX,RDT)

IMPLICIT DOUBLE PRECISION(A-H, O-Z)
PARAMETER (IS=90,JS=40)

DIMENSION RDT(JS,IS),DX(IS)

DO J=1,7 !10
DO I=1,IX-1
    DDX = DDX + DX(I)
    END DO
END DO

DO J=1,7
    DO I=1,IX-1
        RDT(J,I) = DX(I)/DDX
    END DO
END DO

DO J=8,jz
    DO I=1,IX-1
        RDT(J,I) = 0.0D00
    END DO
END DO

I=IX
DO J=1,JZ
    RDT(J,I) = 0.0D00
END DO

TEST=0.0D00 !test to check if the sum of all RDT is equal to 1.
DO J=1,JZ
    DO I=1,IX
        TEST=TEST + RDT(J,I)
    END DO
END DO

RETURN
END
```

```
*****
*          *
*          ETDIST_2D          *
*          *
* This subroutine uses daily potential evapotranspiration to compute the          *
* crop evapotranspiration (Eta) by using the appropriate crop coefficient.          *
* Then Eta is distributed over the day with a sinusoidal function to find the          *
* evapotranspiration rate(ETRATE). From that, the extraction rate of each          *
* cell is computed and linearly adjusted to meet the evapotranspiration rate.          *
*** ****
SUBROUTINE ETDIST_2D (
.DYN,TEND,TSTART,TIME24,IDAD,JZ,IX,TAREA,WCWP,WCFC,DY,NLayers,
.NBeginRow,NEndRow,WC,ETP,RDT,DZ,DX,SINIT,S,Smax,LAH,Kc)

PARAMETER (IS=90, JS=40, LD=365,PI=3.141592654)
IMPLICIT DOUBLE PRECISION(A-H, K,O-Z)
DOUBLE PRECISION LAH
CHARACTER*15 DYN

DIMENSION WC(JS,IS),ETP(LD),RDT(JS,IS),DZ(JS),DX(IS),S(JS,IS),
.NBeginRow(8),NEndRow(8),WCWP(8),WCFC(8)

IF(DYN == 'INITIAL') THEN
  DO J=1,JZ
    DO I=1,IX
      S(j,i) = Sinit
    END DO
  END DO

  RETURN
END IF

TCYCLE = TEND - TSTART
OMEGA = 2.0 * PI / TCYCLE
DAYTIM = TIME24 - TSTART

IF(TIME24 < TSTART)THEN
  ETPP = ETP(IDAY-1)
ELSE
  ETPP = ETP(IDAY)
END IF
!GO TO 10
*****
! Calculation of Crop Evapotranspiration
! JOP = 37  !1996      ! julian day of planting(varies for each year)
! JOP = 34  !(1997)    ! julian day of planting(varies for each year)
! JIS = 22          ! duration of initial stage
! JDS = 27          ! duration of development stage
! JMS = 38          ! duration of middle stage
! JLS = 20          ! duration of late stage
! IDS = JOP+JIS     ! julian day of beginning of development stage
! IMS = IDS+JDS     ! julian day of beginning of middle stage
! ILS = IMS+JMS     ! julian day of beginning of development stage
! Kci = 0.30d00      ! Initial crop coefficient
```

```

Kcm = 1.150d00      ! Middle crop coefficient
Kce = 0.750d00      ! End crop coefficient
*****  

If(IDAY <= IDS) Kc = Kci      !Crop coefficient for initial stage  

If (IDAY > IDS .AND. IDAY <= IMS) then  !Crop coefficient for development stage
  Kc = Kci + (IDAY-IDS)*(Kcm - Kci)/JDS
  End if  

If (IDAY > IMS .AND. IDAY <= ILS) Kc = Kcm  !Crop coefficient for middle stage  

If(IDAY > ILS) then      !Crop coefficient for late stage
  Kc = Kcm + (IDAY-ILS)*(Kce - Kcm)/JLS
  End if  

ETa = Kc * ETPP      ! Actual evapotranspiration
*****  

!  Computation of total profile evapotranspiration rate, ETRATE, at
!  a given time with a sinusoidal distribution.
ETMAX = ETa / TCYCLE
ETRATE = ETMAX * (1 + SIN(OMEGA*DAYTIM - PI*0.50D00))      ! mm/hr
ETRATE = ETRATE*0.10D00 ! Convert to cm/hr
*****  

!  If the ETP is distributed uniformly over the day(cm/hr)
!  etrate = etp(iday)/240.0      !ETP in mm/day
*****  

!  Computation of soil water extraction rate, S(J,I), and linear
!  adjustment of the sum of S(J,I) over all cells, SUMOFS, to make
!  sure that the total evapotranspiration rate, ETRATE, is met.  

IF(ETRATE == 0.0) THEN
  DO J=1,JZ
  DO I=1,IX
    S(J,I) = 0.0
  END DO
  END DO
  RETURN
END IF  

CC  = 10.0
SUMOFS = 0.0  

DO L=1, NLayers
  NBR = NBeginRow(L)
  NER = NEndRow(L)
  DELTAWC = WCFC(L) - WCWP(L)
  DO J=NBR,NER
    DO I=1,IX
      RWC = (WC(J,I) - WCWP(L)) / DELTAWC
      IF(RWC > 1.0) RWC = 1.0
      IF(RWC <= 0.0) THEN
        S(J,I) = 0.0
      END IF
    END DO
  END DO
END IF

```

```

GO TO 20
END IF

! Compute the fraction of the ERate to be extracted at each cell
! in terms of cm3/hr -- a function of the root distribution term, RDT.
  FRACTN = ETRATE * TAREA * RDT(J,I)

! Compute the extraction of each cell in terms of cm3/hr as modified by
! the relative available soil water content term.
  S(J,I) = FRACTN * RWC**(ETRATE / RWC / CC)
  SUMOFS = SUMOFS + S(J,I)

20  END DO
    END DO
  END DO
! Linear adjustment -- CF is the correction factor that forces the
! computed total profile extraction rate to equal the predetermined
! ERate.

  IF(SUMOFS == 0.0d00) THEN
    CF = 1.0
  ELSE
    CF = ETRATE * TAREA / SUMOFS
  END IF

! Computation of the corrected cell extraction rate and conversion to units of cm/(cm-hr).
! Finding the magnitude of largest extraction rate in the mesh
  Smax = 0.0
  DO J=1,JZ
    DO I=1,IX
      S(J,I) = S(J,I) * CF / DZ(J) / (DX(I) * DY)
      If( Smax < Abs(S(j,i)) ) Smax = Abs(S(j,i))
    END DO
  END DO
  TEST=0.0
  DO J=1, JZ
    DO I=1, IX
      TEST = TEST+ S(J,I)
    END DO
  END DO

  RETURN
END

```

```
*****
*          WATFLOW_2D
*
* This subroutine calculates the flow at each interior node and at the boundaries
* (runoff, seepage, deep percolation).
*****
SUBROUTINE WATFLOW_2D(
.DYN,IX,JZ,QSINIT,QBINIT,QLINIT,QRINIT,DX,DZ,K1,K2,K3,K4,H,TIME24,
.Cum_time,Time_End_Sim,Hour,LDD,LHH,Depth,WC,SWC,Precip,QS,QB,QL,
.QR,fluxdelta,NWFZ,NWFX,COND,SINK,Q1,Q2,Q3,Q4,QBWF,wf_depth,a,IDAY,
.oldh,QIRRI,wtdepth,CONDs,D1,D2,D3,D4,Time_Begin_Sim,KS,
.bottom,CONTROLPRINT,SURFRUN,LAH,QRUNOFF,IL1,IL2,JL,IC,
.SEEP)

PARAMETER (IS=90, JS=40,LD=365)
IMPLICIT DOUBLE PRECISION(A-H,K, O-Z)
DOUBLE PRECISION LAH
CHARACTER*15 DYN
CHARACTER*15 CONTROLPRINT
CHARACTER*15 SURFRUN,SEEP
DIMENSION QL(JS),QR(JS),QB(IS),QS(IS),K1(JS,IS),K2(JS,IS),
.K3(JS,IS),K4(JS,IS),DX(IS),DZ(JS),H(JS,IS),PRECIP(LD,0:23),
.Q1(js,is),Q2(js,is),Q3(js,is),Q4(js,is),DEPTH(JS),WC(js,is),
.Deltaflux(js,is),SINK(JS,IS),COND(JS,IS),fluxdelta(js,is),
.oldh(js,is),wtdepth(is),SWC(JS,IS),D1(JS),D2(JS),D3(IS),D4(IS),
.QRUNOFF(IS),SEEP(JS),KS(JS)
*****
! Initialize fluxes
IF(DYN == 'INITIAL') THEN
  DO J=1, JZ
    DO I=1,IX
      IF(I == 1) THEN
        QL(J) = QLINIT
      ELSE
        Q3(J,I) = 0.0
      END IF
      IF (I == IX-1) THEN
        QR(J) = QRINIT
      ELSE
        Q4(J,I) = 0.0
      END IF
      IF (J == 1) THEN
        QS(I) = QSINIT
      ELSE
        Q1(J,I) = 0.0
      END IF
      IF (J == JZ) THEN
        QB(I) = QBINIT
      ELSE
        Q2(J,I) = 0.0
      END IF
    END DO
  END DO

```

```

I=IX-1
  WRITE(12,3000) TIME24, IDAY, Cum_Time, LAH
  WRITE(12,3100)
    DO J=1,JZ
      WRITE(12,3200) DEPTH(J), H(j,i), Q1(j,i), Q2(j,i), Q3(j,i), Q4(J,I),
      . WC(J,I), COND(J,I), SWC(J,I), sink(j,i)
    END DO
    WRITE(12, *)
13  RETURN
  END IF
***** ! Set fluxes equal 0 at the beginning of each time step.
  IF (DYN == 'INTEG') THEN
    SURFRUN = 'FALSE' ; SEEP(J) = 'FALSE'
    Qmax = 0.0D00 ; QBFW = 0.0D00; A= 0.0D00; C= 0.0D00
    DRAINRUN = 'FALSE'
    DO J=1,JZ
      DO I=1,IX
        SINK(J,I) = 0.0D00
        Q1(J,I)=0.0D00; Q2(J,I)=0.0D00; Q3(J,I)=0.0D00; Q4(J,I)=0.0D00
        fluxdelta(j,i) = 0.0D00; deltaflux(j,i) = 0.0D00
      END DO
      END DO
      DO I = 1, IX
        QSRUNOFF(I) = 0.0D00
      END DO
***** ! Calculate fluxes for the cells
2100 DO J=1,JZ-1
  DO I=1,IX-2

    IF (J == 1) THEN
      Q1(j,i) = PRECIP(LDD,LHH)
    ELSE
      Q1(j,i) = - K1(J,I) * ((H(J,I) - H(J-1,I) ) / D1(J) - 1.0)
    END IF

    Q2(j,i)= - K2(J,I) * ((H(J+1,I) - H(J,I) ) / D2(J) - 1.0)

    IF(I == 1) THEN
      Q3(J,I) = 0.0
    ELSE
      Q3(j,i) = - K3(J,I) * ((H(J,I) - H(J,I-1) ) / D3(I))
    END IF

    Q4(j,i) = - K4(J,I) * ((H(J,I+1) - H(J,I) ) / D4(I))

  END DO
  END DO
***** ! Calculate seepage at the lateral of the drain.
2200 I = IX-1

  Do J=1, NWFZ      !NWFZ = row of the bottom of the drain

  If (J == 1) then

```

```

Q1(j,i) = PRECIP(LDD,LHH)
Else
  Q1(j,i) = -K1(J,I) * ((H(J,I) - H(J-1,I)) / D1(J) - 1.0)
End if
  Q2(j,i) = -K2(J,I) * ((H(J+1,I) - H(J,I)) / D2(J) - 1.0)
  Q3(j,i) = -K3(J,I) * ((H(J,I) - H(J,I-1)) / D3(I))

  If(h(j,i) < 0.0d00) then
    Q4(j,i) = 0.0d00
  Else
    Q4(j,i) = Q3(J,I) - !K4(J,I)*H(J,I)/DX(I)
  End if

  If(Q4(J,I) > 0.0D00) then
    SEEP(J) = 'TRUE'
  Else
    SEEP(J) = 'FALSE'
    Q4(J,I) = 0.0D00
  End if

End do

2300  Do J=NWFZ+1,JZ-1
  Q1(j,i) = -K1(j,i) * ((H(j,i) - H(j-1,i)) / D1(j) - 1.0)
  Q2(j,i) = -K2(j,i) * ((H(j+1,i) - H(j,i)) / D2(j) - 1.0)
  Q3(j,i) = -K3(j,i) * ((H(j,i) - H(j,i-1)) / D3(i))
  Q4(j,i) = -K4(j,i) * (H(j,i+1) - H(j,i)) / DX(i)
End do
*****
! Implement bottom boundary condition(relationship between position of water table
! and flux at the bottom).

J=JZ
DO I=1,IX-1
  Q1(JZ,i) = -K1(j,i) * ((H(j,i) - H(j-1,i)) / D1(j) - 1.0)

  IF(I == 1) THEN
    Q3(j,i) = 0.0
  ELSE
    Q3(j,i) = -K3(j,i) * ((H(j,i) - H(j,i-1)) / D3(i))
  END IF

  Q2(J,I) = 0.001*EXP(0.0173*(H(JZ,I)+DZ(JZ)/2.0D00)) !BOTTOM=120 cm
!  Q2(J,I) = 0.000D00 ! used to simulated no-deep percolation
  QB(i) = Q2(JZ,i)
  Q4(j,i) = -K4(j,i)*(H(j,i+1) - H(j,i)) / D4(i)

END DO
*****
! Implement condition for surface runoff
2500  j=3 ! row where runoff takes place
  DO I=1,IX-1
    IF(H(j,i) >= 0.0d00) then
      SURFRUN = 'TRUE'
      Q1(1,I) = 0.0D00
      QS(I) = 0.0D00
    End if
  End do

```

```

QSRUNOFF(I) = PRECIP(LDD,LHH)
END IF
END DO
*****
! Calculates net flux for each cell.
2800 DO J=1,JZ
    DO I=1,IX
        fluxdelta(j,i) = (Q1(j,i) - Q2(j,i))/DZ(J) +
        . (Q3(j,i) - Q4(j,i))/DX(I)
    END DO
    END DO
*****
! Update fluxes at boundaries
2900 DO J=1,JZ
    DO I=1,IX
        IF (I == 1)    QL(J) = Q3(J,I)
        IF (I == IX-1) QR(J) = Q4(J,I)
        IF (J == 1)    QS(I) = Q1(J,I)
        IF (J == JZ)   QB(I) = Q2(J,I)
    END DO
    END DO
*****
IF(CONTROLPRINT == 'TRUE') THEN
! IF(TIME24 == 0.0D00) THEN ! PRINT DAILY OUTPUT
    I=IX-1
    WRITE(12,3000) TIME24, IDAY, Cum_Time, LAH
3000  FORMAT('Hour = ',F7.3,3X,'DAY = ',I4,3X,'Time of simulation = ',F7.3,
. 1X,'hr',3X,'Annual Hour = ',F10.0)

    WRITE(12,3100)
3100 FORMAT(T14,'H(cm)',T25,'Q1',T34,'Q2',T43,'Q3',T50,'Q4',T60,'WC',
. T70,'COND',T80,'SWC',t90,'sink')

    DO J=1,JZ
    WRITE(12,3200) DEPTH(J),H(j,i),Q1(j,i),Q2(j,i),Q3(j,i),Q4(J,I),
. WC(J,I),COND(J,I),SWC(J,I),sink(j,i)
3200 FORMAT(F7.2,F12.3,8f9.5)
    END DO

    WRITE(12,*)*
    END IF
*****
1300 RETURN
ENDIF

END

```

```
*****
*          *
*          TIME_2D          *
*          *
* This subroutine determines the time step and updates the time-dependent variables. *
*****
```

SUBROUTINE TIME_2D(
.DYN,IX,JZ,S,DX,DZ,fluxdelta,DTMAX,DTMIN, SINK,precip,H,
.Time_Begin_Sim,Cum_Time,TIME24,IDAY,DT,HOUR,LDD,LHH,LAH,DEPTH,
.Time_End_Sim,Q1,Q2,Q3,Q4,a,b,WC,SWC,COND,CONTROLPRINT,
.PRINTCONTROL,Time_of_irrigation)

PARAMETER (IS=90, JS=40,LD=365)
IMPLICIT DOUBLE PRECISION(A-H,K, O-Z)
DOUBLE PRECISION LAH
CHARACTER*15 DYN
CHARACTER*15 CONTROLPRINT
DIMENSION DX(IS),DZ(JS),DEPTH(JS),fluxdelta(js,is),S(js,is),
.SINK(JS,IS),precip(l0:0:23),q1(js,is),q2(js,is),q3(js,is),
.H(js,is),wc(js,is),SWC(JS,IS),Q4(JS,IS),COND(JS,IS)

IF (DYN == 'INITIAL') THEN
 LDD = IDAY
 LHH = Time_Begin_Sim
 HOUR = Time_Begin_Sim - REAL(LHH)
 Cum_Time = 0.0d00
 TIME24 = Time_Begin_Sim
 LAH = (IDAY-1)*24 + LHH ! annual hour
 PRINTIME = 0.0d00
 Time_of_irrigation = 0.0d00

RETURN
ENDIF

```
*****
IF (DYN == 'INTEG') THEN
    CONTROLPRINT = 'FALSE'
! Compare net flux plus extraction rate for each cell and choose
! the largest magnitude to be assigned to EXTMAX
    EXTMAX = 0.0D00
    OLD_DT = DT
    DO J= 1, JZ
        DO I = 1, IX
            EXT = S(j,i) + Abs(fluxdelta(j,i)) + SINK(J,I)
            IF(EXT > EXTMAX) EXTMAX = EXT
        END DO
    END DO
```

! Determining the time step and the cumulative time.

IF (EXTMAX == 0.0) THEN
 DT = DTMAX
 GO TO 160
END IF

DELTAWCmax = 0.002 ! maximum change in water content

```

DT = DELTAWCmax/EXTMAX

IF (DT >= OLD_DT) DT = 1.20D00*OLD_DT
IF (DT >= DTMAX) DT = DTMAX
IF (DT <= DTMIN) DT = DTMIN

! ****
! DT = 0.050D00 ! use this statement to fix a value of DT
! ****

160    b = precip(ldd,lhh) ! precipitation at previous time step
        HOUR = HOUR + DT
        LAH = LAH + DT
        IF (HOUR >= 1.0000d00) THEN
            DT = 1.0000d00 + DT - HOUR
            HOUR = 0.0000d00
            LHH = LHH + 1
        LAH = LAH + 1
        ENDIF

        Cum_Time = Cum_Time + DT
        TIME24 = TIME24 + DT
        PRINTIME=PRINTIME + DT
        IF(PRINTIME >= PRINTCONTROL) THEN
            CONTROLPRINT='TRUE'
            PRINTIME = 0.0D+00
        END IF

        IF (LHH == 24) THEN
            TIME24 = 0.0000
            IDAY = IDAY + 1
            LDD = LDD + 1
            LHH = 0
        END IF

1300 RETURN
        ENDIF
    END

```

```
*****
*          RESET_2D
*
* This subroutine evaluates the coefficients of the banded matrix equation
* AH = R where A has MBAND = IX*2+1 bands (including the zero
* bands C enclosed between the A and B and E and F terms and is of the
* order of NMAX = IX*JZ. The subroutine stores the coefficients in the
* C(NMAX,MBAND).
* ****
SUBROUTINE RESET_2D(
.IX,JZ,NWFZ,IRRICONTROL,DT,DZ,DX,K1,K2,K3,K4,QS,QB,QR,QL,QBWF,SWC,
.S,SINK,H,DEPTH,WF_DEPTH,OLDH,WTDEPTH,QIRRI,D1,D2,D3,D4,
.SURFRUN,SEEP,LAH,Time_of_irrigation,IL1,IL2,JL,IC,NWFX,KS,COND,WTA)

PARAMETER (IS=90, JS=40)
IMPLICIT DOUBLE PRECISION(A-H,K,O-Z)
DOUBLE PRECISION LAH
CHARACTER*10 IRRICONTROL
CHARACTER*15 SURFRUN,SEEP

DIMENSION DX(IS),DZ(JS),K1(JS,IS),K2(JS,IS),K3(JS,IS),K4(JS,IS),
.S(JS,IS),QS(JS),QB(JS),QR(JS),QL(JS),H(JS,IS),SWC(JS,IS),KS(js),
.SINK(JS,IS),C(JS*IS,IS*2+1), R(IS*JS),DEPTH(JS),oldh(js,is),
.WTDEPTH(JS),D1(JS),D2(JS),D3(JS),D4(JS),SEEP(JS),COND(JS,IS)

! Compute the number of diagonals, MBAND, in the solution matrix.
! Compute the i-index of the array C(NMAX,MBAND) that the
! coefficients of the main diagonal terms will occupy.

NMAX = IX * JZ
MBAND = IX * 2 + 1
MID = ( MBAND + 1 ) / 2.0D00

! Initialize the array C(N,MBAND), which contains only elements
! enclosed by the outer bands of the matrix

DO N=1,NMAX
DO M=1,MBAND
C(N,M) = 0.0D00
END DO
END DO
*****
! Set up the interior grid points
20 DO J=2,JZ-1
NN = IX * (J-1)
DO I=2,IX-1
N = NN + I
C1 = SWC(J,I)
C(N,1) = -K1(J,I) / (D1(J)**2.0D00)
C(N,MBAND) = -K2(J,I) / (D2(J)**2.0D00)
C(N,MID-1) = -K3(J,I) / (D3(I)**2.0D00)
IF(I==IX-1 .AND. J<=NWFZ) THEN
C(N,MID+1) = 0.0
ELSE
C(N,MID+1) = -K4(J,I) / (D4(I)**2.0D00)

```

```

END IF
C(N,MID) = C1/DT - C(N,1) - C(N,MID-1) - C(N,MID+1)
- C(N,MBAND)
IF(I==IX-1 .AND. J<=NWFZ) THEN
  R(N) = C1*H(J,I)/DT + (K1(J,I)/D1(J) - K2(J,I)/D2(J)) - S(J,I) -
  SINK(J,I) - QR(J)/DX(I)
  ELSE
  R(N) = C1*H(J,I)/DT + (K1(J,I)/D1(J) - K2(J,I)/D2(J)) - S(J,I) -
  SINK(J,I)
END IF

END DO
END DO
*****
! Set up the boundary conditions

! Variable flux boundary condition at the surface (J=1)
J = 1
DO I=1,IX-1
  N = I
  C1 = SWC(J,I)

  IF(I == 1) THEN
    C(N,MID+1) = -K4(J,I) / D4(I)**2.0D00
    C(N,MBAND) = -K2(J,I) / D2(J)**2.0D00
    C(N,MID) = C1/DT - C(N,MID+1) - C(N,MBAND)
    R(N) = C1*H(J,I)/DT + (QS(I)/DZ(J) - K2(J,I)/D2(J))
    - S(J,I) - SINK(J,I) + QL(j)/dx(i)
    GO TO 30
  END IF

  C(N,MID-1) = -K3(J,I) / D3(I)**2.0D00
  C(N,MBAND) = -K2(J,I) / D2(J)**2.0D00
  C(N,MID+1) = -K4(J,I) / D4(I)**2.0D00
  C(N,MID) = C1/DT - C(N,MID-1) - C(N,MID+1) - C(N,MBAND)

  R(N) = C1*H(J,I)/DT + (QS(I)/DZ(J) - K2(J,I)/D2(J)) - S(J,I)
  - SINK(J,I)

30 END DO
*****
! Set up boundary conditions for the last row, J=JZ.
60 J = JZ

69 NN = IX * (JZ-1)
DO I=1,IX-1
  N = NN + I
  C1 = SWC(J,I)

  IF(I == 1) THEN
    C(N,1) = -K1(J,I) / D1(J)**2.0D00
    C(N,MID+1) = -K4(J,I) / D4(I)**2.0D00
    C(N,MID) = C1/DT - C(N,1) - C(N,MID+1)
    R(N) = C1*H(J,I)/DT + (K1(J,I)/D1(J) - QB(I)/DZ(J))
    - S(J,I) - SINK(J,I) + QL(j)/dx(i)
    GO TO 70
  END IF

```

```

END IF

C(N,1) = -K1(J,I) / D1(J)**2.0D00
C(N,MID-1) = -K3(J,I) / D3(I)**2.0D00
C(N,MID+1) = -K4(J,I) / D4(I)**2.0D00
C(N,MID) = C1/DT - C(N,1) - C(N,MID-1) - C(N,MID+1)
R(N) = C1*H(J,I)/DT + (K1(J,I)/D1(J) - QB(I)/DZ(J))
. - S(J,I) - SINK(J,I)
70 END DO
*****
! Constant flux boundary condition at the line of symmetry (I=1)
! QL(J) = 0.0

80 I = 1
N = 1

DO J=2,JZ-1
N = N + IX

C1 = SWC(J,I)
C(N,1) = -K1(J,I) / (D1(J)**2.0D00)
C(N,MID+1) = -K4(J,I) / (D4(I)**2.0D00)
C(N,MBAND) = -K2(J,I) / (D2(J)**2.0D00)
C(N,MID) = C1/DT - C(N,1) - C(N,MID+1) - C(N,MBAND)
R(N) = C1*H(J,I)/DT + (K1(J,I)/D1(J) - K2(J,I)/D2(J)) -
. S(J,I) - SINK(J,I) + QL(j)/dx(i)

END DO
*****
! Set the water pressure constant at I=IX (column of the water furrow)
I=IX

DO J=1,JZ
N= IX * J
C1 = 1.0
C(N,1) = 0.0
C(N,MID-1) = 0.0
C(N,MBAND) = 0.0
C(N,MID) = C1/DT
R(N) = C1*H(J,I)/DT
END DO
*****
IRRICONTROL = 'FALSE'

! GO TO 300 ! to simulate 1996
GO TO 400 ! to simulate 1997
!GO TO 600 ! no irrigation
*****
300 IF(LAH > 1544. .AND. LAH < 2384.) GO TO 600 !period with no irrigation
IF(LAH > 2544. .AND. LAH < 2632.) GO TO 600 !period with no irrigation
IF(LAH > 2904. .AND. LAH < 2968.) GO TO 600 !period with no irrigation
IF(LAH > 3298. .AND. LAH < 4000.) GO TO 600 !period with no irrigation
*****set up irrigation condition*****
IF(LAH <=1352.) then
IF (wtdepth(IC) >= -40.0d00) IRRICONTROL = 'FALSE' ! there is no irrigation
IF (wtdepth(IC) <= -40.6d00) IRRICONTROL = 'TRUE' ! there is irrigation

```

```

rangewt= wta-wtdepth(ic)
IF(wtdepth(IC) < -40.0d00 .AND. wtdepth(IC) > -40.60d00) THEN
  IF(RANGEWT < 0.0D00 ) THEN
    IRRICONTROL = 'TRUE'
  ELSE
    IRRICONTROL = 'FALSE'
  END IF
END IF
go to 500
END IF

  IF (wtdepth(IC) >= -42.0000) IRRICONTROL = 'FALSE' ! there is no irrigation
  IF (wtdepth(IC) <= -42.5d00) IRRICONTROL = 'TRUE' ! there is irrigation
  rangewt= wta-wtdepth(ic)
  IF(wtdepth(IC) < -42.0d00 .AND. wtdepth(IC) > -42.50d00) THEN
    IF(RANGEWT < 0.0D00 ) THEN
      IRRICONTROL = 'TRUE'
    ELSE
      IRRICONTROL = 'FALSE'
    END IF
  END IF
  GO TO 500
*****
! 1997
400 IF(LAH < 1380.) GO TO 600 !period with no irrigation
  IF(LAH > 1728. .AND. LAH < 1856.) GO TO 600 !period with no irrigation
  IF(LAH > 1976. .AND. LAH < 2076.) GO TO 600 !period with no irrigation
  IF(LAH > 2484. .AND. LAH < 2652.) GO TO 600 !period with no irrigation
  IF(LAH > 2697. .AND. LAH < 3084.) GO TO 600 !period with no irrigation
  IF(LAH > 3176.) GO TO 600 !period with no irrigation

  IF(LAH <=1500.) then
    IF (wtdepth(IC) >= -40.5d00) IRRICONTROL = 'FALSE' ! there is no irrigation
    IF (wtdepth(IC) <= -41.6d00) IRRICONTROL = 'TRUE' ! there is irrigation
    rangewt= wta-wtdepth(ic)
    IF(wtdepth(IC) < -40.50d00 .AND. wtdepth(IC) > -41.60d00) THEN
      IF(RANGEWT < 0.0D00 ) THEN
        IRRICONTROL = 'TRUE'
      ELSE
        IRRICONTROL = 'FALSE'
      END IF
    END IF
    go to 500
  END IF

  IF(LAH >1500. and. LAH <=2192.) then
    IF (wtdepth(IC) >= -38.8d00) IRRICONTROL = 'FALSE' ! there is no irrigation
    IF (wtdepth(IC) <= -39.4d00) IRRICONTROL = 'TRUE' ! there is irrigation
    rangewt= wta-wtdepth(ic)
    IF(wtdepth(IC) < -38.80d00 .AND. wtdepth(IC) > -39.40d00) THEN
      IF(RANGEWT < 0.0D00 ) THEN
        IRRICONTROL = 'TRUE'
      ELSE
        IRRICONTROL = 'FALSE'
      END IF
    END IF
  END IF

```

```

END IF
GO TO 500
END IF

IF(LAH > 2192.) THEN
  IF (wtdepth(IC) >= -40.9d00) IRRICONTROL = 'FALSE' ! there is no irrigation
  IF (wtdepth(IC) <= -41.4d00) IRRICONTROL = 'TRUE' ! there is irrigation
  rangewt= wta-wtdepth(ic)
  IF(wtdepth(IC) < -40.90d00 .AND. wtdepth(IC) > -41.40d00) THEN
    IF(RANGEWT < 0.0D00 ) THEN
      IRRICONTROL = 'TRUE'
    ELSE
      IRRICONTROL = 'FALSE'
    END IF
  END IF
  go to 500
END IF
*****
! Set the right-hand side for the irrigating cells.
500  IF(IRRICONTROL == 'TRUE') THEN
510  Time_of_irrigation = Time_of_irrigation + DT
      J=JL; I=IL1          ! IRRIGATION CELL 1
      N = IX*(J-1) + I
      R(N) = R(N) + 0.5d00*QIRRI/DZ(J)

      J=JL; I = IL2        !IRRIGATION CELL 2
      N = IX * (J-1) + I

      R(N) = R(N) + QIRRI/DZ(J)

    END IF
*****
600  do j=1,jz
      do i=1,ix
        oldh(j,i) = h(j,i)
      end do
    end do

CALL BANDSOLVE_2D(C, NMAX, MBAND, R)

L = 0
DO J=1,JZ
DO I=1,IX
  L = L + 1
  H(J,I) = R(L)
END DO
END DO

! Check the occurrence of ponding at the water furrow.
I=IX-1
  DO J=NWFZ+1,JZ

  ! IF( H(J,I) <= (depth(j) - nwfz*dz(j)) ) THEN      ! no ponding
  ! IF( H(J,I) <= (depth(j) - WF_depth + 20.00) ) THEN !ponding 17.50 cm
  ! H(J,IX) = H(J,I)

```

```
ELSE
!      H(J,IX) = depth(j) - nwfz*dz(j)      ! no ponding
!      H(J,IX) = depth(j) - WF_depth + 20.00  !ponding 17.50 cm
END IF
END DO

900 RETURN
END
```

```
*****
*          *
*          BANDSOLVE_2D
*          *
* BANDSOLVE is an algorithm to solve the matrix equations AX = B
* when the matrix A is of large order and sparse such that a narrow band
* centered on the main diagonal includes all the non-zero elements.
* Parameter N is the order of A, and M is the width of the band (total
* number of diagonals enclosed by the two outermost bands), necessarily an
* odd number of elements. BANDSOLVE is very efficient because it
* operates only on the banded portion of the matrix A, given in the
* N by M array C. The band elements of a given row of A appear in
* the same row of C but shifted such that element A(i,j) becomes
* C(i,j-1+(M+1)/2). All band elements whether zero or nonzero must
* be given. The values of undefined elements of C, such as C(1,1) or
* C(N,M) are irrelevant. The array V initially contains the vector
* B. After solution, the array V contains the answer vector X. The
* contents of array C are destroyed during solution which is done by
* Gauss elimination with row interchanges, followed by back
* substitution. The array C in subroutine REDIST is already in the
* N by M form and does not need further conversion to go into
* BANDSOLVE.
*****
```

SUBROUTINE BANDSOLVE_2D(C, N, M, V)

```
IMPLICIT DOUBLE PRECISION(A-H, O-Z)
PARAMETER (IS=90, JS=40, LD=365)
DIMENSION C(JS*IS,IS*2+1), V(IS*JS)
INTEGER PIV, R
```

* ----- ROW SHIFTING AND ZERO PLACEMENT -----

```
LR = (M + 1) / 2
```

```
DO 20 R=1,LR-1
DO 20 I=1,LR-R
  DO 10 J=2,M
    C(R,J-1) = C(R,J)
10  CONTINUE
    C(R,M) = 0.0
    C(N+1-R,M+1-I) = 0.0
20  CONTINUE
```

```
!  ROW INTERCHANGE
DO I=1,N-1
  PIV = I

  DO R=I+1,LR
    IF(ABS(C(R,1)).GT.ABS(C(PIV,1))) PIV = R
  END DO
```

```
IF(PIV .NE. I) THEN
  DO J=1,M
    TEMP = C(I,J)
    C(I,J) = C(PIV,J)
```

```

C(PIV,J) = TEMP
END DO
TEMP = V(I)
V(I) = V(PIV)
V(PIV) = TEMP
END IF

```

! TRIANGULARIZATION

```
V(I) = V(I) / C(I,1)
```

```

DO J=2,M
C(I,J) = C(I,J) / C(I,1)
END DO

```

```

DO R=I+1,LR
TEMP = C(R,1)
V(R) = V(R) - TEMP * V(I)

```

```

DO J=2,M
C(R,J-1) = C(R,J) - TEMP * C(I,J)
END DO
C(R,M) = 0.0
END DO

```

```
IF(LR .NE. N) LR = LR + 1
```

```
END DO
```

! BACK SOLUTION

```
V(N) = V(N) / C(N,1)
JM = 2
```

```
DO R=N-1,1,-1
```

```

DO 100 J=2,JM
V(R) = V(R) - C(R,J) * V(R-1+J)
END DO

```

```
IF(JM .NE. M) JM = JM + 1
```

```
END DO
```

```
RETURN
END
```

```

* ****
*          MASSBAL_2D
*
* This subroutine computes the mass balance of the soil profile by two different ways
* to check the stability of the model:
* Method 1 sums the water contents of each grid in the soil profile to the total outflows .
* Method 2 sums the total inflows to the initial storage.
* Porc_mass is the error (%) of the relation between method 1 and 2.
* ****
SUBROUTINE MASSBAL_2D(
.DYN,IX,JZ,DX,DZ,DY,TAREA,BOTTOM,QB,QL,QS,QR,S,WC,WCS,IRRICONTROL,
.QIRRI,DT,Drain,Delta_mass,Error_mass,Porc_mass,Storage,QRUNOFF,
.Sim_mass,Storage_initial,Storage_maximum,Runoff, SINK,NWFZ,
.Root_extraction,Cum_perc,Cum_irrig,Water_in,Old_storage,
.Actual_balance,NLayers,QBWF,H,b,Cum_precip,SURFRUN,Seepage,
.PRECIP, LDD, LHH,EXCESS,IL1,IL2,JL)

PARAMETER (IS=90, JS=40,LD=365)
IMPLICIT DOUBLE PRECISION(A-H, O-Z)
CHARACTER*15 ::DYN
CHARACTER*10 IRRICONTROL
CHARACTER*15 SURFRUN

DIMENSION DZ(JS),DX(IS),QB(IS),QR(JS),QS(IS),QL(JS),WC(JS,IS),
.S     S(JS,IS),WCS(8),SINK(JS,IS),H(JS,IS),QRUNOFF(IS),
.S     PRECIP(LD,0:23)

! Initialize the cumulative infiltration and extraction

IF(DYN == 'INITIAL') THEN
  Cum_precip = 0.0D+00      ! cumulative precipitation
  Root_extraction = 0.0D+00 ! cumulative root extraction
  Storage = 0.0D+00        ! water storage in the current time step
  Old_storage = 0.0d+00     ! simulated storage in the previous time step
  Actual_balance = 0.0d+00 ! sum of total inflows, drainage, and root
                           ! extractions to the initial storage, Storage_init,
                           ! Runoff = 0.0d+00           ! cumulative runoff
                           ! Cum_irrig = 0.0D+00        ! cumulative irrigation
                           ! Cum_perc = 0.0D+00        ! cumulative deep percolation
                           ! Cum_precip = 0.0d00       ! cumulative precipitation
                           ! Seepage = 0.0d00          ! cumulative seepage

! Calculate initial storage
DO J=1, JZ
  DO I=1, IX-1
    Storage = Storage + WC(J,I) * DZ(J) * DX(I)*DY
  END DO
END DO

Storage_initial = Storage
Old_Storage = Storage
Actual_balance = Storage_initial
RETURN
ENDIF

```

! Compute cumulative infiltration, irrigation, extraction, deep percolation, and runoff.

IF (DYN == 'INTEG') THEN

```

Storage = 0.0D00      ! water stored in the profile at each time step
Uptake = 0.0D00       ! root extraction during time step
Delta_irrig = 0.0D00  ! irrigation during the time step
Delta_perc = 0.0D00   ! deep percolation during the time step
Delta_mass = 0.0D00   ! difference between water that enters and
! leaves the profile during the time step.
Delta_runoff = 0.0D00 ! runoff during time step
Delta_precip = 0.0d00 ! precipitation during time step

```

DO J=1, JZ

DO I=1, IX-1

```

Storage = Storage + WC(J,I) * DZ(J) * DX(I)*DY
Uptake = Uptake + S(J,I) * DT * DZ(J) * DX(I)*DY

```

END DO

END DO

DO I=1, IX-1

Delta_perc = Delta_perc + QB(I) * DX(I) * DT * DY

END DO

I=IX-1

DO J=1,JZ

```

Delta_seepage = Delta_seepage + QR(J)*DZ(J)*DY*DT

```

END DO

DO I=1,IX-1

Delta_runoff = delta_runoff + QSRUNOFF(I)*DX(I)*DY*DT

END DO

IF (IRRICONTROL == 'TRUE') THEN

Delta_irrig = 0.5*QIRRI*DT*DX(IL1) + QIRRI*DT*DX(IL2)

END IF

DO I=1,IX-1

Delta_precip = Delta_precip + b*dx(i)*dt

END DO

```

Delta_mass = Delta_precip + Delta_irrig - Uptake - Delta_perc
- Delta_runoff - Delta_seepage

```

```

Cum_precip = Cum_precip + Delta_precip      ! CUMULATIVE
Root_extraction = Root_extraction + Uptake   ! CUMULATIVE
Cum_irrig = Cum_irrig + Delta_irrig          ! CUMULATIVE
Cum_perc = Cum_perc + Delta_perc            ! CUMULATIVE
Runoff = Runoff + Delta_runoff              ! CUMULATIVE
Seepage = Seepage + Delta_seepage           ! CUMULATIVE

```

! Calculation of the actual mass balance

Actual_balance = Actual_balance + Delta_mass

```
! Calculation of the simulated mass balance
Sim_mass = Storage

Porc_mass = 100.0*abs( 1.0 - (Storage+Root_extraction+Runoff+
.   Cum_perc+Seepage)/(Storage_initial+Cum_irrig+Cum_precip) )

RETURN
ENDIF

END
```

```
*****
*          OUTPUT_2D
* This subroutine is designed to print data to different output files
* ****
SUBROUTINE OUTPUT_2D(
.DYN,SOIL_ID,JZ,IX,IDAY,Cum_Time,Time_End_Sim,IENDAY,TIME24,DT,
.Storage_initial,Storage,Actual_balance,Water_in,Time_Begin_Sim,
.Root_extraction,Cum_irrig,Cum_perc,Sim_mass,QS,LAH,B,Seepage,
.Porc_mass,Runoff,QB,QIRRI,PRECIP,LDD,LHH,RADIUS,BOTTOM,NITER,
.DEPTH,H,WTDEPTH,WT_Initial,Q1,Q2,Q3,Q4,SINK,Cum_precip,
.Time_of_irrigation,Kc)

IMPLICIT DOUBLE PRECISION(A-H,O-Z)
DOUBLE PRECISION LAH,Kc
PARAMETER (IS=90, JS=40,LD=365)
CHARACTER*15 DYN
CHARACTER*20 SOIL_ID

DIMENSION QB(IS),PRECIP(LD,0:23),RADIUS(IS),DEPTH(JS),H(JS,IS),
.WTDEPTH(is),QS(is),Q1(JS,IS),Q2(JS,IS),Q3(JS,IS),Q4(JS,IS),
.SINK(JS,IS)

IF (DYN .EQ. 'INITIAL') THEN

      WRITE(11,5)
5   FORMAT(T20,'Water table depth (cm)',/)
      WRITE(11,6) (I, I=1,IX)
6   FORMAT(16X,7I10)
!   WRITE(11,*) RADIUS(13)
      WRITE(11,7) (RADIUS(I), I=1,IX)
7   FORMAT('TIME24',2X, 'IDAY',2X, 'HOUR',37F10.2)
!   WRITE(11,*) LAH, WTDEPTH(13)
      WRITE(11,320) TIME24, IDAY, LAH, (WTDEPTH(i), I=1,IX)

      WRITE(6,*) ' ****'
      WRITE(6,*) '*'
      WRITE(6,*) '*'          WATABLE          '*'
      WRITE(6,*) '*'
      WRITE(6,*) '*'          CODE FOR SIMULATING WATER FLOW FROM SUB-DRIP  '*'
      WRITE(6,*) '*'          IRRIGATION IN TWO DIMENSIONAL VARIABLY      '*'
      WRITE(6,*) '*'          SATURATED POROUS MEDIA          '*'
      WRITE(6,*) '*'
      WRITE(6,*) '*'
      WRITE(6,*) '*'          JADIR APARECIDO ROSA          '*'
      WRITE(6,*) '*'          GAINESVILLE, FL          '*'
      WRITE(6,*) '*'          2000          '*'
      WRITE(6,*) '*'
      WRITE(6,*) ' ****'
      WRITE(6,*) '*'
      WRITE(6,*) 'Running...'

      WRITE(6,9) TIME24, IDAY, Cum_Time, DT, LAH
9   FORMAT('Time    =',F11.5,' hr',2X,'Day =',I3,6X,
.   'Cumulative Time =',F12.5,' hrs',/,
.   'Time Step =',F10.5,' hr',17X,'Annual hour = ',F10.3,/)

```

```

      WRITE(6,*)
!  Write the initial parameters for the simulation.
      WRITE(7,10) SOIL_ID
10  FORMAT('TWO-DIMENSIONAL SIMULATION OF A SOIL PROFILE',//,
.    'Soil: ',A,//,
.    'Upper Boundary condition at Soil Surface: Flux Density =
.    precipitation')

40  WRITE(7,50) BOTTOM,QIRRI,WT_Initial
50  FORMAT('Lower Boundary condition at Depth of ',F6.0,' cm: ',
.    'Flux Density = variable',//,
.    'Left Boundary condition at I = 1/2: Flux Density =
.    no-flux',//,
.    'Right Boundary condition at I = IX+1/2: Flux Density =
.    no-flux',//,
.    'Irrigation rate by sub-drip lines = ',F9.2,' cm/hr',//,
.    'Initial depth of water table = ',F9.2,' cm',//)

      WRITE(7,60) JZ,IX
60  FORMAT('The Number Of Vertical Increments = ',I3,//,
.    'The Number Of Radial Increments = ',I3,/) 

70  WRITE(7,80) IDAY, Time_Begin_Sim, IENDAY, Time_End_Sim,LAH
80  FORMAT('Begin day = ',I3,16x,'Time = ',2X,F9.2,' hrs',//,
.    'End day = ',I4,16x,'Total Time of Simulation = ',
.2X,F9.2,' hrs',//,'Annual hour = ',2X,F10.3)
      WRITE(7,90) Time_of_irrigation
90  FORMAT('Time_of_irrigation = ',F10.5,2x,'hr')
      WRITE(7,*)

      WRITE(8,255) TIME24, IDAY, LAH
      WRITE(8,260) (RADIUS(I), I=1,IX)
      DO J=1,JZ
      WRITE(8,270) DEPTH(J), (H(J,I), I=1,IX)
      END DO
      WRITE(8,*)

      WRITE(13,*) 'CUMULATIVE RUNOFF,SEEPAGE AND IRRIGATION'
      WRITE(13,95)
95  FORMAT('TIME24',2X,'IDAY',2X,'HOUR',T24,'SEEPAGE',T34,'RUNOFF',
.    T45,'TOTAL',T52, 'Cum-irrig')
      RETURN
      ENDIF
*****
      IF (DYN .EQ. 'INTEG') THEN
!
      IF(LHH == 0) THEN    ! PRINT DAILY BALANCE

      WRITE(7,220) TIME24, IDAY, Cum_Time, DT, NITER, LAH
220  FORMAT('Time = ',4X,F11.5,' hr',2X,'Day = ',I3,6X,
.    'Cumulative Time = ',F12.5,' hrs',//,
.    'Time Step = ',F10.5,' hr',16X,'Iteration = ',I5,/,
.    'Annual hour = ', F10.0)
      WRITE(7,90) Time_of_irrigation
      write(7,225) ldd,lhh,Kc

```

```

225  format('ldd = ',i5,10x,'lhh = ',i5,10x,'Kc = ',f5.3)
      WRITE(7,230) Storage_initial,Cum_irrig,Cum_precip,Cum_perc,
      .Root_extraction,Seepage,Runoff,Storage,Actual_balance,Sim_mass,
      .Porc_mass

230  FORMAT('Storage initial',t40,f15.4,' cm3',/,
      . 'Sum of irrigation applications',t40,f15.4,' cm3',/,
      . 'Sum of precipitations',t40,f15.4,' cm3',/,
      . 'Sum of deep percolations',t40,f15.4,' cm3',/,
      . 'Sum of root extractions',t40,f15.4,' cm3',/,
      . 'Seepage', t40,f15.4, ' cm3',/,
      . 'Sum of runoff',t40,f15.4,' cm3',/,
      . 'Storage at end of simulation',t40,f15.4,' cm3',//,
      . 'Cumulative mass balance',t40,f15.4,' cm3',/,
      . 'Cumulative simulated mass',t40,f15.4,' cm3',//,
      . 'Mass balance Error (%)',t40,F10.3,/) 

      WRITE(7,250) b,QB(1)
250  FORMAT('Inflow Rate at Upper Surface =',f13.4,' cm/hr',/
      . 'Outflow Rate at Lower Surface =',f13.4,' cm/hr',//)

      WRITE(8,255) TIME24,IDAD,LAH
255  FORMAT('Hour = ',F5.2,3X,'DAY = ',I4,3x,'Annual hour = ',F10.0,
      .1x,'hr')

      WRITE(8,260) (RADIUS(I), I=1,IX)
260  FORMAT(5X,71F10.2)

      DO 300 J=1,JZ
      WRITE(8,270) DEPTH(J), (H(J,I), I=1,IX)
270  FORMAT(F6.2,90F10.2)
300  CONTINUE
      WRITE(8,*)
350  WRITE(7,360)
360  FORMAT(//)

!      END IF

310  WRITE(11,320) TIME24,IDAD,LAH, (WTDEPTH(i), I=1,IX)
!      WRITE(11,*) LAH, WTDEPTH(13)
320  FORMAT(f6.0,I4,F8.0,37f10.3)

      TOTAL = SEEPAGE+RUNOFF
      WRITE(13,330) TIME24,IDAD,LAH,Seepage,Runoff,Total,Cum_irrig
330  FORMAT(F7.0,I4,F8.0,4F10.3)

      RETURN
      ENDIF
      END

```

LIST OF REFERENCES

Allen, R.G., L.S. Pereira, D. Raes, and M. Smith. 1998. Crop evapotranspiration: guidelines for computing crop water requirements. FAO Irrigation and Drainage Paper 56. FAO, Rome.

Amerman, C.R. and E.J. Monke. 1977. Soil water modeling II: On sensitivity to finite difference grid spacing. Transactions of the ASAE 20:478-484,488.

Amoozegar, A. and A.W. Warrick. 1986. Hydraulic conductivity of saturated soils: Field methods. In: Klute, A., ed. Methods of Soil Analysis, Part 1: Physical and Mineralogical Methods. Monograph No. 9. Am. Soc. Agronomy, Madison, WI.

ASAE . 1996. Soil and water terminology. ASAE Standards. S526.1, ASAE, St. Joseph, MI.

Belmans, C., J.G. Wesseling, and R.A. Feddes. 1983. Simulation model of the water balance of a cropped soil: SWATRE. Journal of Hydrology 63:271-286.

Bengtson, R.L., R.S. Garzon, and J.L. Fouss. 1993. A fluctuating watertable model for the management of a controlled-drainage/subirrigation system. Transactions of the ASAE 36:437-443.

Boersma, L. 1965a. Field measurements of hydraulic conductivity below a water table. In: Black, C. A., ed. Methods of Soil Analysis. Monograph No. 9. Am. Soc. Agronomy, Madison, WI.

Boersma, L. 1965b. Field measurements of hydraulic conductivity above a water table. In: Black, C. A., ed. Methods of Soil Analysis. Monograph No. 9. Am. Soc. Agronomy, Madison, WI.

Bower, H. 1974. Developing drainage design criteria. In: Schilfgaarde, J. (Ed.). Drainage for agriculture. Agronomy 11, American Society of Agronomy, Madison, WI.

Brandt, A., E. Bresler, N. Diner, I. Ben-Asher, J. Heller, and D. Goldberg. 1971. Infiltration from a trickle source: I. Mathematical Models. Soil Sci. Soc. Am. Proc. 35:675-682.

Brooks, R.H. and A.T. Corey. 1964. Hydraulic properties of porous media. *Hydrology Paper No. 3*, Colorado State Univ., Fort Collins, CO.

Brutsaert, W.F. 1971. A functional iteration technique for solving the Richards equation applied to two dimensional infiltration problems. *Water Resources Research* 7:1583-1596.

Camp, C.R. 1998. Subsurface drip irrigation: a review. *Transactions of the ASAE* 41:1353-1367.

✗ Campbell, K.L., J.S. Rogers, and D.R. Hensel. 1974. Watertable control for potatoes in Florida. *Transactions of the ASAE* 21:701-705.

Capece, J.C., K.L. Campbell, and L.B. Baldwin. 1988. Estimating runoff peak rates from flat, high-water-table watersheds. *Transactions of the ASAE* 31(1):74-81.

Capece, J.C., K.L. Campbell, L.B. Baldwin, and K.D. Konyha. 1987. Estimating runoff volumes from flat, high-water-table watersheds. *Transactions of the ASAE* 30:1397-1402.

Carlisle, V.W., F. Sodek, M.E. Collins, L.C. Hammond, and W.G. Harris. 1989. Characterization data for selected Florida soils. *Soil Sci. Research Rpt. No. 89-1*. Univ. of Florida, Gainesville, FL.

Celia, M.A. E.T. Bouloutas, and R.L. Zarba. 1990. A general mass-conservative numerical solution for the unsaturated flow equation. *Water Resources Research* 26:1483-1496.

Chung, S.O., A.D. Ward, and C.W. Schalk. 1992. Evaluation of the hydrologic component of the ADAPT water table management model. *Transactions of the ASAE* 35:571-579.

Clark, G.A., C.D. Stanley, and P.R. Gilreath. 1990. Fully enclosed subsurface irrigation for water management. *Proc. Florida Tomato Institute, 19-30. Veg. Crops Special Series Rep. SS-VEC-001*. Fla. Coop. Ext. Svc. University of Florida, Gainesville.

Clark, G.A. and C.D. Stanley. 1992. Subirrigation by microirrigation. *Applied Engineering In Agriculture* 8:647-652.

Clement, T.P., W.R. Wise, and F.J. Molz. 1994. A physically based, two-dimensional, finite-difference algorithm for modeling variably saturated flow. *Journal of Hydrology* 161:71-90.

Coleman, G. and D.G. DeCoursey. 1976. Sensitivity and model variance analysis applied to some evaporation and evapotranspiration models. *Water Resources Research* 12:873-879.

Dane, J.H. and F.H. Mathis. 1981. An adaptive finite difference scheme for the one-dimensional water flow equation. *Soil Sci. Soc. Am. J.* 45:1048-1054.

Desmond, E.D., A.D. Ward, N.R. Fausey, and S.R. Workman. 1996. Comparison of daily water table depth prediction by four simulation models. *Transactions of the ASAE* 39:111-118.

Dogan, A. 1999. Variably saturated three-dimensional rainfall driven groundwater pumping model. Ph. D. Dissertation. Univ. of Florida, Gainesville, FL.

Evans, R.O. and R.W. Skaggs. 1989. Design guidelines for water table management systems on coastal plain soils. *Applied Engineering in Agriculture* 5:539-548.

FAO. 1980. Drainage design factors. FAO Irrigation and Drainage Paper No. 38, Food and Agricultural Organization of the United Nations, Rome, Italy.

Feddes, R.A., P.J. Kowalik, and H. Zaradny. 1978. Simulation of field water use and crop yield. PUDOC, Wageningen, The Netherlands.

Feddes, R.A., P. Kabat, P.J.T. van Bakel, J.J.B. Bronswijk, and J. Halbertsma. 1988. Modelling soil water dynamics in the unsaturated zone – state of the art. *Journal of Hydrology* 100:69-111.

Fouss, J.L., R.W. Skaggs, J.E. Ayars, and H.B. Belcher. 1990. Water table control and shallow groundwater utilization. In: G.J. Hoffman, T.A Hoffman, and K.H. Solomon (Eds.). *Management of farm irrigation systems*. ASAE Monograph No. 9, ASAE, St. Joseph, MI. pp.783-824.

Fredlund, M.D., D.G. Fredlund, and G.W. Wilson. 1997. Prediction of the soil-water characteristic curve from grain-size distribution and volume-mass properties. Presented at the 3rd Brazilian Symposium on Unsaturated Soils. Rio de Janeiro, Brazil.

Gilley, J.R. and E.R. Allred. 1974. Infiltration and root extraction from subsurface irrigation laterals. *Transactions of the ASAE* 17:927-933.

Hanks, R.J. and G.L. Ashcroft. 1980. *Applied soil physics*. Springer-Verlag, New York.

Havard, P. 1993. *LINKFLOW: A linked saturated-unsaturated water flow model for drainage and subirrigation*. Ph. D. Dissertation. McGill University, Montreal, Quebec, Canada.

Haverkamp, R.I. and M. Vauclin. 1979. A note on estimating finite difference interblock hydraulic conductivity values for transient unsaturated flow. *Water Resources Research* 15:181-187.

Haverkamp, R.I. and M. Vauclin. 1981. A comparative study of three forms of the Richards equation used for predicting one-dimensional infiltration in unsaturated soil. *Soil Sci. Soc. Am. J.* 45:13-20.

Haverkamp, R.I., M. Vauclin, J. Touma, P.J. Wierenga, and G. Vachaud. 1977. A comparison of numerical models for one-dimensional infiltration. *Soil Sci. Soc. Am. J.* 41:285-294.

Heatwole, C.D., K.L Campbell, and A.B. Bottcher. 1987. Modified CREAMS hydrology model for coastal plain flatwoods. *Transactions of the ASAE* 30(4):1014-1022.

Hillel, D. 1998. Environmental soil physics. Academic Press, San Diego, CA.

Hills, R.G., I. Porro, D.B. Hudson, and P.J. Wierenga. 1989. Modeling one-dimensional infiltration into very dry soils. I. Model development and evaluation. *Water Resources Research*. 25:1259-1269.

Hopmans, J.W. and J.N.M. Stricker. 1989. Stochastic analysis of soil water regime in a watershed. *Journal of Hydrology* 105:57-84.

Huang, K., B.P. Mohanty, M.Th. van Genuchten. 1996. A new convergence criteria for the modified Picard iteration method to solve the variably saturated flow equation. *Journal of Hydrology* 178:69-91.

Jensen, K.H. 1983. Simulation of water flow in the unsaturated zone including the root zone. Institute of Hydrodynamics and Hydraulic Engineering, Technical University of Denmark, Lyngby, Denmark.

Jnad, I., G.J. Sabbagh, and B.J. Lesikar. 1998. Numerical model to simulate three-dimensional transient flow from subsurface drip irrigation. ASAE Paper No. 98-2174, ASAE, St. Joseph, MI.

Johnson, Jr., M.H., D.L. Thomas, and B.D. McLendon. 1993. Controlled-drainage/subirrigation system automation based on soil water potential. *Transactions of the ASAE* 36:751-759.

Jones, J.W., L.H. Allen, S.F. Shih, J.S. Rogers, L.C. Hammond, A.G. Smajstrla, and J.D. Martsolf. 1984. Estimated and measured evapotranspiration for Florida climate, crops, and soils. *Florida Agric. Exp. Stn. Bull.* 840.

Kandil, H.M. and L.S. Willardson. 1992. Relating crop-yield response to water-table fluctuations. *Journal of Irrigation and Drainage Engineering* 118:113-121.

Kanwar, R.S., H.A. Rizvi, M. Ahmed, R. Horton, and S.J. Marley. 1989. Measurement of field-saturated hydraulic conductivity by using Guelph and velocity permeameters. *Trans. of the ASAE* 32(6):1885-1890.

Kirkland, M.R., R.G. Hills, and P.J. Wierenga. 1992. Algorithms for solving Richards' equation for variably saturated soils. *Water Resources Research* 28:2049-2058.

Klute, A. and C. Dirksen. 1986. Hydraulic conductivity and diffusivity: laboratory methods. In: Klute, A. (Ed.). *Methods of soil analysis. Part 1. Physical and mineralogical methods*. Soil Science Society of America Book Series No. 5, Madison, WI.

Knisel, W.G.,[ed]. 1980. CREAMS: A field-scale model for chemicals, runoff, and erosion from agricultural management systems. *Conservation Research Report No. 26*. USDA-SEA, Washington, DC.

Koorevaar, P., G. Menelik, and C. Dirksen. 1983. *Elements of soil physics*. Elsevier, Amsterdam, The Netherlands.

Kutilek, M. and D.R. Nielsen. 1994. *Soil hydrology*. Catena Verlag, Germany.

Lafolie, F., R. Guennelon, and M.Th. van Genuchten. 1989. Analysis of water flow under trickle irrigation: I. Theory and numerical solution. *Soil Sci. Soc. Am. J.* 53:1310-1318.

Lappala, E.G., R.W. Healy, and E.P. Weeks. 1993. Documentation of computer program VS2D to solve the equations of fluid flow in variably saturated porous media. U.S. Geological Survey, Water Resources Investigations Report 83-4099, Denver, CO.

Leonard, R.A., W.G. Knisel, and D.A. Still. 1987. GLEAMS: Groundwater loading effects of agricultural management systems. *Transactions of the ASAE* 30:1403-1418.

Luckner, L., M.Th. van Genuchten, and D.R. Nielsen. 1989. A consistent set of parametric models for the two-phase flow of immiscible fluids in the subsurface. *Water Resources Research* 25:2187-2193.

Madramootoo, C.A., G.T. Dodds, and A. Papadopoulos. 1993. Agronomic and environmental benefits of water table management. *Journal of Irrigation and Drainage Engineering* 119:1052-1065.

Milly, P.C.D. 1985. A mass-conservative procedure for time-stepping in models of unsaturated flow. *Adv. Water Resources* 8:32-36.

Molz, F.J. 1981. Models of water transport in the soil-plant system: A review. *Water Resources Research* 17:1245-1260.

Mualem, Y. 1976. A new model for predicting hydraulic conductivity of unsaturated porous media. *Water Resources Research* 12:513-522.

Mualem, Y. 1986. Hydraulic conductivity of unsaturated soils: Prediction and formulas. In: Klute, A. (Ed.). *Methods of soil analysis. Part 1. Physical and mineralogical methods*. Soil Science Society of America Book Series No. 5, Madison, WI.

Nwadukwe, P.O., S. Abdulmumin, Y. Arora, and I.F. Ike. 1989. Effects of irrigation frequency and water table depths on root growth and yield of tomato in a tropical soil. *Agricultural Water Management* 16:241-249.

Oosterbaan, R. J., and H. J. Nijland. 1994. Determining the saturated hydraulic conductivity. In: Ritzema, H. P., ed. *Drainage Principles and Applications*. ILRI Publication No. 16, Wageningen, The Netherlands.

Oron, G. 1981. Simulation of water flow in the soil under sub-surface trickle irrigation with water uptake by roots. *Agricultural Water Management* 3:179-193.

Pan, L. and P.J. Wierenga. 1995. A transformed pressure head-based approach to solve Richards' equation for variably saturated soils. *Water Resources Research* 31:925-931.

Philip, J.R. 1968. Steady infiltration from buried point source and spherical cavities. *Water Resources Research* 4:1039-1047.

Philip, J.R. 1971. General theorem on steady infiltration from surfaces with application to point and line sources. *Soil Sci. Soc. Am. Proc.* 35:867-871.

Pitts, D.J., Y.J. Tsai, D.L. Myhre, D.L. Anderson, and S.F. Shih. 1993. Influence of water table depth on sugarcane grown in sandy soils in Florida. *Transactions of the ASAE* 36:777-782.

Prasher, S.O., S.F. Barrington, and A.M. Darbary. 1994. Economical design of water table management systems in humid areas. *Computers and Electronics in Agriculture* 10:229-244.

Ragab, R.A. and F. Amer. 1986. Estimating water table contribution to the water supply of maize. *Agricultural Water Management* 11:221-230.

Rathfelder, K. and L.M. Abriola. 1994. Mass conservative numerical solutions of the head-based Richards equation. *Water Resources Research* 30:2579-2586.

Remson, I., G.M. Hornberger, and F.J. Molz. 1971. Numerical methods in subsurface hydrology. John Wiley & Sons, New York, NY.

Rosa, J.A. 1993. Niveis de drenagem para a cultura do feijoeiro em varzeas. *Pesquisa Agropecuaria Brasileira* 28:947-954.

Rosa, J.A. and A.G. Smajstrla. 1999. Determination of saturated hydraulic conductivity in high water table soils using a simple water table level measurement device. *Soil Crop Sci. Soc. Florida Proc.* 58:62-66.

Rubin, J. 1967. Numerical method for analyzing hysteresis-affected post-infiltration redistribution of soil moisture. *Soil Sci. Soc. Am. Proc.* 31:13-20.

Schnabel, R.R. and E.B. Richie. 1984. Calculation of internodal conductances for unsaturated flow simulations: A comparison. *Soil Sci. Soc. Am. J.* 48:1006-1010.

Shirmohammadi, A., D.L. Thomas, and M.C. Smith. 1991. Drainage-subirrigation design for Pelham Loamy Sand. *Transactions of the ASAE* 34:73-80.

Šimunek, J., T. Vogel, and M.Th. van Genuchten. 1994. The SWMS_2D code for simulating water flow and solute transport in two-dimensional variably saturated media. U.S. Salinity Laboratory, Agricultural Research Service, Riverside, CA.

Skaggs, R.W. 1978. A water management model for shallow water table soils. Report No. 134. Raleigh, N.C.: Water Resources Research Institute, Univ. of North Carolina.

Skaggs, R.W. 1992. Drainage and water management modeling technology. Proceedings of the Sixth International Drainage Symposium, pp. 1-11, ASAE, St. Joseph, MI.

Smajstrla, A.G. 1982. Irrigation management for the conservation of limited water resources. Office of Water Research and Technology of the Department of the Interior. Water Conservation Research Program (WRC-80).

Smajstrla, A.G., B.J. Boman, G.A. Clark, D.Z. Haman, D.S. Harrison, F.T. Izuno, D.J. Pitts, and F.S. Zazueta. 1991. Efficiencies of Florida agricultural irrigation systems. Bul. 247. Fla. Coop. Ext. Svc. University of Florida, Gainesville.

Smajstrla, A.G., S.J. Locascio, and D.R. Hensel. 1995. Subsurface drip irrigation of potatoes. *Proc. Fla. State Hort. Soc.* 108:193-195.

Smajstrla, A.G., S.J. Locascio, and D.P. Weingartner. 1996. Improving seepage irrigation efficiency for potato production using automatic subsurface drip irrigation systems. Project Completion Report. St. Johns River Water Management District Contract No. 95J113, 1996. University of Florida, Gainesville.

Smajstrla, A.G., S.J. Locascio, and D.P. Weingartner. 1998. Improving seepage irrigation efficiency for potato production using automatic subsurface drip irrigation systems. Project Completion Report. St. Johns River Water Management District Contract No. 95J113, 1998. University of Florida, Gainesville.

Smajstrla, A.G., S.J. Locascio, D.P. Weingartner, and D.R. Hensel. 2000. Subsurface drip irrigation for water table control and potato production. *Applied Engineering in Agriculture* 16(3) in press.

Snyder, G.H., W.H. Burdine, J.R. Crocket, G.Gascho, D.S. Harrison, G. Kidder, J.W. Mishoe, D.L. Myhre, F.M. Pate, and S.F. Shih. 1978. Water table management for organic soil conservation and crop production in the Florida Everglades. *Florida Agric. Exp. Stn. Bull.* 801.

Stanley, C.D. and G.A. Clark. 1991. Water table management using microirrigation tubing. *Soil Crop Sci. Soc. Florida Proc.* 50:6-8.

Stephens, D.B. 1995. *Vadose zone hydrology*. CRC Press, Inc., Boca Raton, FL.

Stone, K.C. 1987. Measurement and simulation of soil water status under field conditions. Ph. D. Dissertation. Univ. of Florida, Gainesville, FL.

USDA-SCS. 1983. Soil survey of St. Johns County, Florida. United States Department of Agriculture, Soil Conservation Service.

Vauclin, M., D. Khanji, and G. Vachaud. 1979. Experimental and numerical study of a transient, two-dimensional unsaturated water table recharge problem. *Water Resources Research* 15:1089-1101.

van Genuchten, M.Th. 1980. A closed-form equation for predicting the hydraulic conductivity of unsaturated soils. *Soil Sci. Soc. Am. J.* 44:892-898.

van Genuchten, M.Th., F.J. Leij, and S.R. Yates. 1991. The RETC code for quantifying the hydraulic functions of unsaturated soils. Robert S. Kerr Environmental Research Laboratory, U.S. Environmental Protection Agency, Ada, OK.

Vauclin, M., G. Vachaud , and D. Khanji. 1975. Two dimensional numerical analysis of transient water transfer in saturated-unsaturated soils. In: G.C. Vansteenkiste(Ed.). *Modeling and simulation of water resources systems*. North-Holland, Amsterdam, pp. 299-323.

Vellidis, G. 1989. Measured and simulated soil water redistribution and extraction patterns of drip-irrigated tomatoes above a shallow water table. Ph. D. Dissertation. Univ. of Florida, Gainesville, FL.

Vogel, T., K. Huang, R. Zhang, and M. Th. van Genuchten. 1996. The HYDRUS code for simulating one-dimensional water flow, solute transport, and heat movement in variably-saturated media. U.S. Salinity Laboratory, Agricultural Research Service, Riverside, CA.

Warrick, A.W. 1974. Time dependent linearized infiltration. I. Point sources. *Soil Sci. Soc. Am. Proc.* 38:383-386.

Warrick, A.W. 1991. Numerical approximations of Darcian flow through unsaturated soil. *Water Resources Research* 27:1215-1222.

Williamson, R.E. and G.J. Kriz. 1970. Response of agricultural crops to flooding: depth of water table and soil composition. *Transactions of the ASAE* 13:216-220.

Wise, W.R. 1991. Discussion of 'On the relation between saturated conductivity and capillary retention characteristics', by S. Mishra and J.C. Parker, September-October 1990 issue, vol 28, no. 5, pp. 775-777. *Ground Water* 29:272-273.

Wise, W.R., T.P. Clement, and F.J. Molz. 1994. Variably saturated modeling of transient drainage: sensitivity to soil properties. *Journal of Hydrology* 161:91-108.

Workman, S.R. and R.W. Skaggs. 1990. PREFLO: A water management model capable of simulating preferential flow. *Transactions of the ASAE* 33:1939-1948.

Workman, S.R. and R.W. Skaggs. 1991. Evaluation of the water management model PREFLO. *Transactions of the ASAE* 34:2053-2059.

Wösten, J.H.M. and M.Th. van Genuchten. 1988. Using texture and other soil properties to predict the unsaturated soil hydraulic properties. *Soil Sci. Soc. Am. J.* 52:1762-1770.

Zazueta, F.S., M. Carrillo, and G.A. Clark. 1994. A simple equation to estimate soil-water movement from trickle sources. *Soil Crop Sci. Soc. Florida Proc.* 53:39-42.

Zazueta, F.S., A.G. Smajstrla, and D.S. Harrison. 1985. A simple numerical model for the prediction of soil-water movement from trickle sources. *Soil Crop Sci. Soc. Florida Proc.* 44:72-76.

BIOGRAPHICAL SKETCH

Jadir Aparecido Rosa was born January 26, 1959 in Passos, Minas Gerais State, Brazil.

In 1977, Jadir began his undergraduate program in Agricultural Engineering at the Federal University of Viçosa. In 1981, he received his Bachelor of Science in Agricultural Engineering, and in 1986 his Master of Sciences in Agricultural Engineering.

His professional experience includes two years (May 1982- July 1984) as assistant researcher at EMBRAPA - Brazilian Agricultural Research Corporation, one year as Professor of Agricultural Engineering (May 1986-August 1987) at the University of Uberaba, and researcher in Agricultural Engineering at the Parana State Agricultural Research Institute (1987 - present).

In January 1996, he began his Ph.D. program of study at the University of Florida with a scholarship from the Brazilian government.

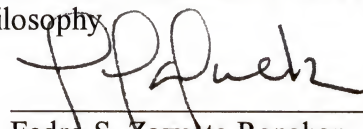
Jadir has a son, Lucas, and a daughter, Bruna.

I certify that I have read this study and that in my opinion it conforms to acceptable standards of scholarly presentation and is fully adequate, in scope and quality, as a dissertation for the degree of Doctor of Philosophy.



Kenneth L. Campbell, Chairman
Professor of Agricultural and Biological Engineering

I certify that I have read this study and that in my opinion it conforms to acceptable standards of scholarly presentation and is fully adequate, in scope and quality, as a dissertation for the degree of Doctor of Philosophy.



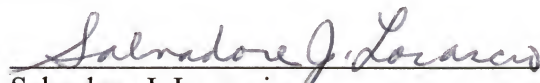
Fedro S. Zazueta Ranahan
Professor of Agricultural and Biological Engineering

I certify that I have read this study and that in my opinion it conforms to acceptable standards of scholarly presentation and is fully adequate, in scope and quality, as a dissertation for the degree of Doctor of Philosophy.



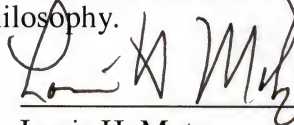
Dorota Z. Haman
Professor of Agricultural and Biological Engineering

I certify that I have read this study and that in my opinion it conforms to acceptable standards of scholarly presentation and is fully adequate, in scope and quality, as a dissertation for the degree of Doctor of Philosophy.



Salvadore J. Locascio
Professor of Horticultural Sciences

I certify that I have read this study and that in my opinion it conforms to acceptable standards of scholarly presentation and is fully adequate, in scope and quality, as a dissertation for the degree of Doctor of Philosophy.

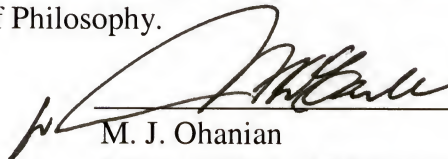


Louis H. Motz

Associate Professor of Civil Engineering

This dissertation was submitted to the Graduate Faculty of the College of Engineering and to the Graduate School and was accepted as partial fulfillment of the requirements for the degree of Doctor of Philosophy.

May 2000



M. J. Ohanian

Dean, College of Engineering

Winfred M. Phillips

Dean, Graduate School